



**Final Study Project**  
**MASTER'S IN BIOMEDICAL ENGINEERING**

**Gripper design for an assistive robot in a  
hospital environment**

Barcelona, 17 June 2023  
Author: Jaume Oriol Lladó  
Director: Júlia Borràs Sol  
Tutor: Alicia Casals i Gelpí

Performed at: Institut de Robòtica i Informàtica  
Industrial (IRI), CSIC-UPC



UNIVERSITAT DE  
BARCELONA



UNIVERSITAT POLITÈCNICA  
DE CATALUNYA

Registration Date:

## MASTER IN BIOMEDICAL ENGINEERING

### Final Master's Project Record

STUDENT NAME:

TITLE OF THE PROJECT:

DIRECTOR AND TUTOR OF THE PROJECT:

(Specify Center, Department, Company, Hospital, etc. where they are associated)

Signed:

Digitally signed  
by BORRAS  
SOL JULIA -  
DNI  
43736258X

Dr/a.  
Project's Director

Signed:

ALICIA CASALS  
GELPI - DNI  
36957994F  
(TCAT)

Digitally signed by  
ALICIA CASALS  
GELPI - DNI  
36957994F (TCAT)  
Date: 2023.03.21  
23:06:17 +01'00'

Dr/a.  
Project's Tutor

Signed:

JAUME  
ORIOL  
LLADO - DNI  
41562009C

Firmado digitalmente  
por JAUME ORIOL  
LLADO - DNI  
41562009C  
Fecha: 2023.03.21  
17:43:53 +01'00'

Student

Signed:

Firmado por JORDI  
FONOLLOSA MAGRINYA -  
DNI \*\*\*5987\*\* (TCAT)  
Fecha: 25/05/2023  
22:16:20 CEST

Dr. Jordi Fonollosa  
UPC Coordinator  
MSc in Biomedical Engineering

Signed:

CASTAÑO  
LINARES  
OSCAR -  
52408576V

Dr. Óscar Castaño  
UB Coordinator  
MSc in Biomedical Engineering

## Resume

The main idea of this project is to design a robotic gripper capable of separating layers of plastic or cloth, with the objective of opening sealed surgical bags used in hospitals and if possible, to unfold folded cloths. A preliminary study of existing projects related to the task of separating cloth layers has been carried out, in order to design a gripper that satisfies the needs of nurses and the design conditions established by Institut de Robòtica i Informàtica Industrial (IRI). These conditions are the dimensions of the final product which must include a roller at the tip of one of the fingers which is used to move the layers.

A test-bench has been designed with the SolidWorks software and developed with a 3D printer, with which studies have been carried out with the materials chosen to manufacture the gripper. With the results obtained, the properties, characteristics and relationships that the different chosen materials must have have been determined. The adhesive property of the materials has been achieved studying the friction between the layers and the materials. On the other hand, superficial modifications of the rollers surface have been discarded, due to a lack of necessary resources, and the use of other mechanisms such as needles or sandpaper to avoid damaging the cloths has also been ruled out.

With the studies carried out, a pair of materials have been found which fulfils the objective of separating two layers of fabric. The material used to manufacture the roller is a Shore 80A hardness resin which has lower friction coefficients with the layers than the material used to cover the second finger. This material is Ecoflex 00-50 which has a hardness lower than the Shore A scale. It has been seen that despite being a very adherent material, it is easy to wash once the lint from the cloth has stuck.

## Glossary

PPE – Protective Medical Equipment

EA – Electroadhesion

PR – Pressure force exerted by the roller

NR – Normal force created from the PR

FR – Force exerted by the roller to carry away the layer

FFRA – Friction force between the roller and layer A

FFAB – Friction force between layer A and B

FFBC – Friction force between layer B and C

Surface – ABS Surface

SGI – Short Glove

LGI – Long Glove

BH – Blue Hat

WH – White Hat

GaPI – Gauze's Plastic

GaPa – Gauze's Paper

GIPI – Glove's Plastic

GIPa – Glove's Paper

PIAp – Plastic Apron

BNC – Blue Nurse's Coat

WNC – White Nurse's Coat

NCPI – Nurse's Coat Plastic

PiC – Pillowcase

LN – Linen Napkin

WR – Waffle Rag

ST – Small Towel

## Index

1. Introduction.....	4
2. Problem Statement.....	6
2.1. Objectives.....	7
2.2. Background .....	7
2.3. Materials Research.....	11
2.4. Friction Coefficients Calculations.....	13
2.5. Materials Choice.....	15
3. Experimental Development.....	16
3.1. Friction Coefficient Experiments .....	16
3.1.1. Results and Discussion .....	19
3.2. Test-bench Experiments.....	20
3.2.1. Test-bench Operation .....	26
3.2.2. Results and Discussion .....	27
4. Gripper Design .....	31
Conclusions and Future Work.....	35
Bibliography.....	36
Annexes.....	37

## 1. Introduction

This project arises from the need to find solutions to the manipulation of soft objects, in particular, at Institut de Robòtica i Informàtica Industrial (IRI), CSIC-UPC, they have focused on the procedure of opening sealed surgical bags, bags that inside contain sterilised medical materials and instrumentation (Figure 1.1). Due to an, IRI European Project in collaboration with the team of nurses and doctors from the Hospital Clinic, this task was selected after a user needs and requirements study with the team. Doctors and nurses explain how at each surgery they have to open around 79-80 surgical bags, meaning a total of 160-210 bag openings at each operating room each morning. Therefore, if we could solve even partially this task we could have a big impact.

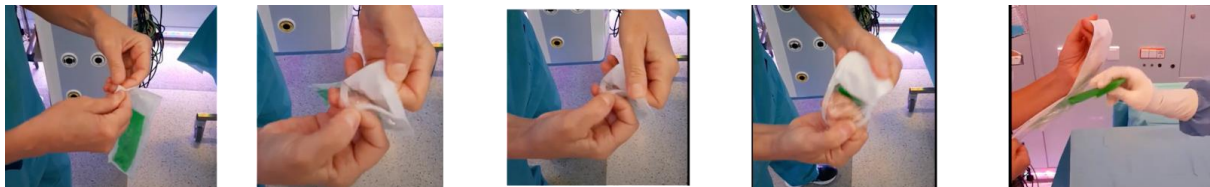


Figure 1.1: Summary of the task of opening surgical bags. They came in different sizes. From left to right, first you separate layers, then you pull them. Often users then regrasp the center and pull again, to finally offer the content to the other nurse/doctor.

The main difficulty of this task is the separation of the layers of plastic that have to be grasped and pulled in order to open the bag. To carry out this procedure, the design of some terminal elements is proposed, which will be accommodated in the base of an already existing robotic arm gripper. These terminal elements are intended to be formed by a roller made of a materials which has the necessary properties to allow the separation of two layers of fabric, which in this case would be the two layers that make up the surgical bag. Once the two layers are separated, the second terminal element would act as a clamp to finish separating the two layers. This project is only a branch of a much larger European Project, SoftEnable, which is carried out in different research centers in Europe.

SoftEnable, formally known as “Towards Soft Fixture-Based Manipulation Primitives Enabling Safe Robotic Manipulation in Hazardous Healthcare and Food Handling Applications”, is an European project started in October 2022 and it will last until September 2026. In this project, based on the notions of soft fixture-enabled manipulation primitives, a new framework for manipulation actions involving delicate and deformable objects is proposed, since it has been seen that there is a great need for the implementations of robust methods to manipulate fragile and soft objects. An important part of this method is the design of specialized grippers. Specially designed robotic grippers for a particular job are very common in industrial robotic

applications involving rigid objects such as metal bars. We propose a gripper design specially conceived for this task, but with generality in mind to perform other tasks, such as unfolding clothes from a folded state, that also requires layer separation.

SoftEnable focuses both on the food handling sector (fresh food handling) in which they want to assist industry workers with collaborative robotics, and on the wellness and medical sector where they want to demonstrate how soft fixtures can be used by robotic systems assisting workers in the sector by reducing their stress and exposure to risks that may exist when preparing, dressing, undressing or safely depositing protective medical equipment (PPE). This project is carried out collectively between different European research and industry partners such as Ocado Innovation Limited in England, KTH Royal Institute of Technology in Sweden and the Clinical Foundation for Biomedical Research, the Hospital Clínic from Barcelona and the Institute of Robotics and Industrial Informatics, CSIC in Catalonia, among others.

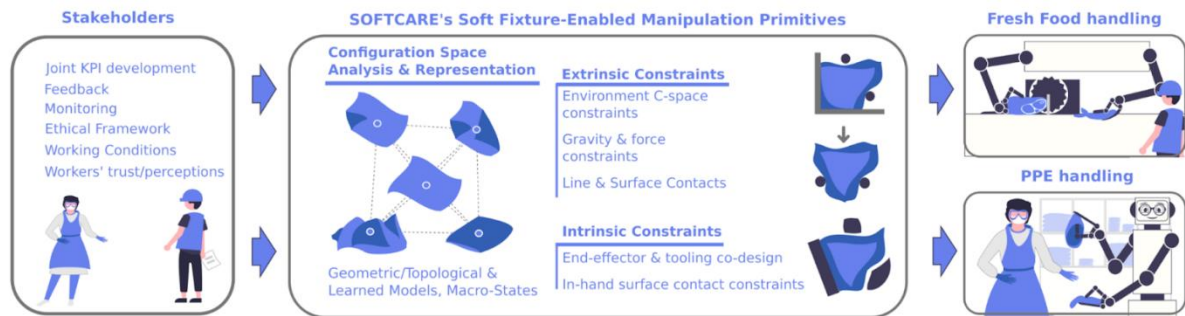


Figure 1.2: Overview of SoftEnable EU project.

Many of the implementations that are intended to be done through SoftEnable are using assistant robots. These robots are designed with interfaces that give them autonomy to interact with people in order to provide support to users. These robots can have a humanoid architecture that helps in robot-human interaction. Another architecture that these robots can have is that of a robotic arm, in which grippers specially designed for the treatment of deformable or soft objects are attached.

## 2. Problem Statement

Compared to the manipulation of rigid objects that have little deformation, in the manipulation of fabrics there is a great difficulty in automating it due to the nature of these materials. Cloths are characterized by low bending stiffness, a complex dynamic behaviour, they are flexible, elastic, and fragile. This makes its manipulation highly unpredictable and complex; you only have to see the behaviour of the fabric when we fold a t-shirt or a sheet. Instead of folding the clothes directly from where they are, we lift and unfold them to consequently fold them in the desired shape.

Another complexity that exists in cloth manipulation is the task of separating two layers of cloth. Although for certain industrial cases this task is automated with vacuum, needles or sticky grippers, in unstructured environments this task is not solved. This is because not all layers are the same, they can vary in materials, physical characteristics, stiffness, surface roughness, etc. Equally, other factors that appear in the stacking of fabric layers must also be taken into account. These factors are the friction coefficients between the layers and the surface on which they are located or the different forces that occur when the layers are manipulated and which depend on the materials of each layer, for example when separating two layers of cotton appears a static force that joins the two layers and makes it difficult to separate them.

When it comes to the procedure of opening surgical bags, to all these factors we must also add other difficulties that appear, since not only do we have two layers arranged one on top of the other, but these two layers are joined together with the other, through a union that can either be made through a type of adhesive substance or through the use of sealing machines that use high temperatures to melt a small part of the layers to join them. Comparing the procedure of separating two layers of fabric that are not attached to the procedure of separating surgical bags, the latter have a considerably reduced surface with which the layers can be grasped, which makes the process of opening the bags even more difficult.

Although all hospitals use surgical bags, these are not always made of the same materials and depending on the use they are given, they do not have the same characteristics. For example, a bag that contains sterilized gloves is made up of two layers of the same plastic material, on the other hand, a bag that contains sterile gauzes is usually made up of a layer of a plastic material to observe the contents of the bag and another of paper treated to have the necessary characteristics to maintain sterility inside. This influences when deciding for which layer you want to start taking the bag, how they should be stored to facilitate their handling or what movements should be made to be able to separate them, since the friction coefficients between the terminal element of the robot and those of the layers varies.



## 2.1. Objectives

Due to the high complexity of the task, the objectives of this thesis will not be that of solving the task as a whole, but to understand well the problem, the parameters that are more relevant, and propose a gripper design as a first step towards a solution.

For this reason, the objectives of this work are:

1. Study the previous works that exist related to the task of layer separation.
2. Design and prototype a test-bench that allows to study the friction requirements of the task, compare materials and choose the best design parameters.
3. Establish relationships between material frictions necessary for the task to work based on the experiments using the test-bench developed in the first objective.
4. Design a first version of a gripper based on the results found to execute the task of “layer separation”.

## 2.2. Background

A lot of research has been carried out in order to achieve the manipulation of fabrics, from clamp designs with different materials that can achieve the adhesion of the layers to the movements that the robot must make to grasp and manipulate the cloth. Conventional end-effectors have been found to have difficulty handling layers of tissue. Successful grippers are usually intrusive ones, meaning that they can damage the material, either using needles, glues or similar technologies, which are only acceptable in industrial scenarios. For this reason, one of the techniques that has been used for the manipulation of layers is the use of air pressure with which the adhesion of the first layer can be achieved by applying negative pressure through the end-effector or by applying the Bernoulli principles where high velocity air flows create low pressure regions that serve to achieve a force that causes the layers to separate.

Although it looks like a great solution, it has several problems, such as poor performance when used to move porous fabrics, plugging of air outlets and fabric vibration among others. Apart from the functional problems, there are also the problems of simulation of the models, which can be computationally expensive, the calculations that must be carried out to achieve the appropriate operating parameters, volume, air flow speed and area that can be difficult to control and which can lead to unexpected results.

Zhenjia Xu et al [\[1\]](#) developed the DextAIRity, a robotic system with 6 degrees of freedom consisting of two robotic arms with parallel grippers (Schunk WSG50 and OnRobot RG2) and a third arm containing a centrifugal air pump capable of producing a maximum air flow of 1100L/s. In this case, they do not use the Bernoulli principles to manipulate the fabrics, but

instead they use direct air flows. When testing the robotic system, they have seen that it has several deficiencies such as the high noise when using the air pump or that the pump they use does not turn on or off instantly, which can be a problem for tasks that require an instant boost of air. However, they have managed to demonstrate the effectiveness of DextAIRity for handling multiple layers of fabrics and that it is highly effective in the process of unfolding large cloths without the need of using large robots or fast movements.

Much research has been carried out for the manipulation of soft objects in which the imitation of the movements performed by human beings when manipulating tissue layers and the imitation of the physiognomy of people's fingers have been sought, as we are capable of varying the friction between the tips of our fingers to achieve the separation of two layers without the need of applying high forces. A design proposal that imitates the human being is for example that of H. Jiang et al [\[2\]](#) who proposed a method based on the variation of frictions, in which they develop a robotic gripper that allows the variation of the friction coefficients between the tips of the fingers. One of the fingers has a flat surface coated with Acrylic which gives it a low friction coefficient and the other finger with a curved shape, has been coated with sandpaper with which they achieve a high friction coefficient. Jiang et al have shown that with their design they are able to slide layers of fabric between two fingers and unfold a piece of cloth. However, it is a complex design, that requires 6 motors and one of the fingers is a tactile sensor, and for our solution we wanted to evaluate if something simpler could be designed by understanding well the problematic of the task.

These abilities of the human being to modify the coefficients of friction between the tips of the fingers and the different materials, is partly due to the mechanical structure of the pads of the fingers and the tissues that form them. When they are harder, they can slide more easily and with less force on surfaces and also provide the security of holding objects without the need to apply high forces to secure them. In robotics, attempts have been made to imitate the functioning of human skin using different materials such as elastomers without succeeding in imitating its characteristics one hundred percent. Spiers et al [\[3\]](#) proposed a mechanism by which they could achieve significant changes in the friction coefficients and in the morphology of the contact area that allowed both grasping the objects and sliding over them. This mechanism consists of the use of elements with low friction that are hidden inside the finger depending on the normal force that is applied when the object comes into contact with the fingers of the clamp, leaving exposed the surface that has high friction. For the development of this clamp, they use ABS as a material for the retractable parts since they achieve hard surfaces with low friction coefficients and for the surface with high friction, they use the Vytaflex30 urethane rubber from Smooth-On. With this design, they have shown that by varying the properties of the frictions, the sliding or movement of rigid objects is achieved

without the need to use tactile sensors, dynamic models or complex controllers, but only a gripper torque controller is needed.

Another way to focus solutions on fabric manipulation is through clothing penetration. Different methods have been used, like sharp objects such as needles, which instead of playing with the materials friction's coefficients for better adhesion, they go through the fabric layers. These methods are not widely used as they can damage the fabrics and their correct operation is affected by the thickness of the layers. Ku et al [4] developed a clamp that mimicked the mouth of lampreys. The forceps made with silicone elastomers have two fingers that contain microneedles at the tips which penetrate the layer of tissue achieving the union of the layer with the gripper. Once the layer is penetrated, the fingers of the gripper close, pinching the layer and allowing its manipulation.

A less invasive method than the previous one has been the use of adhesive surfaces to manipulate tissues. The problem with these methods is that the utensils or materials used have a very short lifespan and stop working as a lot of dust or even lint from the fabrics themselves gets stuck to them. As a solution to these problems, several solutions have been developed that are based on electroadhesion (EA). It is about creating surfaces that, once a voltage is applied to them, an electric field is created between the surface and the first layer of fabric, causing it to adhere to the EA surface. It is a technique that is currently being used in the textile and aerospace industry to handle flexible and flat materials. They cannot be used for objects that are not flat as the electrostatic force created by the EA surface is not strong enough to cause the material layer to stick to it. An advantage of this method is that it can be used for any type of material and for any layer thickness. An example of a gripper that uses electroadhesion is the one developed by Digumarty et al [5] which consists of a gripper with two fingers, one of which is equipped with an EA surface of  $2\text{cm}^2$ . This finger is used to lift a corner of the fabric that together with the second finger moves in the direction of the first grasping the layer. To prevent the fabric's own weight from causing the corner to detach from the finger, it rotates in the opposite direction to the force that attracts the first layer to the second. With this gripper model, Digumarty et al have achieved positive results demonstrating that they are able to handle a wide variety of materials and dimensions, despite having difficulties with materials that present a high roughness surface. By having a small EA surface they are also able to handle fabrics that are not flat on a surface but may be wrinkled, as they only need a small part of the cloth to have a smooth surface to adhere the gripper to. Despite being a method with many advantages, the use of electroadhesion surfaces requires a longer releasing time than other methods as residual electrical charges remain after the current has been cut. In this project, we want to study if we can solve this problem with friction alone.

Other scientists, instead of using electric fields to manipulate tissues, have preferred to use magnetic fields, as for example Dragusanu et al [6] developed the DressGripper, an end effector consisting of two fingers composed of different moving parts which are directed by an internal tendon, when this tendon is stretched, the tips of the fingers come together and when the tension is released, they separate. An electromagnet is placed at the tip of one of the two fingers, while another electromagnet or a small ferromagnetic piece can be found on the other. Both options can be given since depending on the number of electromagnets, the robot requires a greater energy capacity to operate, which entails the incorporation of more batteries but which also implies a greater magnetic force that prevents manipulated fabrics from falling from the gripper. The materials they use are chosen taking into account that the DressGripper has been designed to have a safe human-robot cooperative dressing. They have used polyurethane as it can absorb shocks and reduce unwanted vibrations. For the magnetic elements they have used a soft ferromagnet, as it leaves no residual magnetism and is easily magnetized and demagnetized when activated or deactivated. In this way, they avoid unwanted interactions with magnetic parts that may be in the clothes in which they dress people. This design is not able to separate layers.

Finally, below are two examples of end-effectors that, apart from performing the function of clamps, are made up of rollers as mechanisms to separate the two layers of fabrics to be manipulated. The first end-effector has been specifically designed for handling cotton and wool. This end-effector developed by Yamazaki et al [7], consists of two rollers which are surrounded with the same material that is used in commercial products to remove lint and dust from clothes. The operation of this terminal element can either be by grasping, where the two rollers pinch the piece of fabric to be handled or one of the rollers is placed in a corner of the fabric layer where it is activated, and with the same movement of the roller and the properties of the material used, the cotton layer adheres to the roller.

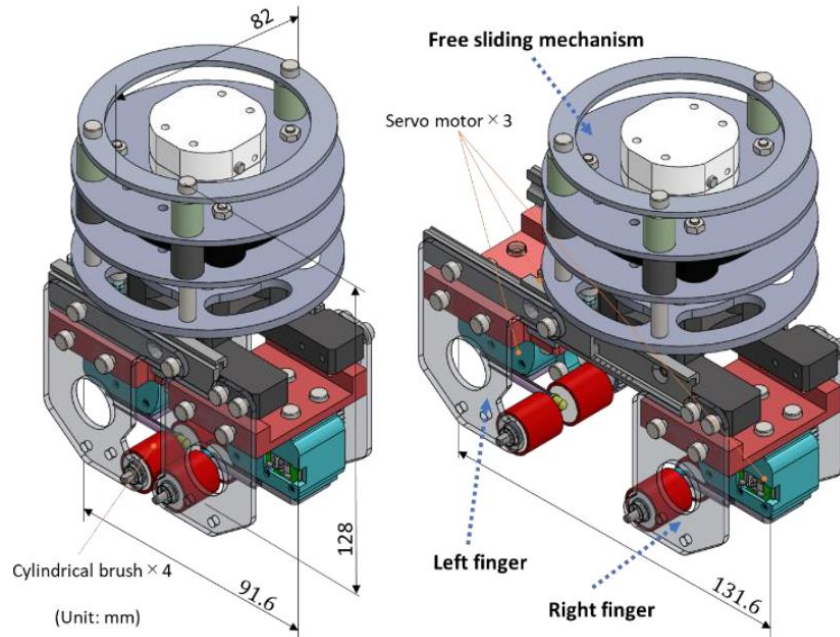


Figure 2.2.1: Overview of the proposed end-effector in [7].

The second end-effector designed by Yuan et al [8] was not designed for the manipulation of soft objects, but to perform in-hand manipulation trajectories to develop an imitation learning-based policy that was able to interpolate between learned trajectories to arrive at depositing the objects in new locations. This gripper consists of the use of spherical rollers located at the tip of three fingers of a gripper. These rollers can rotate in all directions as the gripper fingers contain a motor that orients the roller to the desired position and a motor that activates the rollers. This allows a reorientation of the rollers according to the manipulation that is to be carried out and together with the high friction surfaces of the rollers coated with Smooth-On Mold Star 16 Fast silicone they manage to manipulate the layer without the need to use other elements.

These last two designs use an element that we think can be useful, a roller that allows manipulation at the fingertip to simulate the movement of the fingers when we separate layers, therefore we will study in detail how such roller could interact with the different materials.

### 2.3. Materials Research

In this project it is proposed to design a gripper that, through the use of a roller, is capable both of opening surgical bags and of separating two layers of cloth, for this reason, the most suitable material must be chosen to be able to achieve this goal. Not only do we have to choose a material for the roller, but we also must find a material for the other finger of the gripper since once the layers are separated, the gripper must perform its function of grabbing the fabric and

not letting go. For this reason, what we need to achieve is a high adhesion between the clamp and the tissues.

To achieve this adhesion, the chosen material must produce a high friction between it and the fabric. This could be achieved mechanically using materials such as sandpaper or a Velcro-like structure. But these two options are discarded as they can damage the cloth layers. Therefore, what we have to achieve is to modify the friction coefficient between the gripper and the fabrics using materials that have the appropriate properties since the friction coefficient depends on the physical and mechanical characteristics of the materials to be used. A physical characteristic that can be modified is the surface roughness that the roller and finger can have once they have been built. The higher the surface roughness value, the more friction and adhesion we will achieve between the roller and the first layer.

The surface roughness of an object can be modified by physical processes that attack the surface of the object. For example, surface attacks with chemical products, applications of granules, which are usually done by sandblasting, application of sand at high speed against the object's surface. And other processes such as polishing, which are usually used to reduce surface roughness. The modification of the surface roughness of the roller or the finger are discarded for this project since the necessary machinery is not available to apply the sandblasting treatment or to measure the final roughness. In this case, the surface roughness of the clamp should be high enough to have the greatest adhesion of the fabric but not high enough to cause damage to the clothes.

Another characteristic of materials that can vary the friction coefficient is its hardness. When a material has a low hardness, it tends to have a much higher friction coefficient compared to a high hardness material. Therefore, the less hardness the material has, the greater the adhesion it will provide, but this can become a disadvantage, since this adhesion would not only be achieved between the roller and the fabrics, but also all the things that come into contact with the roller, such as dust or lint. This would cause the friction coefficient to decrease over time. The difference between the friction coefficient of materials with high hardness and those with low hardness is due to the fact that materials with lower hardness have a greater contact area since they deform when a force is applied to them.

To begin the search for the most suitable materials for the manipulation of fabrics using a roller, research must be done in which materials are used in the textile industry. Currently, the industries that handle cloth, use rollers for the transportation of the materials and not for the manipulation of clothes. However, these materials used serve as a guide to know which families of materials the research should focus on. There are several companies that are dedicated to covering rollers with materials for the smooth operation of textile factories, for



example the Italian company Textape covers the rollers of machines with natural rubber, synthetic rubber, PVC and Silicon. On the other hand, the Valencian company, Tecno-Caucho Rolls & Covers, uses more than 300 different rubber elastomers to cover the rollers.

Taking into account the materials already used in industry and in the articles discussed in the previous section, and that we must use materials that have high friction coefficients, which implies that these materials must have low hardness, we can conclude that the materials we will have to use for the manufacture of the roller are from the polymer family.

## 2.4. Friction Coefficients Calculations

As mentioned above, with the materials a high friction coefficient must be achieved between the roller and the first layer of fabric to get it to move, however, not only the friction coefficients that exist between the roller and the first layer, but the friction coefficients between the first layer and the second and the second layer and the surface on which it rests must also be taken into account, considering that we will only have two layers.

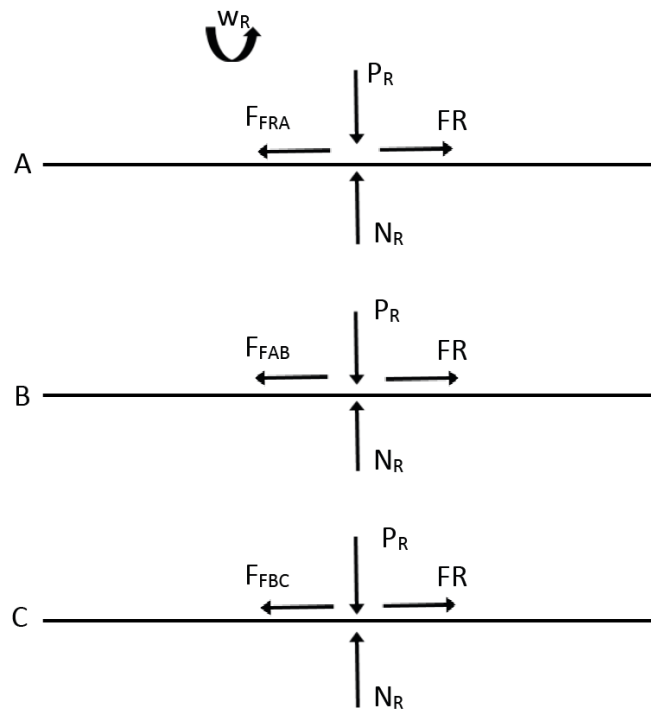


Figure 2.4.1: Diagram of the forces that appear in the layers when pressed with the gripper.

As it can be seen in Figure 2.4.1, when the roller comes into contact with the first layer and is put into operation, different frictional forces appear. To begin with, the layers are named from A being the first to C being the third layer or the surface on which the layers rest. When the roller comes into contact with the layers, a pressure force " $P_R$ " is produced, which is the one exerted by the clamp and which is compensated by the normal force " $N_R$ ". When the roller is put into operation, the frictional force between the roller and the first layer " $F_{FRA}$ " and the force

exerted by the roller to carry away the layer “ $F_R$ ” appear. We can assume that “ $F_R$ ” depends on “ $F_{FRA}$ ” since if “ $F_{FRA}$ ” had a value of 0, no matter how high the force “ $F_R$ ” was, the roller in operation would roll over the layer and it would not be possible to move the first layer. Therefore, to simplify the calculations we discard the force produced by the roller from the calculations.

The objective is to move the first layer and leave the second immobile on the surface, therefore, to move layer A, the frictional force between the roller and layer A “ $F_{FRA}$ ” must have a greater value than the frictional force between layer A and layer B “ $F_{FAB}$ ”. And for layer B to remain immobile in layer C, the frictional force between layer A and layer B “ $F_{FAB}$ ” must have a lower value than the frictional force between layer B and layer C “ $F_{FBC}$ ”.

$$\text{To move A} \rightarrow F_{FRA} > F_{FAB} \quad (\text{Eq.2.4.1})$$

$$\text{To not move B} \rightarrow F_{FAB} < F_{FBC} \quad (\text{Eq.2.4.2})$$

Friction forces are determined by the normal force which is the reaction of the applied force and the friction coefficients between the two materials that are in contact. Therefore, we can develop the previous equations by leaving them as a function of the normal forces and the friction coefficients.

$$N_R \mu_{RA} > N_R \mu_{AB} \quad (\text{Eq.2.4.3})$$

$$N_R \mu_{AB} < N_R \mu_{BC} \quad (\text{Eq.2.4.4})$$

As it can be seen in equations (Eq.2.4.3) and (Eq.2.4.4), the normal force “ $N_R$ ” in all layers is the same, therefore, we can disregard the normal force and compare only the friction coefficients as can be seen in equation (Eq.2.4.5).

$$\mu_{RA} > \mu_{AB} < \mu_{BC} \quad (\text{Eq.2.4.5})$$

Finally, we can conclude that the proper operation of the clamp will only depend on the friction coefficients between the materials. In order to achieve this, materials must be found that satisfy equation (Eq.2.4.5), where the friction coefficients between the roller and the first layer must always be higher than the coefficients between the first two layers and the coefficients between the finger and the second layer must also be higher than the coefficient between the first and the second layer.

All what has been explained in this section are calculations made from hypotheses that must be verified using experimental methods that will be explained in section 3. Experimental Development. Another thing that must be verified through experimentation and cannot be done through calculation is the difference between “ $\mu_{RA}$ ” and “ $\mu_{BC}$ ”. With the equations that have been described, it is not possible to know if they must have the same value or if one must be



greater than the other, but we have the hypothesis that as seen in equation (Eq.2.4.6), at least, the “ $\mu_{BC}$ ” must have a higher value than “ $\mu_{RA}$ ”, as if not, when the roller came into contact with the layer B, it will also carry it away as the coefficient would be higher.

$$\mu_{BC} > \mu_{RA} \quad (\text{Eq.2.4.6})$$

## 2.5. Materials Choice

Based on the characteristics discussed in section 2.2 Materials Research, a list of potentially useful materials for making the gripper has been developed. This list includes the materials used in the articles discussed in section 2.1 Background. It has been seen that the hardness of these materials varies from Shore 30A to Shore 80A. Shore A is the scale used to refer to the hardness of polymers. These urethane-based materials must also be added to those previously tested by the IRI technician. These materials are also urethane-based elastomers with hardness from Shore 10A to Shore 30A. Despite having the necessary characteristics, they deteriorate a lot after a long period of time. Over time, these materials end up having a dark colour, and a significant amount of dust adhered to them, which is difficult to clean and reduces the adhesive properties of the materials. Therefore, they are discarded.

Observing objects from everyday life, it was decided to add styrene to the list, belonging to the group of elastomers, these are materials used in the manufacture of mobile phone covers that have non-slip surfaces among other objects. Another material is paraffin wax, which is used to coat surfboards to prevent your feet from slipping. This is discarded because of the ease with which any substance that comes into contact with it adheres and the difficulty with cleaning it. It is usually removed from the tables and replaced with new wax.

Other materials that have been taken into account are silicones which also belong to the group of elastomers and latex, used in the textile industry to cover rollers. In our case, we want to use the latex used in the coating of clothing surfaces such as soles of socks and other objects to prevent them from slipping. Finally, in order to use the resources that the IRI has, it is proposed to use a resin which can be 3D printed.

Once the list has been made, it is decided to test six materials with different characteristics, the non-slip latex, two silicones with different hardness, Ecoflex with a hardness of 00-50 which is lower than the Shore A scale and Dragon Skin 30 with a hardness of Shore 30A. These two silicones are chosen as they are used in the coating of prostheses for the simulation of human skin. It is also decided to test the Flexible Resin 80A which has a hardness of Shore 80A. And finally, the other two materials that are decided to be tested are Ensoft SD-161-30A and Calprene 411. Both are elastomers used for the manufacture of hand tool handles. However, these two materials could not be tested due to a lack of supply from the companies contacted.

### 3. Experimental Development

This section of the project will discuss the two experiments designed and carried out to determine the friction coefficients between the materials chosen in the previous section 2.4 Materials Choice and the fabrics with which we want to work. These fabrics include surgical bags, gloves, clothing used by doctors and clothing belonging to a set of household clothing. The second experiment that will be carried out to determine which is the most suitable materials to use for the manufacture of the roller.

#### 3.1. Friction Coefficient Experiments

Between two materials there are two friction coefficients, the static coefficients, and the dynamic coefficients. The first is the coefficient that the materials have until the moment they start to move when a force is applied to them. The second coefficient is the one they have once they are already in motion, normally static coefficients tend to have higher values than dynamic coefficients. For our study, since what we want is to achieve the movement of the first layer but not that of the second, what we are interested in knowing is the static friction coefficients between the different materials.

To determine these coefficients, an inclined plane constructed from two wooden slats of sizes 55x16mm and 35x26mm and a hinge, a 1kg diver's weight and different fishing leads that vary from 18g to 100g have been used. A pulley, string and a bag which acts as a container for the leads have been used as seen in Figure 3.1.1. Finally, the angles have been measured with an electronic protractor X000ZX4FUR from Preciva. With these materials three studies are carried out with which three friction coefficients are obtained and finally by averaging the three, the static friction coefficient between two materials is obtained. The basis of the three studies is the same, one of the materials is placed on the surface of the plane and the other on the base of the diver's weight and the inclination angles of the inclined plane and the weights used are measured.



Figure 3.1.1: Photograph of the inclined plane constructed with the materials mentioned.

All the calculus development can be seen in Annexe A. The first study is performed with the body (M) at rest on the inclined plane and the angle of inclination is increased until the body leaves the rest position. With this angle ( $\alpha$ ) and the equation (Eq.A.3), the first friction coefficient is calculated.

$$\mu = \tan \alpha \quad \text{Eq.A.3}$$

The second study is carried out with a greater angle of inclination ( $\beta$ ) than the first study, to ensure that the body (M) is already in motion from the beginning. The body is tied with a cord that is passed through the pulley and to the other end of which an object holder is tied to which weight is gradually added until the body (M) is completely stopped. Then with the angle of inclination ( $\beta$ ), the weight of the body (M) and the total weight added to the carrier (m), the second friction coefficient is calculated using the equation (Eq.A.6).

$$\mu = \frac{M \sin \beta - m}{M \cos \beta} \quad \text{Eq.A.6}$$

Finally, for the third study, the same angle of inclination is used as that used in the second study, the objective of this study is not to leave the body (M) at rest, but to keep adding weights to the object holder until the body (M) slides in the direction of the pulley, up the inclined plane. And with the measurements of the angle ( $\beta$ ), the weight of the body (M) and the weights used ( $m'$ ), the third friction coefficient is calculated using equation (Eq.A.9). Once the three coefficients have been calculated, an average is made and the resulting static friction coefficient is obtained, which is used to make comparisons between the different materials.

$$\mu = \frac{m' - M \sin \beta}{M \cos \beta} \quad \text{Eq.A.9}$$

In order to be able to study the coefficients of the roller materials, the mold that can be seen in Figure 3.1.2 is developed for the realization of a piece with the shape of the diver's weight. This mold is only used for Ecoflex, DragonSkin and Latex materials. This mold has been designed with the SolidWorks software, it consists of three pieces which have measurements approximately 0.5mm larger than the diver's weight used in the studies since this must be placed inside the piece. Once designed and printed in 3d, the interior of the mold's pieces is covered with a release agent, in our case we use Vaseline to facilitate the extraction of the final piece once it has been cured.

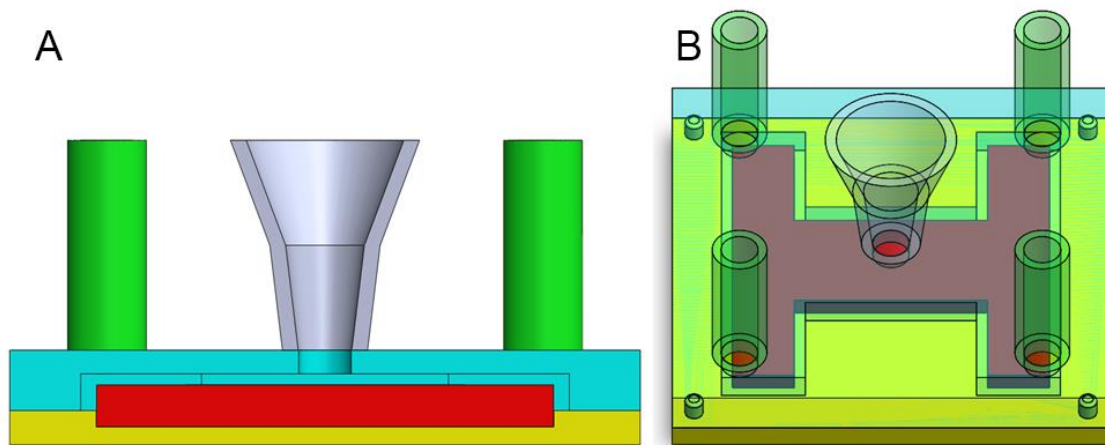


Figure 3.1.2: A) Section view of the mold showing the three pieces with different colours, the funnel and the chimneys. B) View of the mold with the lid, chimneys and funnel transparent to see inside the mold.

The product mixture is prepared with 50-50 amounts of the product and a curing agent supplied by the same company. Finally, once the material is inside the mold, it is placed inside a vacuum pump for 5 minutes at a pressure of 0,9 bars to ensure the elimination of air bubbles inside the mold that could cause defects in the piece. Once the 5 minutes have passed, the pump is opened to leave the material at ambient pressure and the molds are left for the time necessary for a good curing of the materials, in the case of the Ecoflex it is left for 3 hours and the DragonSkin is left 16 hours at rest.

The latex, having a base of water, cures by air, therefore it must not be mixed with a curing agent and when deposited in a closed mold in which air only enters through the funnel and chimneys, it is left to rest inside the 3D printer at a temperature between 40°C and 60°C to evaporate the latex base. The way to deposit the latex inside the mold is different than the other materials because the latex has a much higher viscosity and the spread inside the mold is not uniform. For this reason, the latex is first placed at the base of the mold, then the mold is closed and finished filling through the funnel and chimneys. Finally, since the 80A resin is

printable, the mold is not used, but through the same software, a piece identical to the piece obtained through the molds is designed.

### 3.1.1. Results and Discussion

All the collected data with the inclined plane and performing the calculations to determine the friction coefficients can be found in Annex D. It can be observed that between the different textile layers, the friction coefficients vary considerably, with plastics and papers being those of lowest value and cloth (small towel and waffle rag) with non-uniform rough surfaces the highest. These coefficients calculated between the different layers are the starting point for the comparisons of the different coefficients calculated between the layers and the chosen materials. As has been shown in the equations from the Annex A, the coefficients between the layers are the ones that will mark the values that the other coefficients must have.

It should be noted that all the coefficients calculated between the gloves, including both the short and the long ones, and the other materials, are not exact values due to the type of materials from which they are made. The gloves are made of natural rubber which has a great elastic capacity, this has meant that on many occasions, instead of moving the body M, what moved was the lower layer located on the surface of the inclined plane despite having it attached.

It can also be observed that the coefficients obtained between the layers and the surface on which they rest are of a considerably lower value than the coefficients obtained between the different layers. And it must also be taken into account that the surfaces on which the different hospitals keep the fabrics, we can not ensure or modify the friction coefficients. This assumes that the designed gripper would never be able to separate two layers of cloth. Therefore, it must be taken into account at the time of design, to develop a finger that has a part made with a material that, when it comes into contact with the layers, has a high friction coefficient.

As expected, the material with the lower hardness value (Ecoflex) is the one that has obtained higher friction coefficients compared to the rest. What was not expected is that the DragonSkin material obtained coefficients lower than those of the 80A resin, since this has a higher hardness than DragonSkin. This may be due to the difference between the pieces created with the mold and the part printed with resin as the surface quality is not the same. In the pieces created with molds, on the surface that comes into contact with the plane, there are the marks left by air bubbles and the leftover material that has remained inside the chimneys and the funnel that despite having removed it with caution, a non-uniform surface has been left as can be seen in Figure 3.1.1.1.



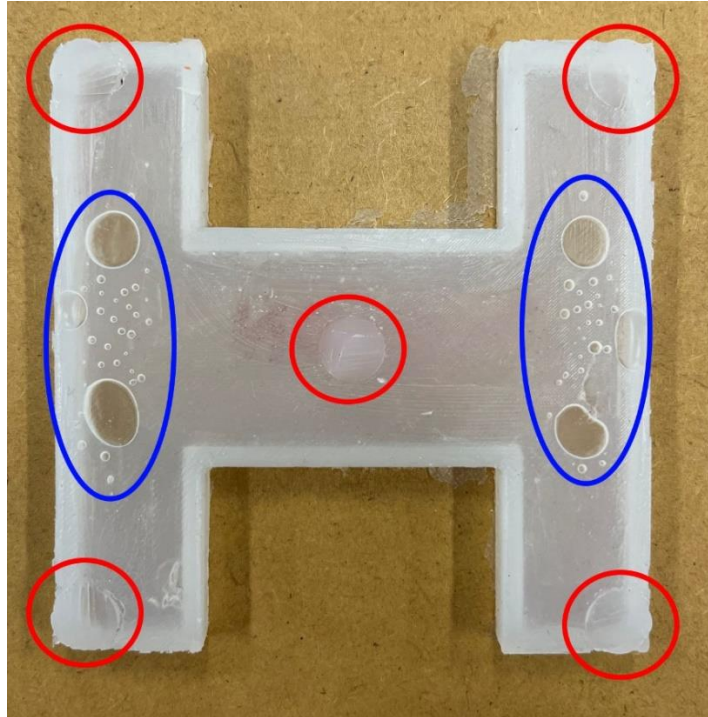


Figure 3.1.1.1: DragonSkin piece image where the leftover marks (red) and bubbles (blue) can be seen.

Given the results obtained, the material that will be used to cover the gripper finger is Ecoflex, as it is the material with the highest coefficients. According to the equations in section 2.4 Friction Coefficients Calculations, if a material with lower coefficients is chosen, as is the case with latex, a material with lower coefficients than latex should be used for the roller. Because on the contrary, when the roller came into contact with the last layer, even though it is touching the latex, it would be carried away by the roller since the friction coefficients between the roller and the layer would be greater than those of the layer and the latex.

### 3.2. Test-bench Experiments

This section of the project describes the development of the experiment carried out to determine which of the four materials is the one that works best when separating two layers of cloth and which is the most successful, which of the four rollers is the one that can be used with more materials. In order to carry out this experiment, it was decided to design, using the SolidWorks software, a test bench with which the different rollers can be tested, and the force applied by the roller on the layers can be measured. The bench is divided into three large parts that include several parts each, the first designed part is the one that simulated the finger of a gripper where the tip houses a roller that can be easily exchanged. The second part of the test bench that has been designed is the base, which includes the accommodation of the finger and the mechanism to move it. Finally, the last part is the rocker which has been designed to be able to measure the pressure forces applied on the cloth.

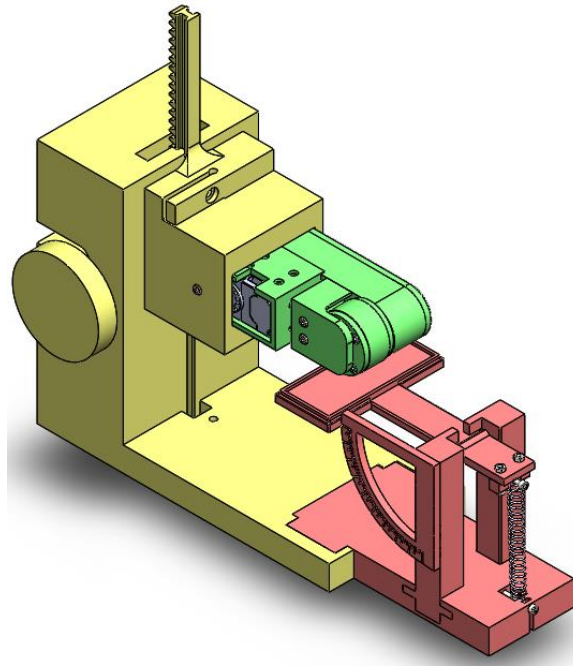


Figure 3.2.1: Test-bench's isometric view. In yellow it can be seen the base, in green the finger and in red the rocker.

The design of this bench has had many variations throughout the project due to factors such as the dimensions of the parts that had to be purchased, such as the motor or the toothed belt, since everything is custom designed and the slightest change in the dimensions of one of the pieces caused the resizing of the other pieces. Other factors that have influenced the variations are assumptions that have been made and that, once the test-bench was finished, were found to be wrong and some parts had to be redesigned. An example is the method used to measure the pressures exerted by the finger in which a linear movement of a spring could not be achieved, which meant an inaccurate calculation of the force.

For the design of the finger, it is decided to use a system of pulleys to transmit the moment of the motor to the roller, achieving a certain distance between the roller and the motor, preventing the roller from having interference in its operation. As it can be seen in Figure 3.2.2, the finger consists of two T5 pulleys with 18 teeth taken from the GrabCAD website which have been modified to be able to incorporate them into the design. One of the pulleys is attached to the motor with 8 M2x12 screws and rests on the finger base plate which houses two bearings 638/3 one for each pulley. The motor is the XM430-W350-R servo motor from Dynamixel Robotis, which can be controlled through the Dynamixel Wizard 2.0 software that has a simple and easy-to-use control interface and allows the control of the servo motor through programming with codes in various languages such as Python or Matlab.

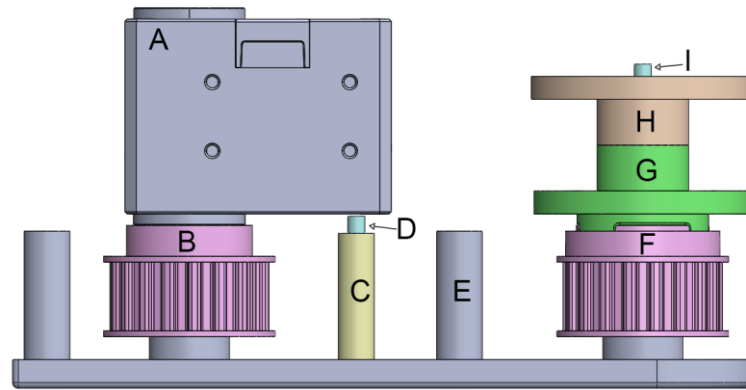


Figure 3.2.2. Internal finger's mechanism on the base plate. A) Engine. B) Engine Pulley. C) Tension Roller. D) Tension Roller Rod. E) Base Plate. F) Roller Pulley. G) Cap Part 1. H) Cap Part 2. I) Roller Rod.

The second pulley is modified to be able to fit with the roller and transmit the engine torque. It is designed with three housings in which three teeth that protrude from the roller are placed. This union tries to imitate the mechanism of a gear. This pulley is traversed by a 3mm diameter and 52mm long shaft. This prevents the fit between the roller and the pulley from receiving shearing stresses when the roller presses the layers and serves to hold the entire assembly in place when the roller is changed. A 5mm diameter roller is incorporated between the two pulleys, which has a core consisting of a 3mm diameter rod. The function of this roller is to tension the T5 belt to prevent its teeth and those of the pulleys from sliding and that there is no proper functioning of the mechanism.

All the internal mechanism of the finger rests on the base plate and is covered by a case in which the motor housing is incorporated, which has been designed with the right measurements so that the engine is fitted and not have unwanted movements caused by the general bench movement. This housing also incorporates the hole for a nut which is used to fix the finger inside its housing. Finally, there is an upper piece to cover the side of the roller and which, together with the built-in bearing, serves as a support for the shaft that goes inside the roller and the pulley.



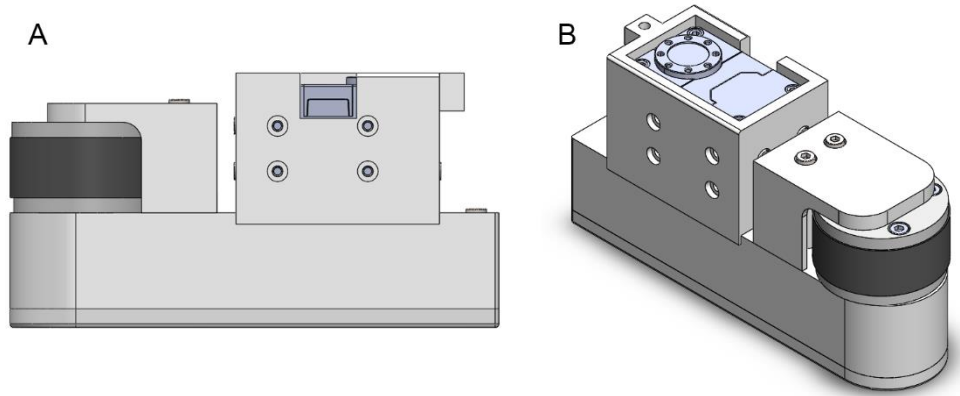


Figure 3.2.3. A) Finger lateral view. B) Finger isometric view.

The base of the test-bench consists of an L-shaped structure in which a modified rack fits to accommodate the previously mentioned finger and which contains a fit that serves to join it with the rocker. Inside the “L” it can be found the mechanism that complements the rack to move the finger vertically. This mechanism has been designed in three parts as it is subjected to torsional and bending forces. Since 3D printers print layer by layer, depending on the orientation of the piece at the time of printing, it may have vulnerable points to external forces. Therefore, by designing this mechanism in three pieces, these weak points disappear.

As it can be seen in Figure 3.2.4, the first part is a toothed wheel with 25 teeth which has the same pitch as the rack. This wheel is set in motion manually through a handle located on the side of the structure, this being the second part of the mechanism. The last piece is a shaft that joins the toothed wheel to the handle and rests at two points on the structure. This is a cylindrical shaft that has been given two hexagonal extrusions to be able to fit with the toothed wheel and the handle to be able to transmit the turning moment.

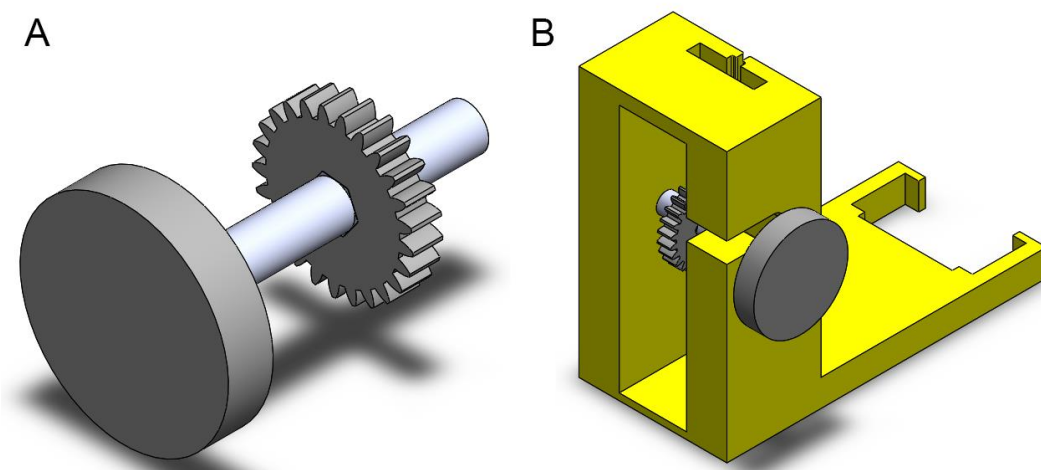


Figure 3.2.4: A) Mechanism Isometric view. B) “L” structure with the where the mechanism can be located.

The rack that meshes with the toothed wheel has an H-shaped structure that allows it to be fitted with the structure that has a guide along which the rack runs. The housing of the finger has also been added, which has the exact measurements of this to prevent that when the roller comes into contact with the surface, due to the reaction forces, the finger does not have oscillatory movement, which would cause errors in the pressure force measurements.

As seen in Figure 3.2.5, the housing contains a hole in which the screw that fixes the finger with the rack goes and there is also a tab that serves to lock the rack at the desired height when changing the roller or the layers. What this tab does is reduce the hole diameter through which the shaft passes, which also serves as an additional guide for the rack. Finally, once this part of the test-bench was printed and assembled, it was observed that this locking mechanism is not needed since there is enough friction between the rack and the guide of the structure for the rack to remain in suspension.

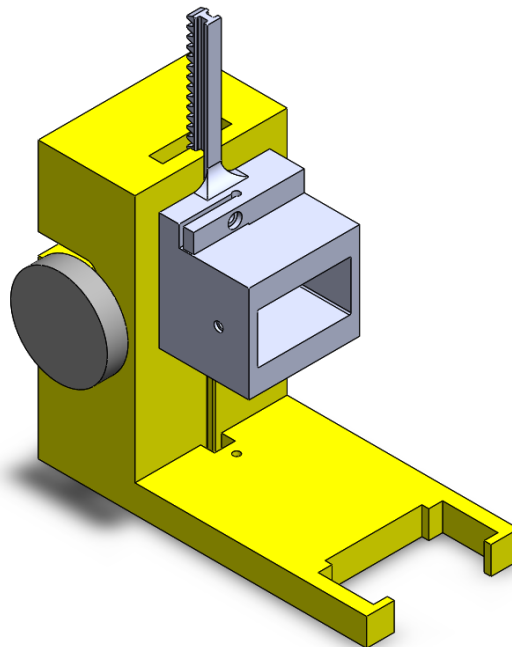


Figure 3.2.5: Base's isometric view.

The third part of the test-bench is the rocker, with which the application forces of the roller are measured. This is achieved thanks to the Hooke's Law and the Law of the Lever explained in Annex B, since on the opposite side of the roller application, there is a spring which extends linearly when the finger applies pressure. A protractor has been incorporated into the rocker to measure the angles, and by means of trigonometry, measure the spring's elongation. The rocker, like the rack drive mechanism, has also been designed in several parts to avoid weak points. First, the part that fits into the "L" structure and acts as the base of the pillars has been designed, and where one of the ends of the spring is connected through a screw and a nut of

metric 3. This allows the spring to be tensioned depending on the forces that you want to apply, the more tensioned the spring, the more force the finger will exert.

Next, the pillars on which the rocker arm rests, were designed. Both pillars have an extrusion that serves to reduce the turning range of the arm. One of the pillars is where the protractor is incorporated, designed so that the measuring point is the axis of rotation of the rocker arm. The arm has been designed in the shape of a "T" to ensure that the entire surface of the roller is in contact with the fabrics. A piece has been added to the other end of the arm that together with an M3 screw and nut serves to connect the spring to the rocker arm. Finally, given that the surface of the arm with the layers has a low friction coefficient, a last piece has been designed that fits exactly with the arm, which acts as a container to deposit the desired material to increase the coefficients. In our case, this piece has been filled with Ecoflex since it is the material with the highest friction coefficients.

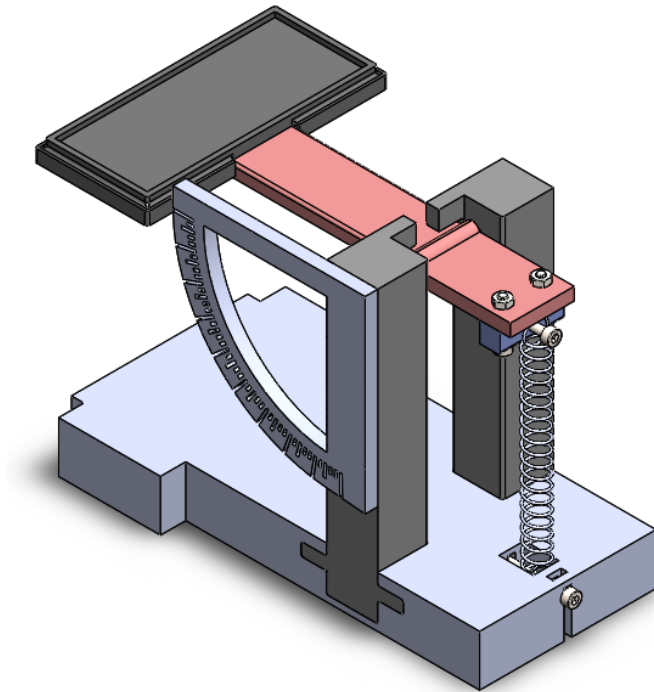


Figure 3.2.6: Rocker's isometric view.

The rollers consist of two pieces that perform the function of the core of the roller that serves to connect the roller with the finger pulley and transmit the movement of the latter. These two pieces are joined with four M3 screws and nuts which at the same time serve to reduce the tensions caused by the turning of the core. For the manufacture of the rollers, as with the friction coefficient experiments, a mold is designed which can be seen in Figure 3.2.7. The mold consists of three 3D printed parts and four rods that are removed once the material has been cured. Once these

rods are removed, there are four holes left in the roller which screws are passed to join the core of the roller. Ecoflex and DragonSkin rollers are made with this mold. Due to the characteristics of latex, the roller of this material cannot be manufactured using the mold as the result is a defective roller. In this case, a one-piece core is designed in which a layer of latex is applied to the surface. And finally, a roller identical to the one obtained with the mold is also designed to be printed with the 80A resin.

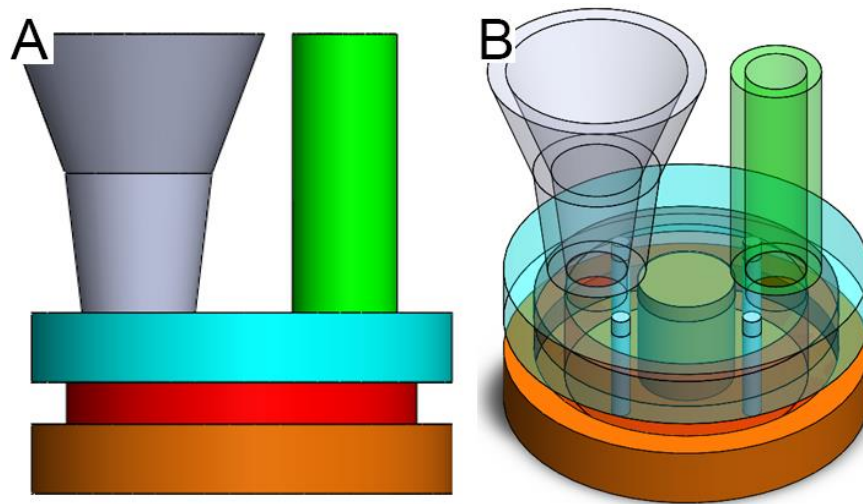


Figure 3.2.7 A) Section view of the mold showing the three pieces with different colours, the funnel and the chimneys. B) View of the mold with the lid, chimneys, and funnel transparent to see inside the mold.

### 3.2.1. Test-bench Operation

To start testing with the bench, once all the parts have been assembled, the servomotor is connected to the computer via a Dynamixel USB adapter and powered by a 12V power supply plugged into the Dynamixel power adapter which is also connected to the USB adapter. Once everything is connected, the software is put into operation and the motor's operating mode is selected. In our case, the engine speed control is used to perform the tests, the engine speed range is from -200 to 200 units, one unit is equivalent to 0,229 rpm. We work with -50 units, which is a rotation speed of 11,45 rpm counterclockwise.

The motor is activated once the layers have been placed on the rocker and the finger has been lowered to the desired position. The range of angles used for the tests is from 0° to 35° changing every 5 degrees. Although the finger can go down to an angle of 40°, this range has been used in order not to force the rocker elements and to facilitate the operation of the bench. As mentioned above, if high forces are to be applied, the spring can be tensioned. It has also been decided to change every 5 degrees since the contact distance between the roller and the

rocker arm at the centre of the rotation of the arm varies by less than a millimetre for each angle. For example, from  $0^\circ$  to  $1^\circ$ , the distance goes from 83,14mm to 83,17mm.

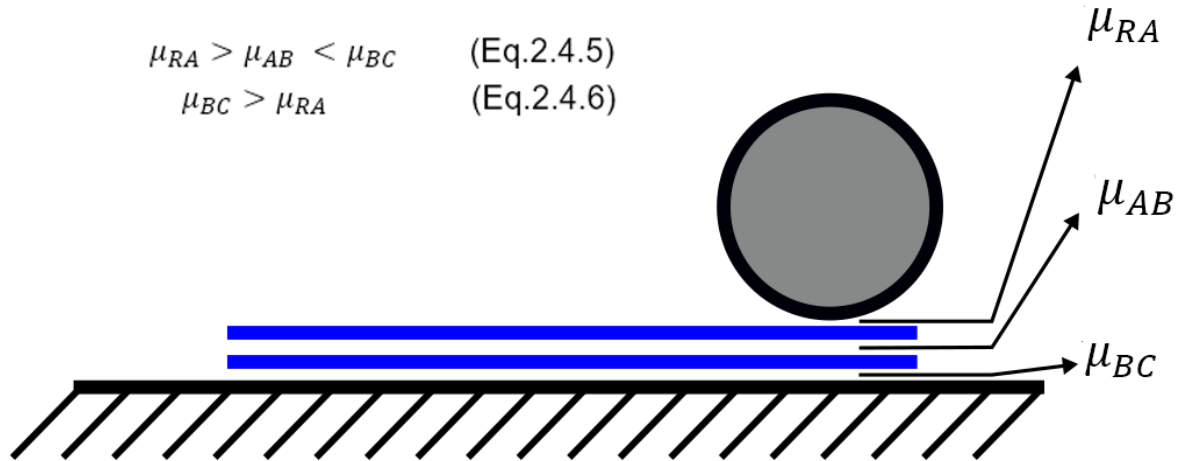
Three tests are performed for each angle, and it is determined whether the material used for the manufacture of the roller meets expectations and is able to separate the layers. This procedure is carried out for each of the fabric materials available and for each roller, therefore a total of 1536 tests are carried out.



Figure 3.2.1.1: Image of the complete test-bench with the connections of the USB and Power adapters to the motor.

### 3.2.2. Results and Discussion

All the detailed results of the experiments can be found in Annex E graphs where each point represents the test done with each force and material. The positive test results are represented with the colour blue and the negative test results are represented with the red colour. Most of the cases we have tested follow our hypothesis, shown in Fig. 3.2.2.1. However, we have detected evidence where the equations (Eq.2.4.5) and (Eq.2.4.6) are not fulfilled but nevertheless the tests have had positive results and vice versa. That means that our hypothesis is only true under certain conditions, and in this section, we will analyse these conditions, that we found can be two: the force exerted by the roller or inaccuracies in the friction coefficient measures.



$$\mu_{RA} > \mu_{AB} < \mu_{BC} \quad (\text{Eq.2.4.5})$$

$$\mu_{BC} > \mu_{RA} \quad (\text{Eq.2.4.6})$$

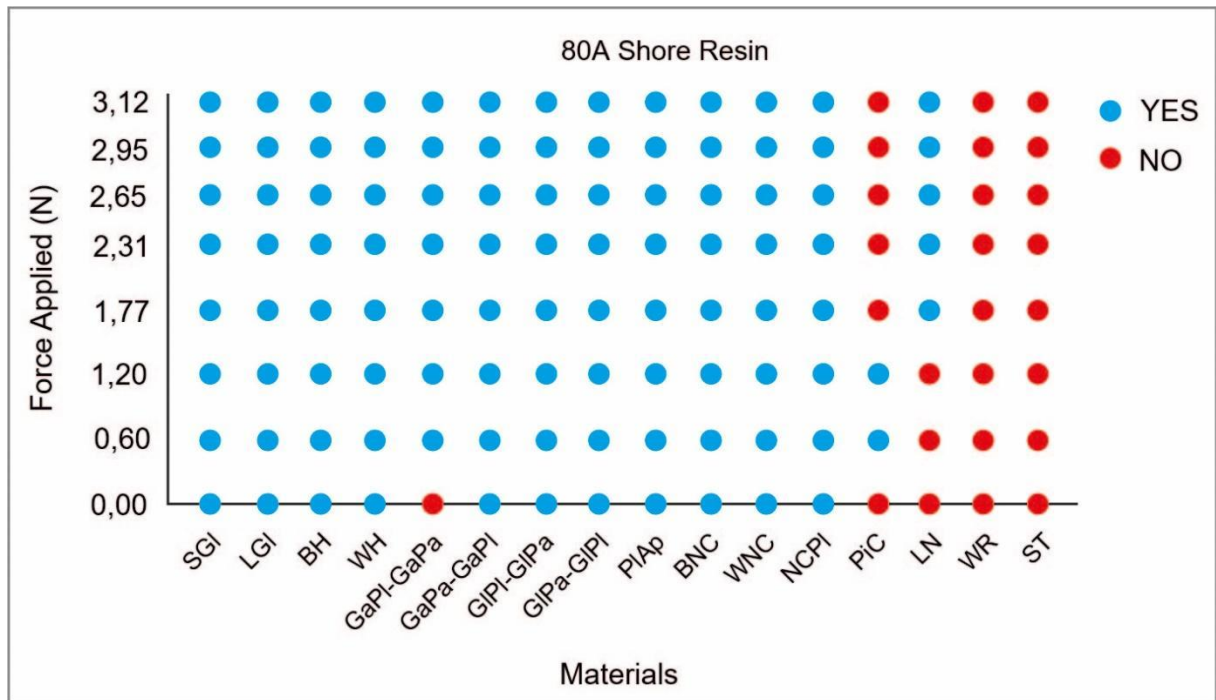
Figure 3.2.2.1 Schematic of the roller and layers where the coefficients can be seen, with a reminder of equations (Eq.2.4.5) and (Eq.2.4.6)

For the case where the condition is fulfilled but the test is negative, we have noticed another important factor is the pressure the roller is exerting. In this case two things can happen: either the roller is not exerting enough force or too much force. When the roller is not exerting enough force none of the layers move, this is the case of the roller made of latex and of the Small Towel where the coefficients are  $\mu_{RA}=0.93$ ,  $\mu_{AB}=0.40$  and  $\mu_{BC}=1.33$  and as it can be seen in the annexes, the tests do not give a positive result until 1.20 N of applied force are reached.

When the roller exerts too much force, both layers move together, this is the case for the roller made of DragonSkin and the paper of the surgical gloves bag (GIPa-GIPI) where the friction coefficients are  $\mu_{RA}=0.69$ ,  $\mu_{AB}=0.33$  and  $\mu_{BC}=0.97$  and it can be seen in the results, from 2.65 N of applied force, the roller does not work correctly.

As can be seen in the Graph 3.2.2.1, the rollers work correctly within a range of pressure forces. In some materials this interval has been determined, but there have been other intervals in which the maximum force has not been determined or the minimum force has not been applied, since the tests have been carried out with a maximum of 3.12 N. In the graph it can clearly be seen the determined range of forces of the case of the Pillowcase where it has a minimum force of 0.60 N and a maximum of 1.2 N. Graph 3.2.2.1 shows the results obtained with the 80A resin roller, which will be used for the manufacture of the gripper as it is the one that has obtained the best results.





Graph 3.2.2.1: Results of the operation of the printed roller with 80A resin. In blue are the tests carried out successfully and in red those where the roller has not been able to separate the layers.

For the case where the condition is not fulfilled but the tests are positive, we think this may be due to inaccuracies in the computation of the friction coefficients. A case would be that of the 80A resin roller with the White Hat, where the coefficients are as follows;  $\mu_{RA}=0.89$ ,  $\mu_{AB}=0.37$  and  $\mu_{BC}=0.84$ , where the equation (Eq.2.4.5) is fulfilled but not the equation (Eq.2.4.6).

Carrying out these tests, we have also come to the conclusion that the roller cannot be applied right at the point where the layer begins but must be located at a distance of at least 1mm from that point. If it is not placed at least 1mm apart, the roller takes the two layers at the same time, this is because the roller is initially already in contact with the two layers, and the pressure exerted does not fall on the layers but on the platform as can be seen in Figure 3.2.2.2.

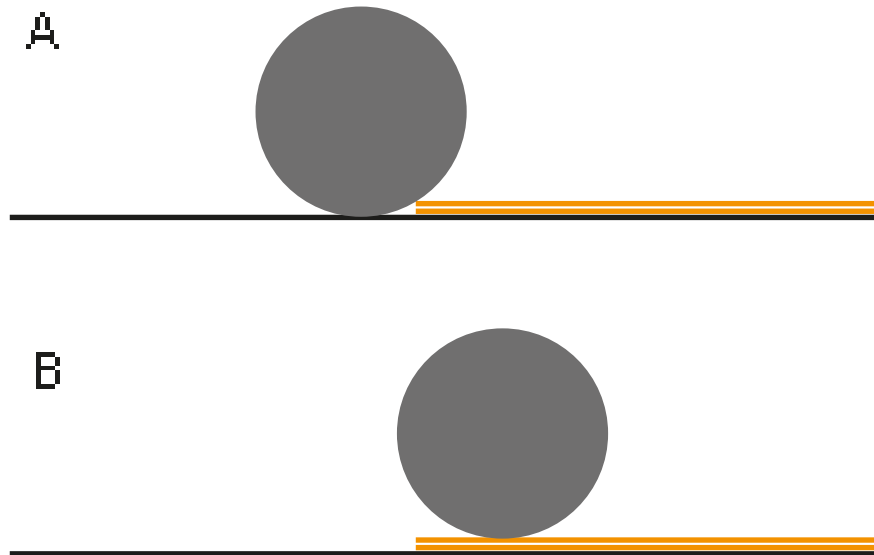


Figure 3.2.2.2: A) Schematic of bad positioning of the roller. B) Schematic of the correct positioning of the roller.

Finally, an important factor to consider is the time that the roller remains in operation, since depending on the fabric and the pressure exerted, the process of separating two layers takes more or less time. There has been tests where the roller has needed more running time to be able to separate the layers. And with the same fabrics it has been seen that by increasing the pressure, the time the roller takes to perform the task is reduced. There have been tests where the roller has been left running longer once it has separated the layers and this has resulted in the last layer being carried away, so when the robot is programmed to perform the task, the time the roller is kept running will have to be controlled.

It was not possible to see the effect of time on the materials since the time elapsed since the manufacture of the pieces can not be considered long enough. However, after performing the 1536 tests, it can be seen a wear mark on the material that covers the rocker arm just where the roller comes into contact with it. It has also been observed that the Ecoflex material is easy to clean if a little moisture is applied to the surface. After carrying out the tests with some cloths such as the towel, lint from it has remained attached to both the roller's surface and the rocker arm's surface.



## 4. Gripper Design

This section introduces the design of the first version of the gripper based on the results obtained from the tests carried out. This design takes into account all the observations made during the experiments, such as the overheating of the engine, which has a maximum working temperature of 80°C. It has also been designed taking into account that we do not want to obtain fingers with high dimensions and weights, since, as seen in previous projects, they would hinder the proper functioning of the robot. For this project, only the fingers of the gripper will be designed. We want to take advantage of the UR5e robot from Universal Robots that we have in the laboratory, which has the interchangeable Hand-E Adaptive grippers with which the fingers can be also exchanged.

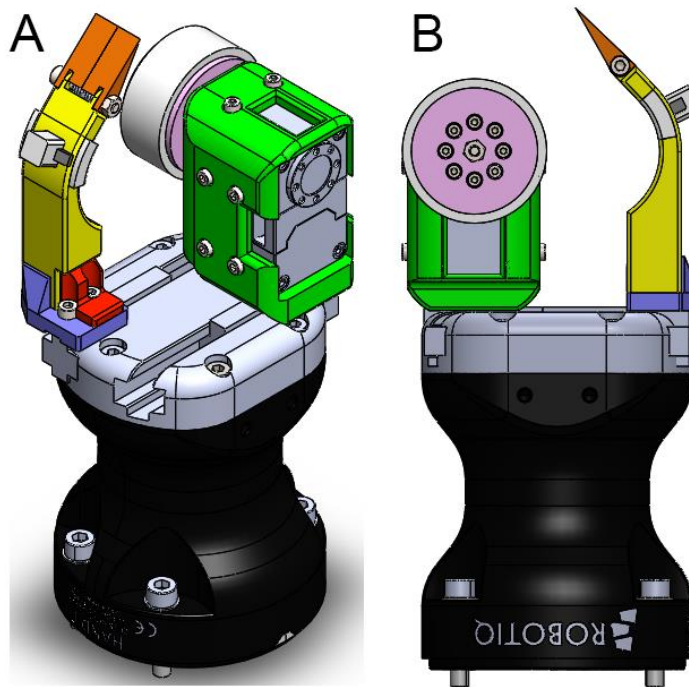


Figure 4.1: A) Gripper's isometric view. B) Gripper's front view.

Therefore, the design has been developed based on the already existing gripper, of which a CAD document has been obtained from the manufacturer's website. Although initially it was wanted to design a gripper with a stationary finger and a mobile finger, due to the short distance of the fingers this has not been possible. If it had been designed with only one mobile finger, the opening of the gripper would have been an inconvenience when working with it. Finally, the gripper consists of two non-independent mobile fingers, in one of the fingers the motor and the roller are housed, and the other finger is where the material (Ecoflex) on which the layers will rest is housed.

Unlike the finger developed on the test-bench, since for the first test we do not need a finger with a large length, it is decided to connect the roller directly to the motor and having seen with the tests that the upper plate that covers the side of the roller is not needed, it has been decided to avoid it in this design to reduce the finger dimensions and avoid unwanted interactions with the layers or other surfaces. What has been designed in a similar way to the test-bench is the engine housing being the only structure of this finger. It has been designed with the exact measurements so that the engine is completely fixed inside, and the number of screw holes has been reduced since it has been seen that by adjusting the housing so much, all the screws that the engine brings to fix it are not necessary. Two slots have been incorporated on each side of the housing to easily plug in the cables. A slot has also been made in the housing base in which the piece of the gripper base will be connected.

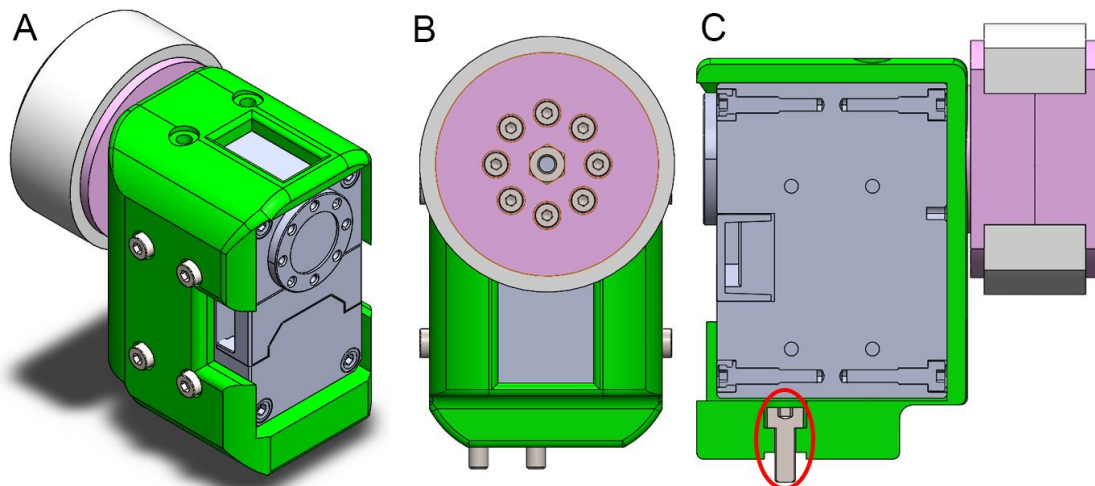


Figure 4.2: A) Finger's isometric view. B) Finger's front view. C) Section view where the base slot and hole for the screw can be seen.

As mentioned above, the maximum temperature at which the engine can work has been taken into account, since with the tests carried out the engine temperature escalated from 25°C to 40°C in a matter of half an hour of interrupted work. And if we want to make the engine work constantly for a certain period of time, the housing must have more openings to be able to dissipate the heat produced by the engine. In this way, a frontal opening has been made, just below the opening in which the roller is inserted and a second opening at the top of the housing. The opening at the back is also maintained so that the engine can be inserted.

In order to be able to assemble this finger, the housing must first be screwed to the piece of the gripper's base, because of how the gripper's base is designed and to avoid developing a finger that overcomes out of the base, the screws must be placed inside the housing. The base of which has been made with sufficient thickness to hide the screws and that they do not collide

with the motor. Next, the engine is inserted and screwed into the lateral sides of the housing and finally the roller is attached to the motor.

To be able to manufacture the roller, a different core from those used for the experimental rollers must be designed, since when the roller is connected directly to the motor, the geometry of the toothed wheel design is not needed. A piece must be developed with a housing for the shaft that comes out of the motor and to also be able to house the screw that joins the two parts of the core. Both pieces that make up the core, like the roller, must have holes through which the screws that fix the roller to the engine must pass.

The second finger of the gripper consists of four parts, the main one being the body of the finger which has a circular shape the size of the roller to achieve the greatest contact once the gripper closes the fingers. This part has also been fitted so that the part containing the Ecoflex material is flush with the surface and does not protrude. This part is fixed to the finger through an extrusion that crosses the body of the finger and contains a hole in which a wedge is inserted to ensure that the part remains completely fixed and has no horizontal movements. As it can be seen in Figure 4.3, at the tip of the finger there is a triangular shaped nail, which consists of two joined pieces whose function is to be placed under the layers of cloth to be able to get them to come into contact with the Ecoflex material to have the last layer adhered to the gripper. A screw and a self-locking nut would be used to attach the nail to the finger. The use of a self-locking nut is chosen to lock the nail to the finger but maintain its movement and to prevent the nut or screw from loosening with the movement of the nail.

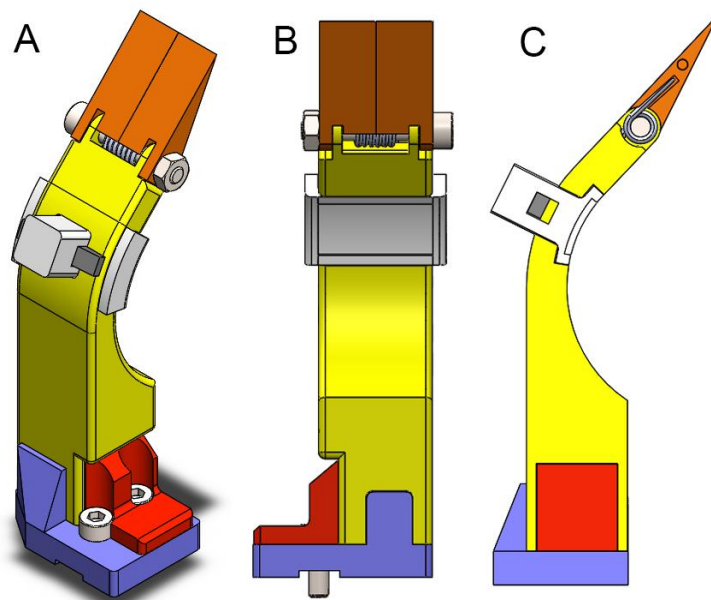


Figure 4.3: A) Finger's isometric view. B) Finger's side view where the base slot can be seen. C) Section view where the spring can be seen.

A spring is housed inside the nail to facilitate the return of the nail to its initial position once the finger is no longer in contact with the surface where the layers are located. Finally, the finger consists of a base that joins it to the base of the gripper. This base has an extrusion that fits inside the body of the finger to hold them together. As with other parts, it is decided to design the base and body of the finger separately to avoid vulnerable points during printing. The base has a slot like the engine housing to fit with the gripper base. A card is also placed at the base, which at the same time is inserted inside the body to reinforce the structure of the finger.

## Conclusions and Future Work

In this project, a study of previous work that already exists related to the task of separating layers has been carried out, with which it has been possible to get ideas of which materials and designs to develop a gripper for the purpose of separating layers. A test bench has also been designed and prototyped to carry out studies with the chosen materials. We have tested 4 materials for the gripper fabrication that have been applied to 15 different fabric objects. A total of 1536 tests have been executed. These experiments allowed us to determine what properties, characteristics, and relationships there must be between the different materials that are to be used and the layers.

The project results allow us to better understand the forces that come into play in the task of grasping individual layers that are piled or folded together. From our initial hypothesis and the results obtained, we have seen that not only the coefficients have to be taken into account, but the force applied also plays a role in the correct roller operation. There is a range of forces where the tests have had a positive result, and not all these ranges have been found, as the maximum force applied has been 3.12 N and there are materials that did not have positive results. However, we have managed to find a pair of materials that, with the cloths and plastics tested, has had the highest number of tests with positive results.

Finally, a design of the first version of the gripper has been made based on the results obtained to perform the layer separation task. In this design, all the observations made during the experiments carried out with the test bench have also been considered.

Despite having carried out the design taking into account many details, in the future the designed gripper must be developed and tested. As it is a first version, once it is manufactured, it will surely have defects and errors which will mean that some of the parts of the gripper will have to be modified. And even a pair of materials that serve to fulfil the task of layer separation have been found, materials with better results and other characteristics can be studied.

Future investigation can be done on finding a way to create a latex roller with the molds used without it coming out defective or look for the necessary resources to make surface modifications to the rollers, an action discarded in this project due to not having the necessary machinery.

## Bibliography

- [1] Xu, Z., Chi, C., Burchfiel, B., Cousineau, E., Feng, S., & Song, S. (2022). Dextairity: Deformable manipulation can be a breeze. arXiv preprint arXiv:2203.01197.
- [2] H. Jiang, X. Jiang, Y. Zhou, H. Chen, P. Li and Y. Liu, "Variable-Friction-Based In-Hand Manipulation of Fabrics Applied to Unfolding Operations," in *IEEE Robotics and Automation Letters*, vol. 7, no. 4, pp. 12259-12266, Oct. 2022, doi: 10.1109/LRA.2022.3216230.
- [3] A. J. Spiers, B. Calli, and A. M. Dollar, "Variable-friction finger surfaces to enable within-hand manipulation via gripping and sliding," *IEEE Robot. Automat. Lett.*, vol. 3, no. 4, pp. 4116–4123, Oct. 2018.
- [4] S. Ku, J. Myeong, H. Y. Kim, and Y. L. Park, "Delicate fabric handling using a soft robotic gripper with embedded microneedles," *IEEE Robot. Automat. Lett.*, vol. 5, no. 3, pp. 4852–4858, Jul. 2020.
- [5] K. M. Digumarti, V. Cacucciolo, and H. Shea, "Dexterous textile manipulation using electroadhesive fingers," in *Proc. IEEE/RSJ Int. Conf. Intell. Robots Syst.*, 2021, pp. 6104–6109.
- [6] Dragusanu, M., Marullo, S., Malvezzi, M., Achilli, G. M., Valigi, M. C., Prattichizzo, D., & Salvietti, G. (2022). The dressgripper: A collaborative gripper with electromagnetic fingertips for dressing assistance. *IEEE Robotics and Automation Letters*, 7(3), 7479-7486.
- [7] Yamazaki, K., & Abe, T. (2021). A Versatile End-Effector for Pick-and-Release of Fabric Parts. *IEEE Robotics and Automation Letters*, 6(2), 1431-1438.
- [8] S. Yuan, L. Shao, C. L. Yako, A. Gruebele, and J. K. Salisbury, "Design and control of roller grasper V2 for in-hand manipulation," in *Proc. IEEE Int. Conf. Intell. Robots Syst.*, 2020, pp. 9151–9158.



# Annexes

## Index

A. Development of Friction Coefficient Calculations .....	40
B. Roller Pressure Forces Calculations .....	42
C. Layers Images.....	44
D. Friction Coefficients Results .....	46
E. Test-bench Results .....	48
<b>F. CAD Exploded View Diagrams and Drawings.....</b>	<b>51</b>
F.1 Mold H Exploded View Diagram .....	52
F.1.1 H Mold Part 1 Drawing.....	53
F.1.2 H Mold Part 2 Drawing.....	54
F.1.3 H Mold Part 3 Drawing.....	55
F.2 Chimney Drawing.....	56
F.3 Funnel Drawing .....	57
F.4 Piece H Resin 80A Drawing .....	58
F.5 Roller Mold Exploded View Diagram .....	59
F.5.1 Roller Mold Part 1 Drawing .....	60
F.5.2 Roller Mold Part 2 Drawing .....	61
F.5.3 Roller Mold Part 3 Drawing .....	62
F.5.4 Rod Drawing.....	63
F.6 Resin 80A Roller Drawing .....	64
F.7 Toothed Latex Roller Drawing .....	65
F.8 Test-bench Exploded View Diagram .....	66
F.8.1 Finger Exploded View Diagram.....	67
F.8.1.1 Base Plate Drawing .....	68
F.8.1.2 Case Drawing .....	69
F.8.1.3 Cap Part 1 Drawing .....	70
F.8.1.4 Cap Part 2 Drawing .....	71
F.8.1.5 Engine Pulley Drawing .....	72
F.8.1.6 Roller Pulley Drawing .....	73
F.8.1.7 Tension Roller.....	74
F.8.1.8 Top Plate Drawing .....	75
F.8.1.9 Roller Rod Drawing .....	76
F.8.1.10 Tension Roller Rod Drawing .....	77
F.8.2 Base Exploded View Diagram.....	78



F.8.2.1 Crank Shaft Drawing.....	79
F.8.2.2 Gear Drawing .....	80
F.8.2.3 Handle Drawing.....	81
F.8.2.4 L Structure Drawing .....	82
F.8.2.5 Rack Drawing .....	83
F.8.3 Rocker Exploded View Diagram .....	84
F.8.3.1 Material Platform Drawing.....	85
F.8.3.2 Pillar with Protractor Drawing .....	86
F.8.3.3 Pillar Drawing.....	87
F.8.3.4 Rocker Arm Drawing .....	88
F.8.3.5 Rocker Base Drawing.....	89
F.8.3.6 Protractor Drawing.....	90
F.8.3.7 Rocker Rod Drawing.....	91
F.8.3.8 Spring Connector Drawing.....	92
F.9 Gripper Exploded View Diagram .....	93
F.9.1 Finger A Exploded View Diagram .....	94
F.9.1.1 Finger A Base Drawing .....	95
F.9.1.2 Gripper's Roller Drawing.....	96
F.9.1.3 Roller Cap Part 1 Drawing .....	97
F.9.1.4 Roller Cap Part 2 Drawing.....	98
F.9.2 Finger B Exploded View Diagram .....	99
F.9.2.1 Cartel Drawing .....	100
F.9.2.2 Finger B Base Drawing .....	101
F.9.2.3 Finger B Body Drawing.....	102
F.9.2.4 Left Tip Drawing .....	103
F.9.2.5 Material Surface Drawing .....	104
F.9.2.6 Right Tip Drawing.....	105
F.9.2.7 Wedge Drawing.....	106

## A. Development of Friction Coefficient Calculations

This section shows the diagrams and equations used to calculate the friction coefficients of the materials. In the first study what we have is a body at rest in an inclined plane like the one shown in Figure A.1, in which it can be observed that at the instant when the body M is at rest, there is the action of the X component ( $P_x$ ) of the weight force (P) and the friction force  $F_F$  in the opposite direction to that of the weight. To determine the coefficient ( $\mu_1$ ) the two forces must be equalized and developed as can be seen in the equation (Eq.A.2).

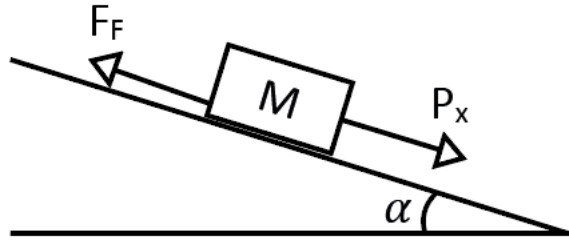


Figure A.1. Force diagram of the first study of the inclined plane.

$$P_x = F_F \quad \text{Eq.A.1}$$

$$Mg \sin \alpha = \mu_1 Mg \cos \alpha \quad \text{Eq.A.2}$$

Finally, having the same weight and gravity on both sides of the equation, they can be eliminated and by isolating  $\mu_1$  the first static friction coefficient is obtained.

$$\mu_1 = \tan \alpha \quad \text{Eq.A.3}$$

In the second study, a second mass (m) comes into play, which is the set of weights added to the object carrier and therefore other forces. When the body M and the carrier objects are connected by a string, a tension force (T) appears as shown in Figure A.2. To determine the coefficient  $\mu_2$  the system presented in the equation (Eq.A.4) has to be resolved.

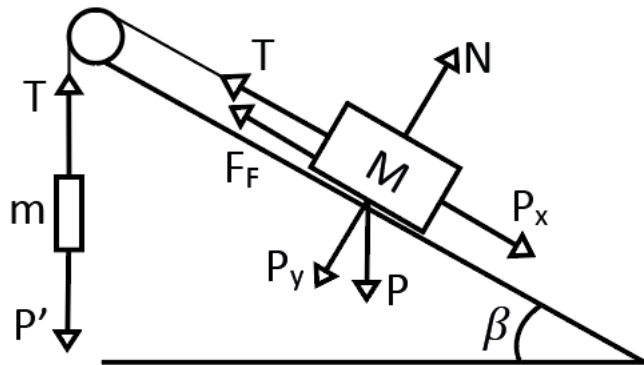


Figure A.2: Force diagram of the second study of the inclined plane.

$$\begin{cases} P_x = T + F_F \\ T = P' \end{cases} \quad \text{Eq.A.4}$$

$$\begin{cases} Mg \sin \beta = T + \mu_2 Mg \cos \beta \\ T = mg \end{cases} \quad \text{Eq.A.5}$$

Finally, substituting the value of the tension (T) and isolating  $\mu_2$ , the second static friction coefficient is obtained.

$$\mu_2 = \frac{M \sin \beta - m}{M \cos \beta} \quad \text{Eq.A.6}$$

In the third study of the friction coefficients, we have the same forces as in the previous study, but the friction force in this case is arranged in the opposite direction, since in this stud the movement of body M is upward in the direction of the pulley. To determine the coefficient  $\mu_3$  the system presented in equation (Eq.A.7) must be solved.

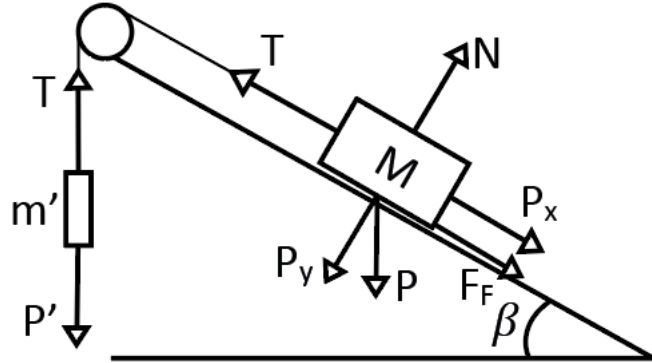


Figure A.3: Force diagram of the third study of the inclined plane.

$$\begin{cases} T = P_x + F_F \\ T = P' \end{cases} \quad \text{Eq.A.7}$$

$$\begin{cases} T = Mg \sin \beta + \mu_3 Mg \cos \beta \\ T = m'g \end{cases} \quad \text{Eq.A.8}$$

Finally, the tensions (T) are equalized and  $\mu_3$  is isolated to obtain the third static friction coefficient.

$$\mu_3 = \frac{m' - M \sin \beta}{M \cos \beta} \quad \text{Eq.A.9}$$

Once the three friction coefficients from each of the calculated studies are obtained, the arithmetic mean of the three is performed as shown in equation (Eq.A.10).

$$\mu = \frac{\mu_1 + \mu_2 + \mu_3}{3} \quad \text{Eq.A.10}$$

## B. Roller Pressure Forces Calculations

This section of the project shows the diagrams and equations used to determine the pressure forces exerted by the roller ( $F_R$ ) on the layers. As a basis for the calculations carried out, it has been used the Hooke's Law and the Law of the Lever. With the Hooke's Law, the force exerted by the spring ( $F_S$ ) is related to the elongation it undergoes when the roller comes into contact with the rocker arm. And with the Law of the Lever, through the moments, the force exerted by the spring is related to the force exerted by the roller. Initially the spring is in its state of rest having an initial length ( $L_0$ ) and an inclination angle ( $\alpha$ ) of  $0^\circ$ .

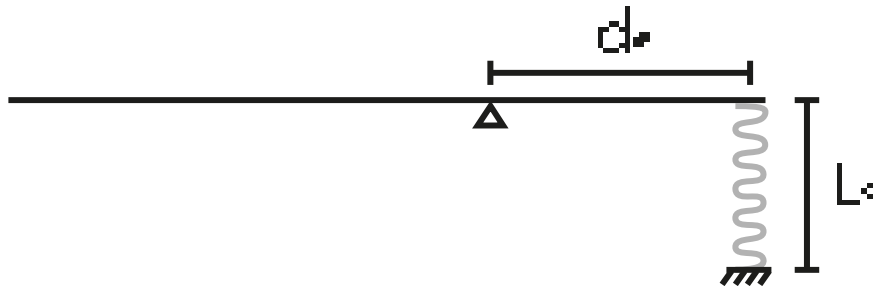


Figure B.1: Schematic of the system at rest.

Once the roller comes into contact with the rocker arm, the inclination angle increases, causing an elongation of the spring, therefore the spring has a new length ( $L_f$ ). The distance at which the spring is located with respect to the tilting point of the rocker arm ( $d_s$ ) is fixed and has a value of 36mm. And the distance at which the roller is from the pivot point ( $d_R$ ) varies according to the inclination angle. Every  $5^\circ$  of inclination, the distance varies by approximately 1mm.

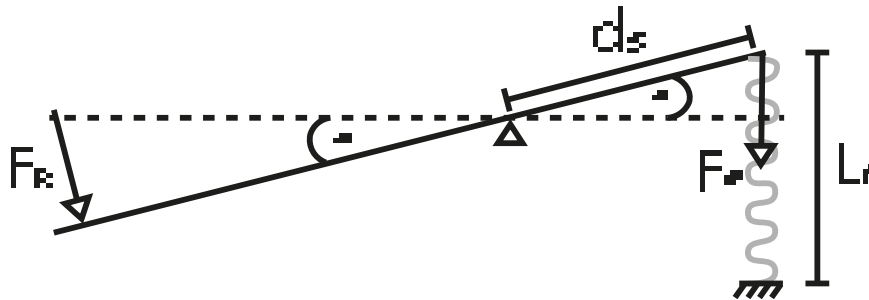


Figure B.2: Schematic of the system once a pressure force has been applied with the roller.

Applying Hooke's Law, equation (Eq.B.2), the force exerted by the spring is determined. The spring constant ( $k$ ) comes determined by the manufacturer and has a value of 0,44 N/mm. The length variation of the spring could be calculated by subtracting between  $L_f$  and  $L_0$ , but since a method to measure the length of the spring has not been designed, this difference in lengths is calculated using trigonometry as can be seen in equation (Eq.B.1).

$$\Delta x = d_s \sin \alpha \quad (\text{Eq.B.1})$$

$$F_S = k \Delta x = k d_s \sin \alpha \quad (\text{Eq.B.2})$$

Once the force exerted by the spring has been calculated, it can be decomposed into its two components as can be seen in Figure B.3. It is assumed that when the roller is in contact with

the platform and is not forced to exert a greater force, the rocker is at a point of equilibrium, therefore, by means of the Law of the Lever, the moments that appear must be equal to zero at the turning point.

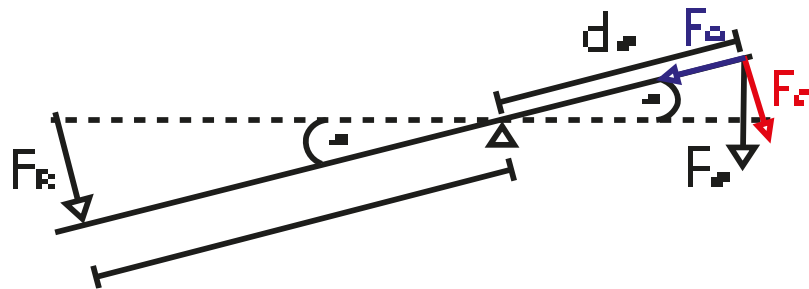


Figure B.3: Diagram of the forces acting on the rocker.

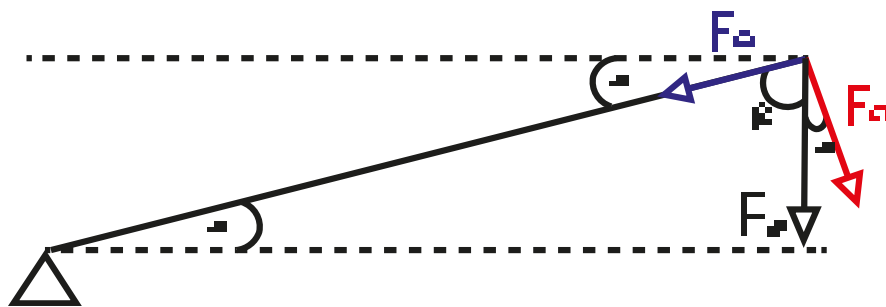


Figure B.4: Extension of Figure B.3 to determine the angles of the spring force components.

$$\sum M = 0 \rightarrow F_R d_R - F_{S1} d_S = 0 \quad (\text{Eq.B.3})$$

$$F_{S1} = F_S \cos \alpha \quad (\text{Eq.B.4})$$

$$F_R = \frac{d_S F_S \cos \alpha}{d_R} \quad (\text{Eq.B.5})$$

## C. Layers Images

Abbreviation	Name	Image	Abbreviation	Name	Image
Surface	ABS Surface		PIAp	Plastic Apron	
SGI	Short Glove		BNC	Blue Nurse's Coat	
LGI	Long Glove		WNC	White Nurse's Coat	
BH	Blue Hat		NCPI	Nurse's Coat Plastic	
WH	White Hat		PiC	Pillowcase	
GaPI	Gauze's Plastic		LN	Linen Napkin	








GaPa	Gauze's Paper		WR	Waffle Rag	
GIPI	Glove's Plastic		ST	Small Towel	
GIPa	Glove's Paper				

Table C.1: Table where the abbreviations, names and photographs of the used cloth and plastics can be seen.

## D. Friction Coefficients Results

Group	Materials	Experiment 1			Experiment 2				Experiment 3		$\mu$ Final
		M (kg)	$\alpha$ (°)	$\mu_1$	M (kg)	$\beta$ (°)	m1 (kg)	$\mu_2$	m2 (kg)	$\mu_3$	
1	SGI-SGI	1	25,58	0,478754957	1	31,00	0,202	0,365200673	0,911	0,461942406	0,435299345
	LGI-LGI INT	1	20,50	0,373884679	1	38,60	0,285	0,433615764	0,925	0,385300723	0,397600389
3	BH-BH	1	24,60	0,457835746	1	30,30	0,13	0,433784519	0,89	0,446460925	0,446027063
4	WH-WH	1	19,60	0,356083983	1	27,50	0,148	0,353714522	0,83	0,415159965	0,374986157
5	GaPI-GaPa	1	14,40	0,25675636	1	23,90	0,148	0,28125838	0,676	0,296261681	0,27809214
6	GIPI-GIPa	1	19,40	0,35215559	1	28,20	0,166	0,347837926	0,74	0,303470087	0,334487868
7	PIAp-PIAp	1	13,00	0,230868191	1	23,50	0,202	0,214543272	0,646	0,269612578	0,238341347
8	BNC-BNC	1	19,20	0,348236844	1	26,40	0,14	0,34010403	0,804	0,401205875	0,36318225
9	WNC-WNC	1	23,00	0,424474816	1	30,90	0,154	0,419014051	0,885	0,432902856	0,425463908
10	NCPI-NCPI	1	6,00	0,105104235	1	17,50	0,198	0,107690022	0,44	0,146054026	0,119616095
11	PiC-PiC	1	29,00	0,554309051	1	45,00	0,389	0,449870924	1,291	0,825749709	0,609976562
12	LN-LN	1	23,60	0,436889258	1	33,10	0,271	0,328394192	1,021	0,566894388	0,444059279
13	WR-WR	1	41,00	0,869286738	1	53,00	0,211	0,976438752	1,661	1,432939453	1,092888314
14	ST-ST	1	51,00	1,234897157	1	57,40	0,215	1,16459989	1,661	1,519287285	1,306261444

Table D.1: Friction coefficients between the two layers of the same fabric.

Group	Materials	Experiment 1			Experiment 2			Experiment 3		μ Final
		M (kg)	α (°)	μ1	β (°)	m1 (kg)	μ2	m2 (kg)	μ3	
1	Surface-SGI	1	22,6	0,416259824	30,3	0,21	0,341127104	0,888	0,44414449	0,400510473
2	Surface-LGI	1	33,6	0,664398412	45,8	0,29	0,612352233	1,234	0,74170292	0,672817855
3	Surface-BH	1	21,4	0,391895715	32,3	0,271	0,311563044	0,857	0,381713261	0,361724006
4	Surface-WH	1	19,6	0,356083983	30,6	0,274	0,273068362	0,832	0,375209498	0,334787281
5	Surface-GaPI	1	9,2	0,161964658	17,5	0,15	0,15801942	0,45	0,156539317	0,158841132
5	Surface-GaPa	1	15	0,267949192	25	0,234	0,208117225	0,674	0,277369059	0,251145159
6	Surface-GIPI	1	15,1	0,269820708	25,4	0,229	0,221329926	0,734	0,337709452	0,276286695
6	Surface-GIPa	1	18,8	0,340427769	28,8	0,274	0,237078729	0,761	0,318662784	0,298723094
7	Surface-PIAp	1	12,2	0,216207653	22,8	0,226	0,1752056	0,57	0,197951739	0,196454997
8	Surface-BNC	1	15,9	0,284857493	28,9	0,258	0,257328968	0,781	0,340068167	0,294084876
9	Surface-WNC	1	15,2	0,271693987	29,2	0,282	0,235828219	0,776	0,330087127	0,279203111
10	Surface-NCPI	1	13,5	0,240078759	30,3	0,346	0,183609498	0,756	0,291259755	0,238316004
11	Surface-PiC	1	17,9	0,322991199	31	0,278	0,276536535	0,899	0,447942805	0,349156846
12	Surface-LN	1	19,4	0,35215559	35,4	0,344	0,288643294	0,984	0,496509664	0,379102849
13	Surface-WR	1	18,5	0,33459532	33,3	0,282	0,319478902	0,899	0,41872948	0,357601234
14	Surface-ST	1	21,5	0,393910476	36,2	0,302	0,35764543	0,965	0,463956315	0,40517074

Table D.2: Friction coefficients between the surface and the different fabrics.

Group	Materials	Experiment 1			Experiment 2			Experiment 3		μ Final
		M (kg)	α (°)	μ1	β (°)	m1 (kg)	μ2	m2 (kg)	μ3	
1	Latex-SGI	1	38,9	0.80689828	44,2	0,192	0.704641691	1,289	0.825535138	0.779025036
2	Latex-LGI	1	40,3	0.848061673	48,1	0,321	0.633858806	1,379	0.950370641	0.810763707
3	Latex-BH	1	32,1	0.627298817	43,1	0,283	0.548198375	1,375	0.947359578	0.707618924
4	Latex-WH	1	28,9	0.552029658	43,2	0,264	0.576907003	1,224	0.740022099	0.622986253
5	Latex-GaPI	1	37,9	0.77847876	43,9	0,248	0.618140505	1,223	0.73499043	0.710536565
5	Latex-GaPa	1	31,6	0.615204105	44,2	0,276	0.587472271	1,178	0.670704118	0.624460165
6	Latex-GIPI	1	29,6	0.568079065	44,6	0,253	0.630809864	1,156	0.63740217	0.612097033
6	Latex-GIPa	1	34,5	0.687280959	46,5	0,304	0.612147265	1,253	0.766502683	0.688643636
7	Latex-PIAp	1	32,1	0.627298817	46,3	0,299	0.613660355	1,256	0.771524713	0.670827962
8	Latex-BNC	1	30,4	0.586696515	46,3	0,35	0.539841715	1,167	0.642703949	0.589747393
9	Latex-WNC	1	29,2	0.55888111	44,6	0,316	0.542329954	1,255	0.776442028	0.625884364
10	Latex-NCPI	1	29,2	0.55888111	46,7	0,292	0.635405506	1,273	0.795002408	0.663096341
11	Latex-PiC	1	34,6	0.689853792	48,6	0,284	0.704827925	1,312	0.84965802	0.748113246
12	Latex-LN	1	32,4	0.634619298	46,9	0,326	0.591508546	1,339	0.891059699	0.705729181
13	Latex-WR	1	37	0.75355405	49,1	0,301	0.694707676	1,385	0.960909291	0.803057006
14	Latex-ST	1	41	0.869286738	51,6	0,303	0.773879377	1,496	1.146758574	0.929974896

Table D.3: Friction coefficients between the latex material and the different fabrics.

Group	Materials	Experiment 1			Experiment 2			Experiment 3		$\mu$ Final
		M (kg)	$\alpha$ (°)	$\mu_1$	$\beta$ (°)	m1 (kg)	$\mu_2$	m2 (kg)	$\mu_3$	
1	Ecoflex-SGI	1	39,1	0,812677955	49	0,062	1,055864716	1,589	1,271669748	1,046737473
2	Ecoflex-LGI	1	48,9	1,146321522	55,3	0,116	1,240417075	1,946	1,974172463	1,45363702
3	Ecoflex-BH	1	40	0,839099631	50,3	0,236	0,835044504	1,501	1,145330784	0,939824973
4	Ecoflex-VH	1	35,2	0,705422401	48,5	0,266	0,728857695	1,477	1,098735665	0,844338587
5	Ecoflex-GaPI	1	41,1	0,872355601	51,5	0,316	0,749553712	1,501	1,154015988	0,925308434
5	Ecoflex-GaPa	1	43,2	0,939062506	54,3	0,256	0,952946452	1,625	1,393074657	1,095027872
6	Ecoflex-GIPI	1	40,6	0,857103661	52	0,284	0,818649166	1,561	1,25554266	0,977098496
6	Ecoflex-GIPa	1	40	0,839099631	52,1	0,27	0,845021311	1,531	1,207771105	0,963964016
7	Ecoflex-PIAp	1	42,6	0,919547138	53,2	0,396	0,675651797	1,643	1,406069195	1,00042271
8	Ecoflex-BNC	1	35,3	0,708039467	44,5	0,215	0,681260369	1,295	0,832934261	0,740744699
9	Ecoflex-WNC	1	36,9	0,750821238	44,3	0,13	0,79421693	1,551	1,191272	0,912103389
10	Ecoflex-NCPI	1	39,3	0,818490516	47	0,124	0,890550091	1,661	1,363121017	1,024053875
11	Ecoflex-PIC	1	38,7	0,801151071	49,3	0,158	0,920312537	1,559	1,228136212	0,98319994
12	Ecoflex-LN	1	41,7	0,8909675	48,3	0,218	0,794669363	1,501	1,133985863	0,939874242
13	Ecoflex-WR	1	42	0,900404044	49,7	0,126	0,984351253	1,874	1,718227012	1,200994103
14	Ecoflex-ST	1	48	1,110612515	53,2	0,136	1,109691459	1,874	1,791696741	1,337333571

Table D.4: Friction coefficients between the Ecoflex material and the different fabrics.

Group	Materials	Experiment 1			Experiment 2			Experiment 3		$\mu$ Final
		M (kg)	$\alpha$ (°)	$\mu_1$	$\beta$ (°)	m1 (kg)	$\mu_2$	m2 (kg)	$\mu_3$	
1	Dragon-SGI	1	35	0,700207538	48,8	0,316	0,662550314	1,431	1,030204872	0,797654242
2	Dragon-LGI	1	29,7	0,57038993	47,9	0,428	0,468322456	1,445	1,048622085	0,695778157
3	Dragon-BH	1	30,7	0,59375655	47,2	0,362	0,547111078	1,393	0,970312125	0,703726584
4	Dragon-VH	1	22	0,404026226	44,2	0,391	0,427061756	1,269	0,797637657	0,542908546
5	Dragon-GaPI	1	24,5	0,455726256	48,5	0,429	0,482864534	1,32	0,861797467	0,600129419
5	Dragon-GaPa	1	26,7	0,502947603	48,5	0,348	0,605106534	1,346	0,90103564	0,669696592
6	Dragon-GIPI	1	23,5	0,434812375	49,5	0,52	0,370169664	1,352	0,91091818	0,57196674
6	Dragon-GIPa	1	30,8	0,59611964	50	0,396	0,575686957	1,352	0,911585021	0,694463873
7	Dragon-PIAp	1	23,7	0,43896931	51	0,458	0,507127953	1,393	0,978601754	0,641566339
8	Dragon-BNC	1	20,1	0,365948033	48	0,569	0,260255358	1,142	0,596079705	0,407427699
9	Dragon-WNC	1	22,1	0,406057892	48	0,533	0,314056514	1,264	0,778405844	0,49950675
10	Dragon-NCPI	1	20,3	0,369911232	49	0,5	0,388241864	1,236	0,733608408	0,497253835
11	Dragon-PIC	1	33,9	0,671972113	50,3	0,328	0,69101721	1,513	1,164116952	0,842368758
12	Dragon-LN	1	34,9	0,697609663	45,8	0,266	0,646777364	1,393	0,969769413	0,77138548
13	Dragon-WR	1	38,8	0,804020643	49,7	0,196	0,876124434	1,561	1,234298524	0,9714812
14	Dragon-ST	1	44,9	0,99651542	51	0,132	1,02514708	1,754	1,552236432	1,191299644

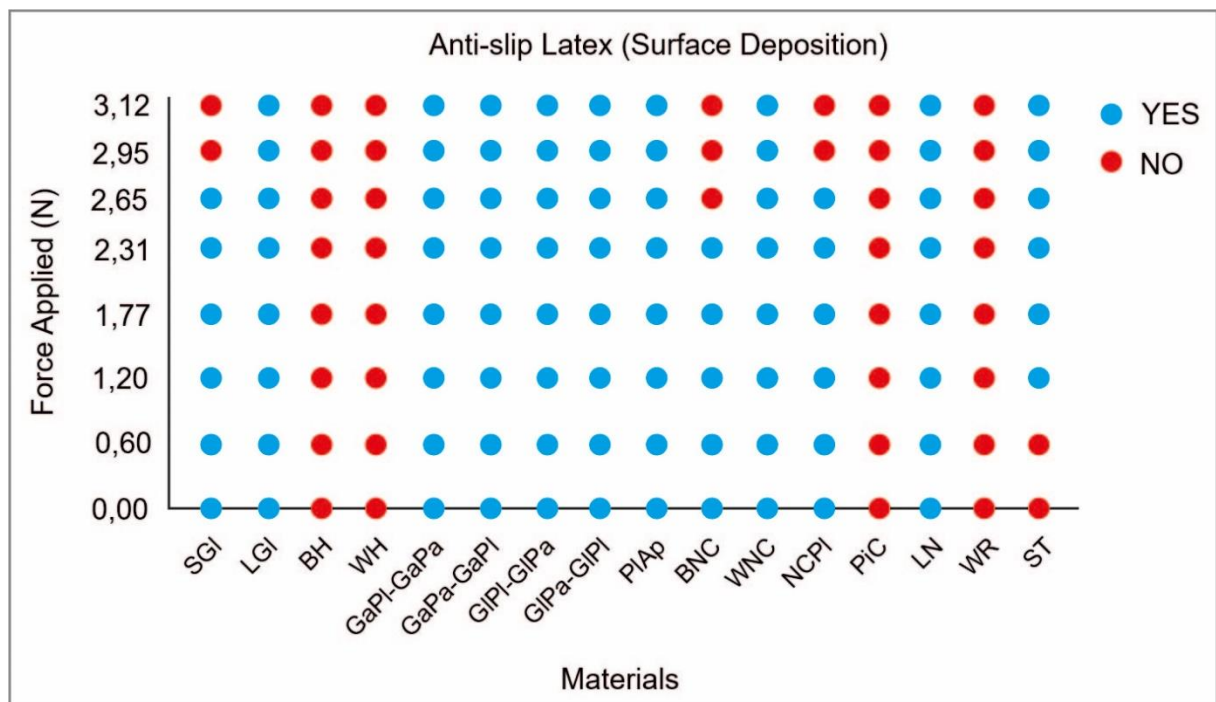
Table D.5: Friction coefficients between the DragonSkin material and the different fabrics.

Group	Materials	Experiment 1			Experiment 2			Experiment 3		$\mu$ Final
		M (kg)	$\alpha$ (°)	$\mu_1$	$\beta$ (°)	m1 (kg)	$\mu_2$	m2 (kg)	$\mu_3$	
1	Resina80A-SGI	1	37,1	0,75629406	47,8	0,186	0,825945497	1,469	1,08407486	0,888771472
2	Resina80A-LGI	1	41	0,869286738	51,4	0,168	0,983395635	1,643	1,380842605	1,077841659
3	Resina80A-BH	1	41,7	0,8909675	51,4	0,136	1,034687584	1,524	1,190100672	1,038585252
4	Resina80A-VH	1	37,6	0,770103672	49,3	0,2	0,85590508	1,44	1,045648417	0,89055239
5	Resina80A-GaPI	1	31,4	0,610402607	47,1	0,374	0,526710602	1,255	0,767505633	0,634872947
5	Resina80A-GaPa	1	37,9	0,77847876	49,1	0,234	0,797038245	1,45	1,060185216	0,878567407
6	Resina80A-GIPI	1	29,7	0,57038993	47,9	0,368	0,55781771	1,337	0,887530629	0,671912756
6	Resina80A-GIPa	1	46,4	1,050103449	51,4	0,182	0,960955408	1,607	1,323139163	1,11139934
7	Resina80A-PIAp	1	30,5	0,589045016	46,6	0,215	0,744555334	1,411	0,996125411	0,776575254
8	Resina80A-BNC	1	34,5	0,687280959	49,2	0,214	0,831003878	1,459	1,074353854	0,864212897
9	Resina80A-WNC	1	33,8	0,669441652	47,7	0,284	0,677002412	1,406	0,990128551	0,778857538
10	Resina80A-NCPI	1	34,3	0,682153749	48,2	0,28	0,698354575	1,44	1,041995749	0,807501358
11	Resina80A-PIC	1	33,9	0,671972113	47,8	0,215	0,782772785	1,439	1,039413433	0,83138611
12	Resina80A-LN	1	38,5	0,795435917	45,7	0,216	0,715466491	1,406	0,988390834	0,833097747
13	Resina80A-WR	1	41,6	0,887841546	52	0,118	1,088277861	1,589	1,301022199	1,092380535
14	Resina80A-ST	1	43,1	0,935783449	61,8	0,1	1,653374643	1,661	1,649974153	1,413044082

Table D.6: Friction coefficients between the 80A resin and the different fabrics.

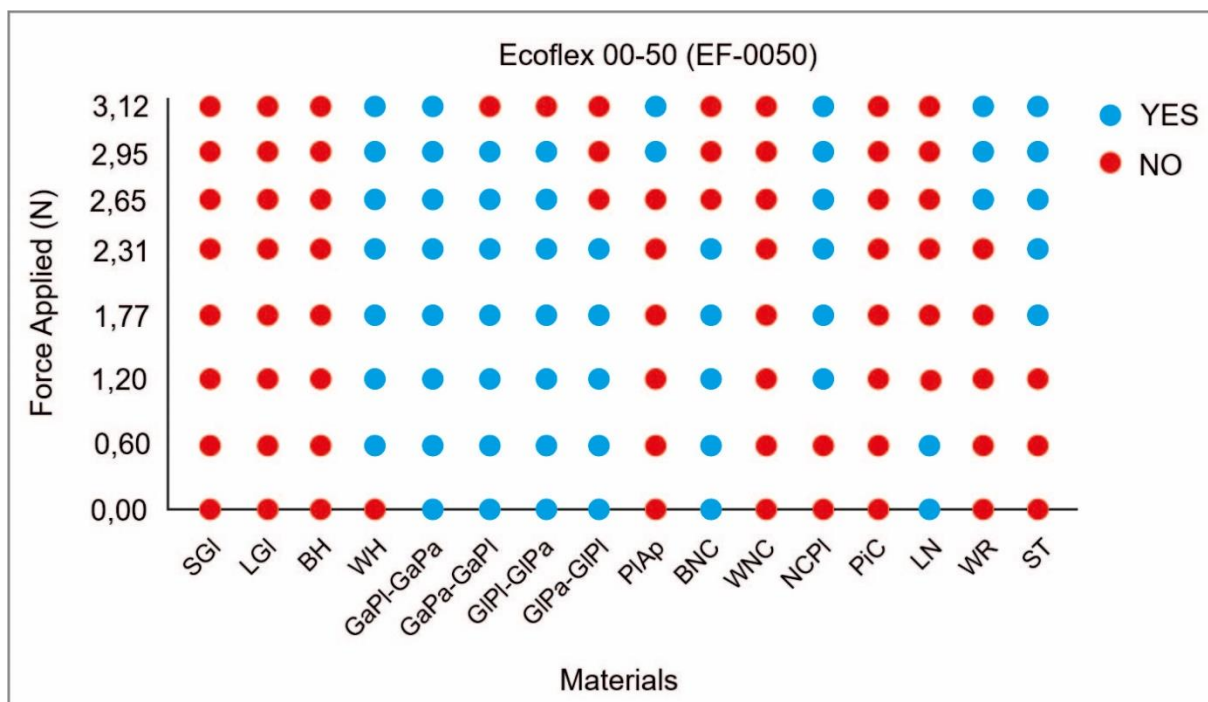
## E. Test-bench Results

In this section it can be seen the graphs of the results obtained with the tests carried out with the test-bench. In blue are the tests carried out successfully and in red those where the roller has not been able to perform the task of separating layers. The order in which the abbreviations of the fabrics appear indicates which part was in contact with the roller and which with the surface coated with Ecoflex. For example, GaPI-GaPa indicates that the GaPI fabric was in contact with the roller and the GaPa fabric was in contact with the surface.

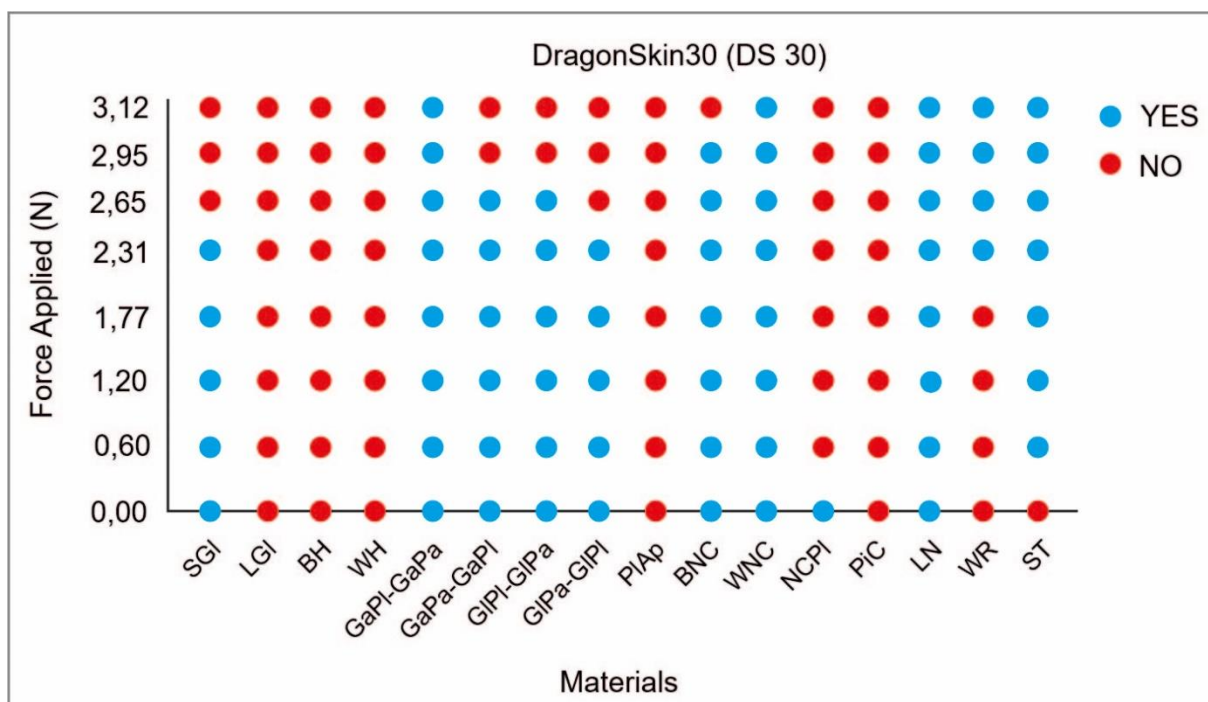


Graph E.1: Results of latex roller operation.

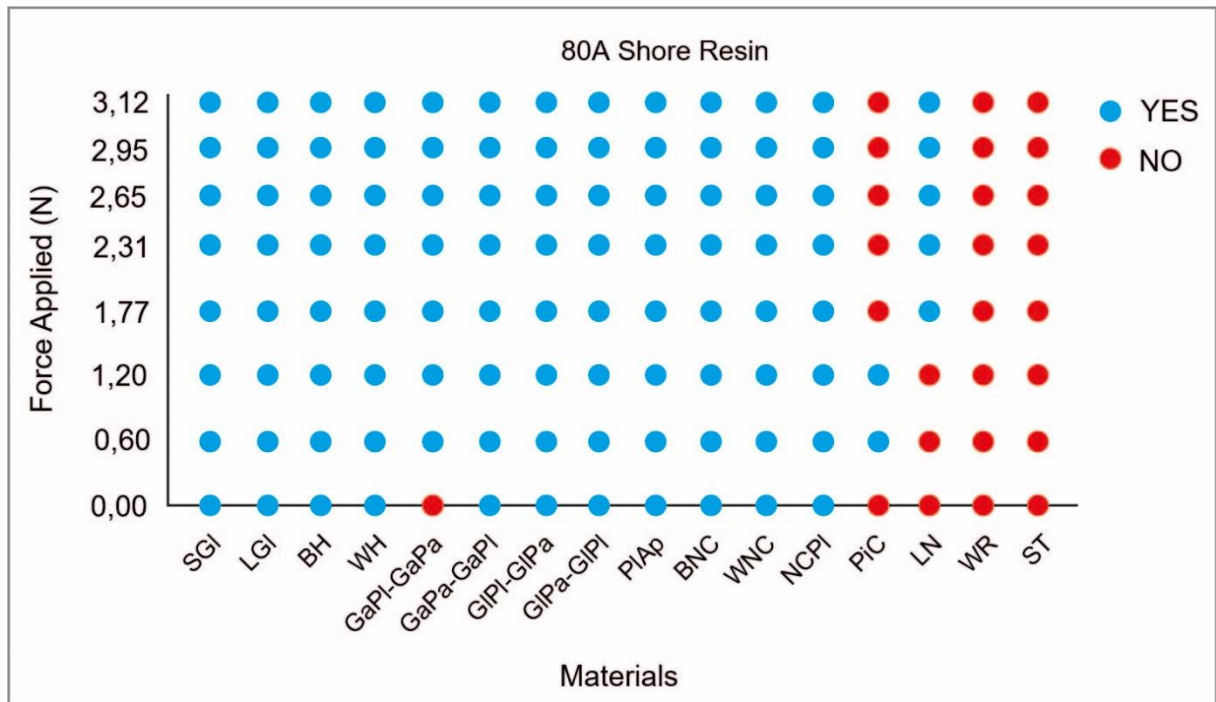




Graph E.2: Results of Ecoflex roller operation.



Graph E.3: Results of DragonSkin roller operation.



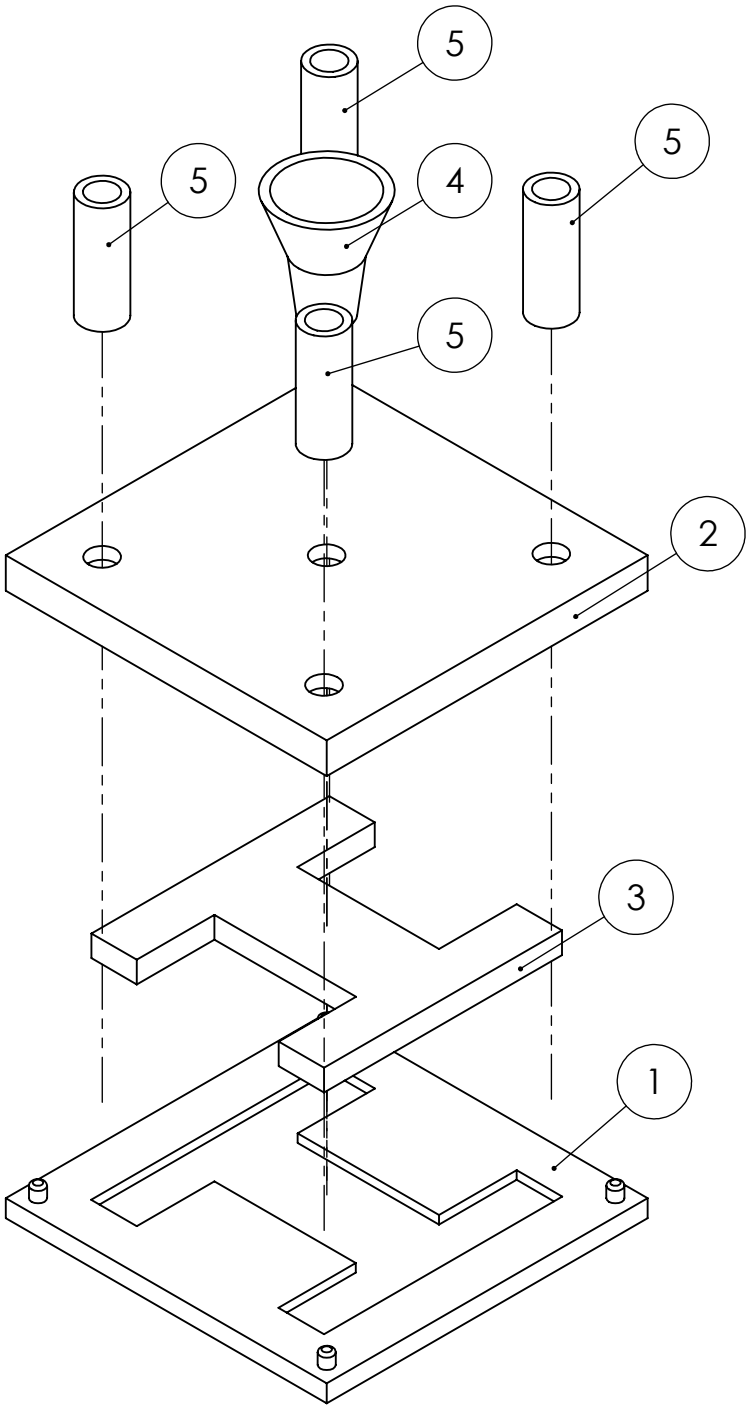
Graph E.4: Results of the 80A resin printed roller operation.






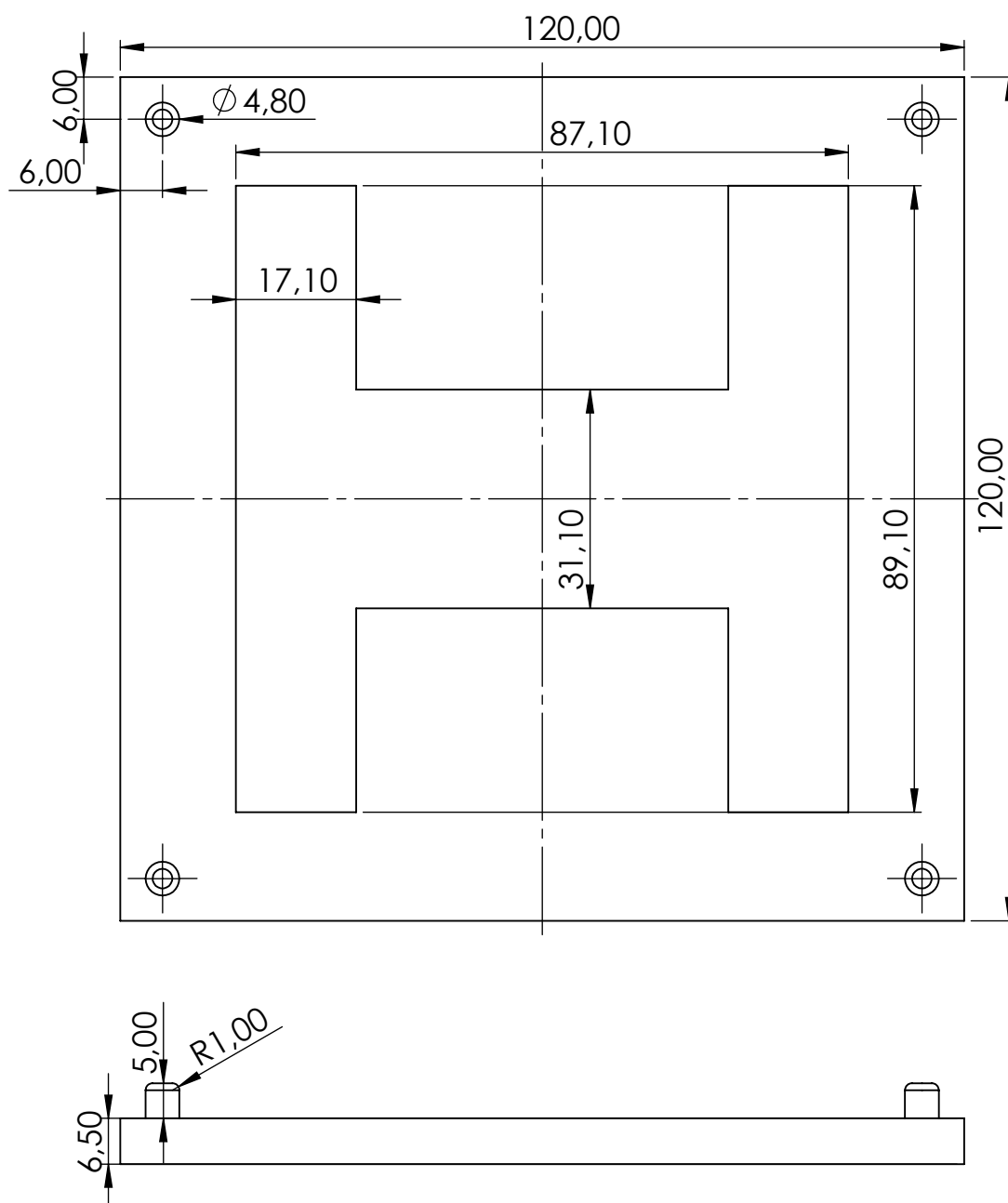
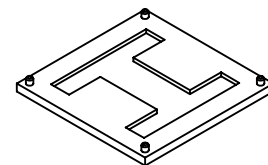
## **F.CAD Exploded View Diagrams and Drawings**



ITEM NO.	PART NUMBER	QTY.
1	H MOLD PART 1	1
2	H MOLD PART 2	1
3	H MOLD PART 3	1
4	FUNNEL	1
5	CHIMNEY	4



GRIPPER DESIGN FOR AN ASSISTIVE ROBOT IN A HOSPITAL ENVIRONMENT			 UNIVERSITAT DE BARCELONA		Part Drawing 1
H MOLD EXPLODED VIEW DIAGRAM					Quantity 1
Checked by	JAUME ORIOL LLADÓ	10/06/2023	Format: DIN A4	Scale 1:2	Projection 
Drawn by	JAUME ORIOL LLADÓ	10/06/2023	Remarks		



GRIPPER DESIGN FOR AN ASSISTIVE ROBOT  
IN A HOSPITAL ENVIRONMENT



UNIVERSITAT DE  
BARCELONA



Part Drawing  
2

Quantity 1

H MOLD PART 1

Format:

DIN A4

Scale

1:1

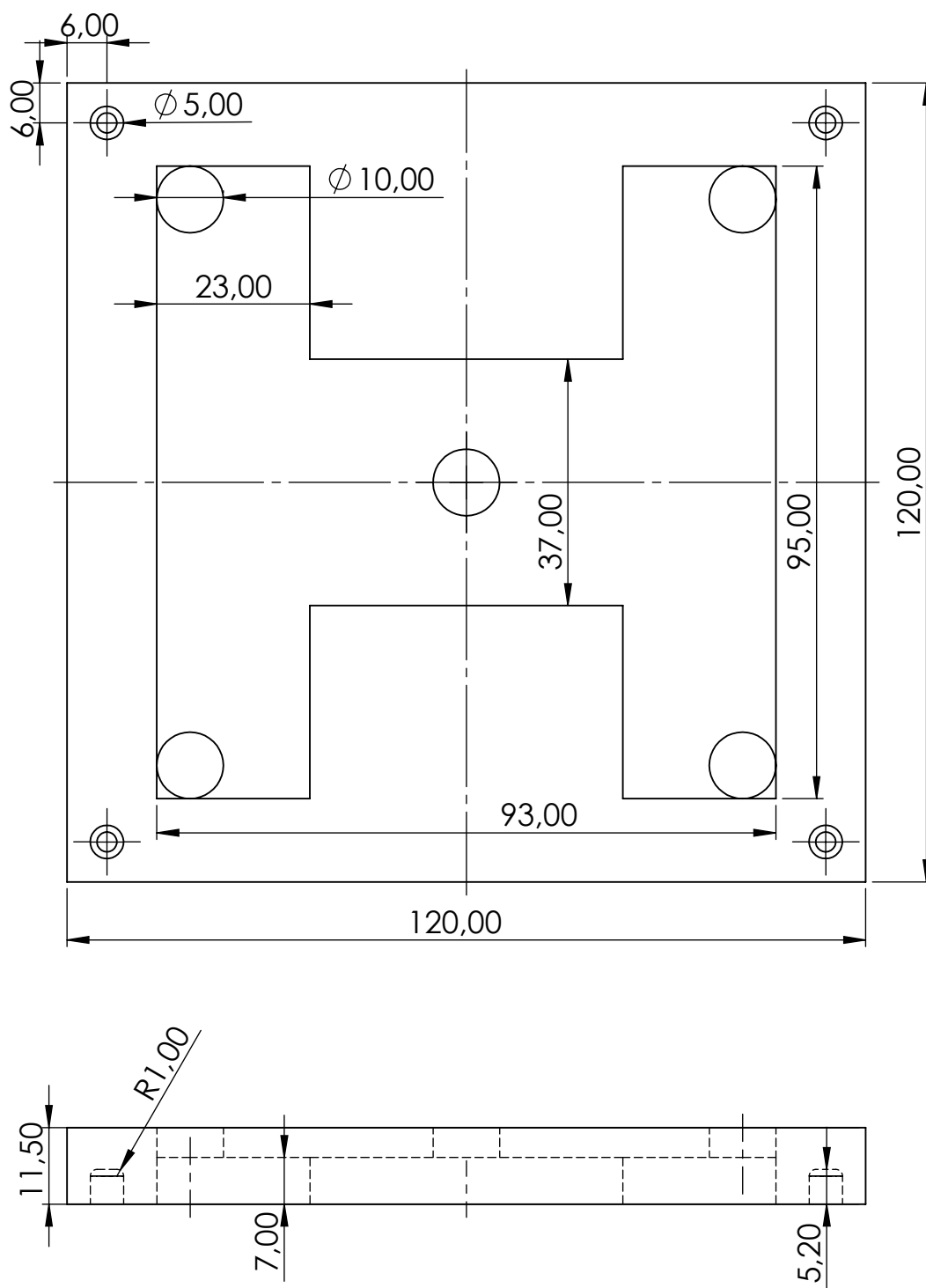
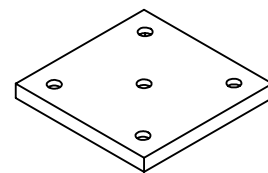
Projection



Checked by JAUME ORIOL LLADÓ 05/05/2023

Drawn by JAUME ORIOL LLADÓ 05/05/2023

Remarks



GRIPPER DESIGN FOR AN ASSISTIVE ROBOT  
IN A HOSPITAL ENVIRONMENT



UNIVERSITAT DE  
BARCELONA



Part Drawing

3

Quantity 1

H MOLD PART 2

Format:

DIN A4

Scale

1:1

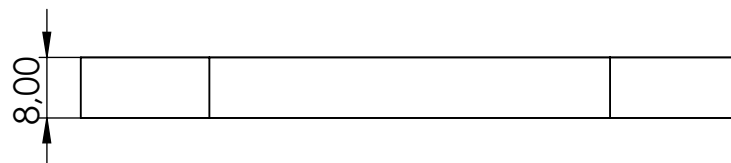
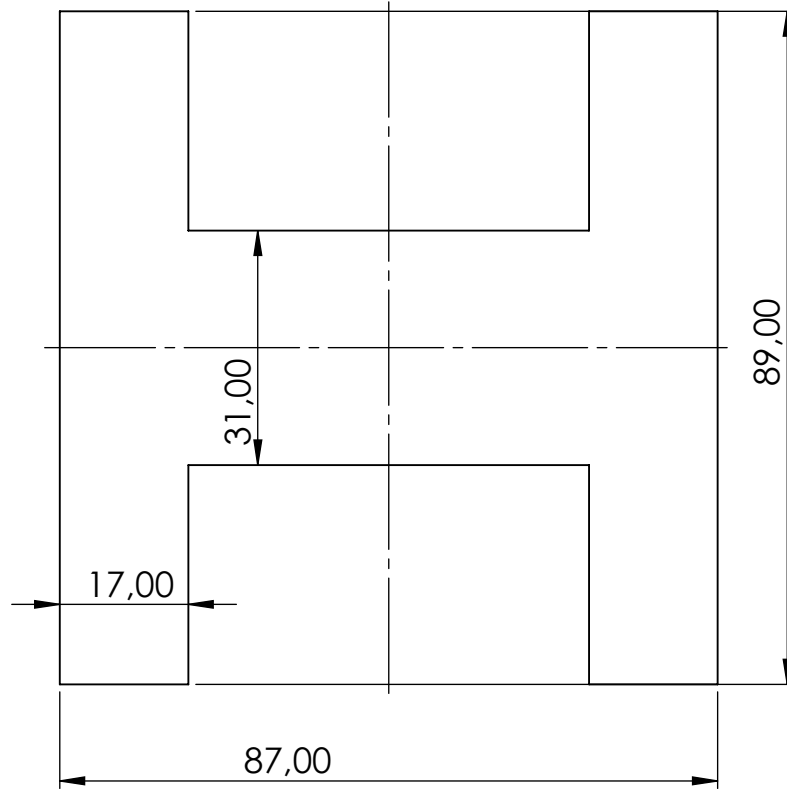
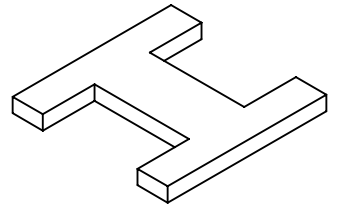
Projection



Checked by JAUME ORIOL LLADÓ 05/05/2023

Drawn by JAUME ORIOL LLADÓ 05/05/2023

Remarks



GRIPPER DESIGN FOR AN ASSISTIVE ROBOT  
IN A HOSPITAL ENVIRONMENT



UNIVERSITAT DE  
BARCELONA



Part Drawing

4

Quantity 1

H MOLD PART 3

Format:

DIN A4

Scale

1:1

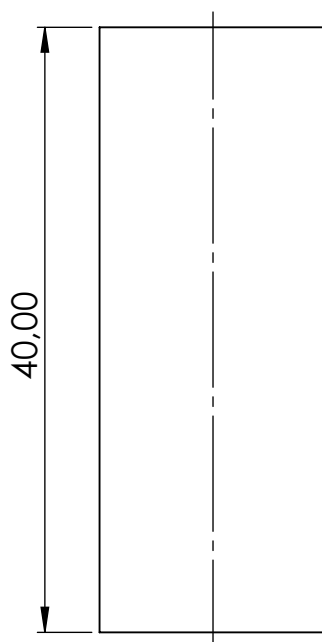
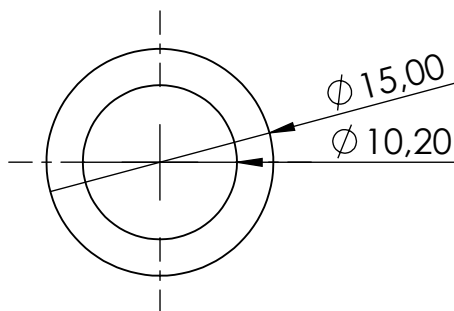
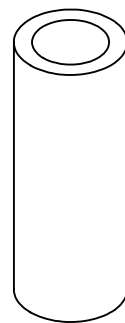
Projection






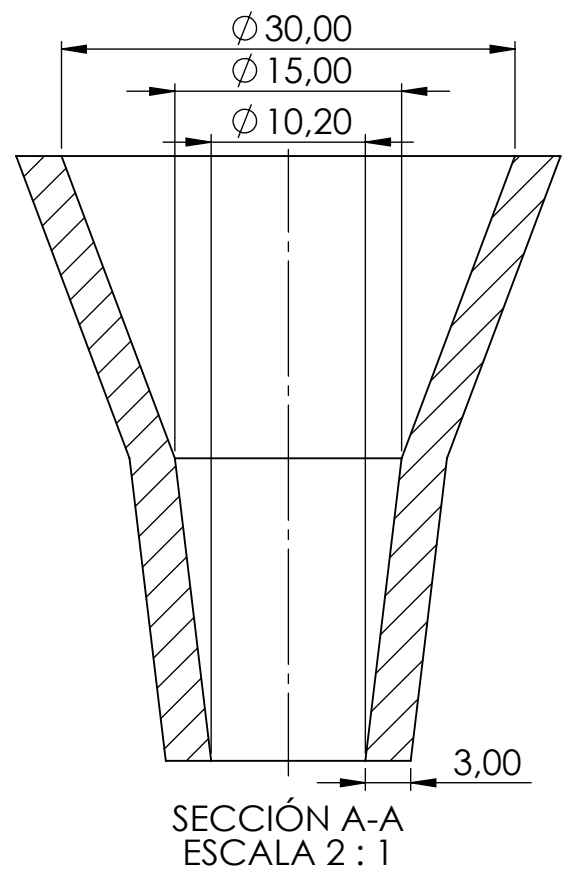
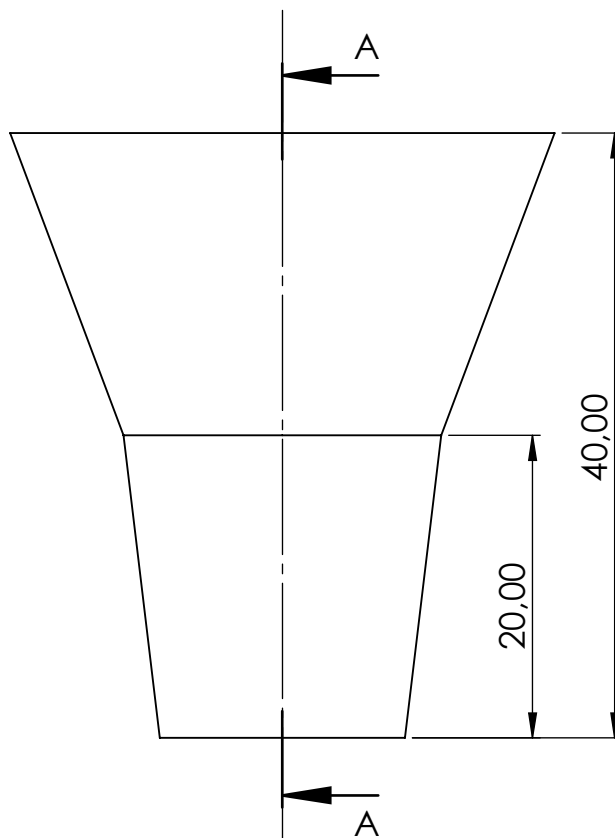
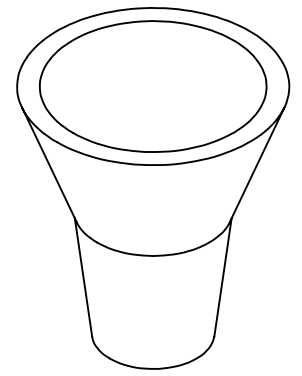
Checked by JAUME ORIOL LLADÓ 05/05/2023

Drawn by JAUME ORIOL LLADÓ 05/05/2023

Remarks



GRIPPER DESIGN FOR AN ASSISTIVE ROBOT IN A HOSPITAL ENVIRONMENT			 UNIVERSITAT DE BARCELONA 	Part Drawing 5	
CHIMNEY				Quantity 5	
Checked by	JAUME ORIOL LLADÓ	05/05/2023	Format:  DIN A4	Scale  2:1	Projection 
Drawn by	JAUME ORIOL LLADÓ	05/05/2023			



GRIPPER DESIGN FOR AN ASSISTIVE ROBOT  
IN A HOSPITAL ENVIRONMENT



UNIVERSITAT DE  
BARCELONA



Part Drawing

6

Quantity 2

FUNNEL

Format:

DIN A4

Scale

2:1

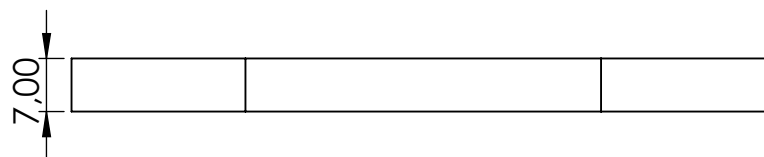
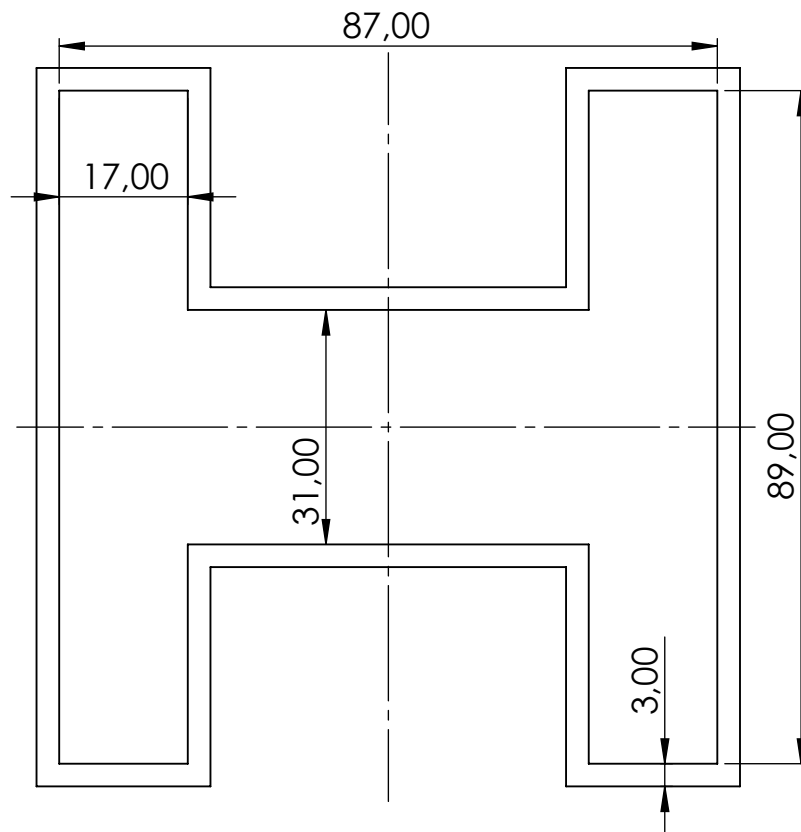
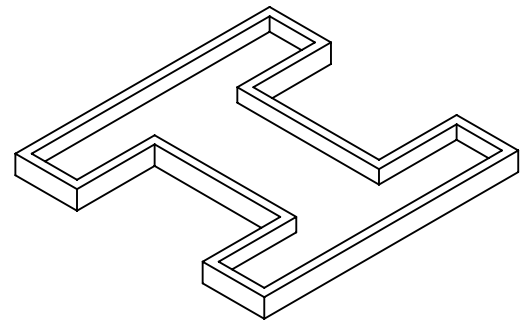
Projection



Checked by JAUME ORIOL LLADÓ 05/05/2023

Drawn by JAUME ORIOL LLADÓ 05/05/2023

Remarks



GRIPPER DESIGN FOR AN ASSISTIVE ROBOT  
IN A HOSPITAL ENVIRONMENT



UNIVERSITAT DE  
BARCELONA



Part Drawing

7

Quantity 1

Projection



PIECE H RESIN 80A

Format:

DIN A4

Scale

1:1

Checked by JAUME ORIOL LLADÓ 05/05/2023

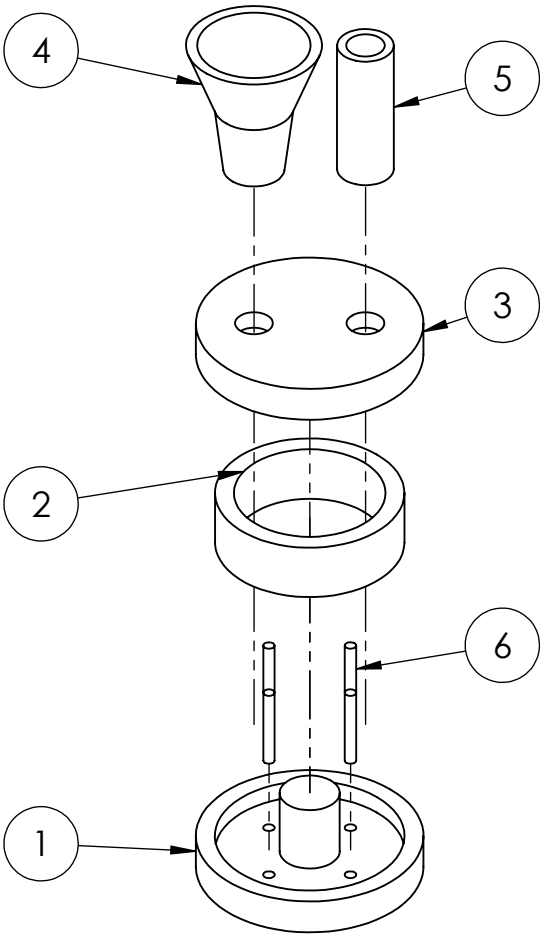
Drawn by JAUME ORIOL LLADÓ 05/05/2023




Remarks

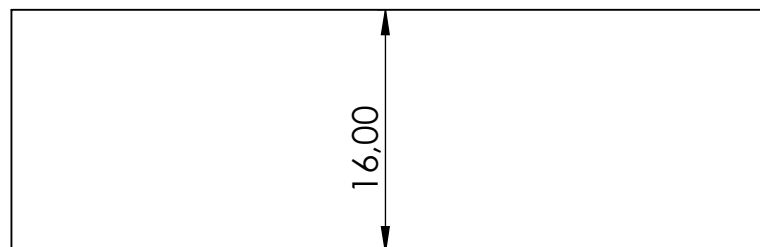
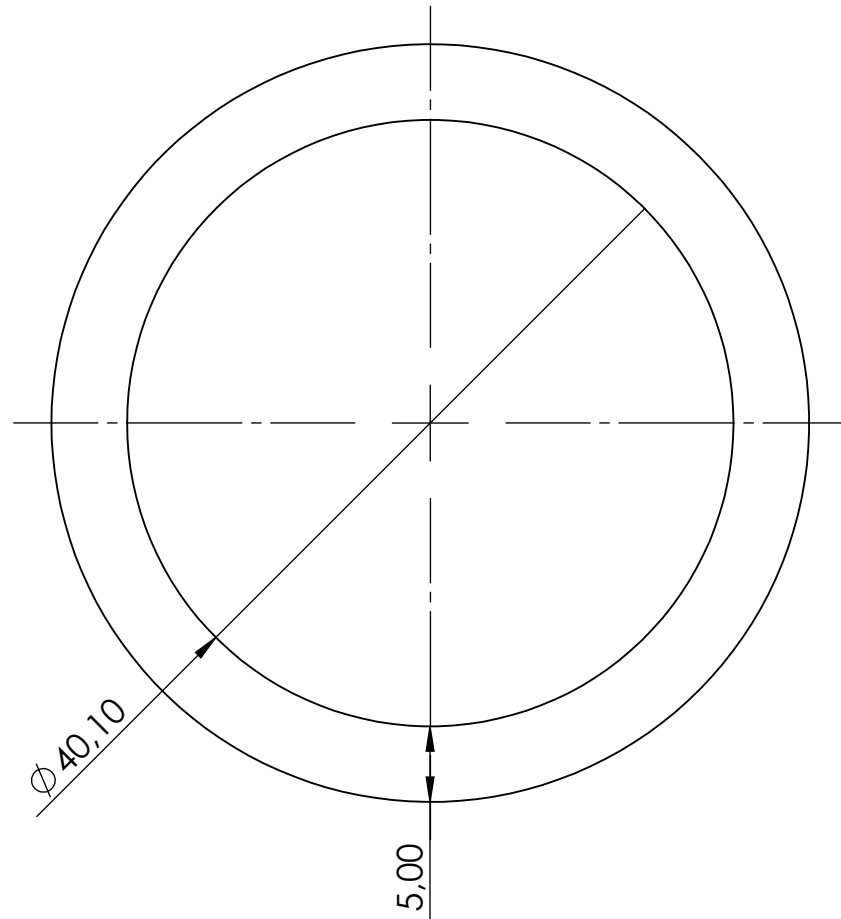
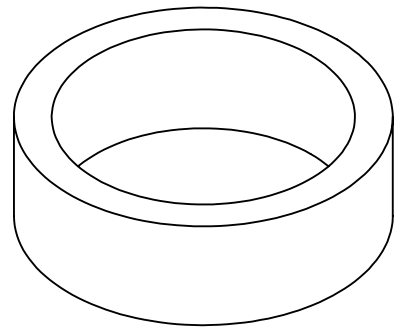
PRINTED WITH RESIN 80A



ITEM NO.	PART NUMBER	QTY.
1	ROLLER MOLD PART 2	1
2	ROLLER MOLD PART 1	1
3	ROLLER MOLD PART 3	1
4	FUNNEL	1
5	CHIMNEY	1
6	ROD	4



GRIPPER DESIGN FOR AN ASSISTIVE ROBOT IN A HOSPITAL ENVIRONMENT			 UNIVERSITAT DE BARCELONA 	Part Drawing 8	
ROLLER MOLD EXPLODED VIEW DIAGRAM				Quantity 1	
Checked by	JAUME ORIOL LLADÓ	10/06/2023	Format: DIN A4	Scale 1:2	Projection 
Drawn by	JAUME ORIOL LLADÓ	10/06/2023	Remarks		



GRIPPER DESIGN FOR AN ASSISTIVE ROBOT  
IN A HOSPITAL ENVIRONMENT



UNIVERSITAT DE  
BARCELONA



Part Drawing

9

Quantity 1

ROLLER MOLD PART 1

Format:

DIN A4

Scale

2:1

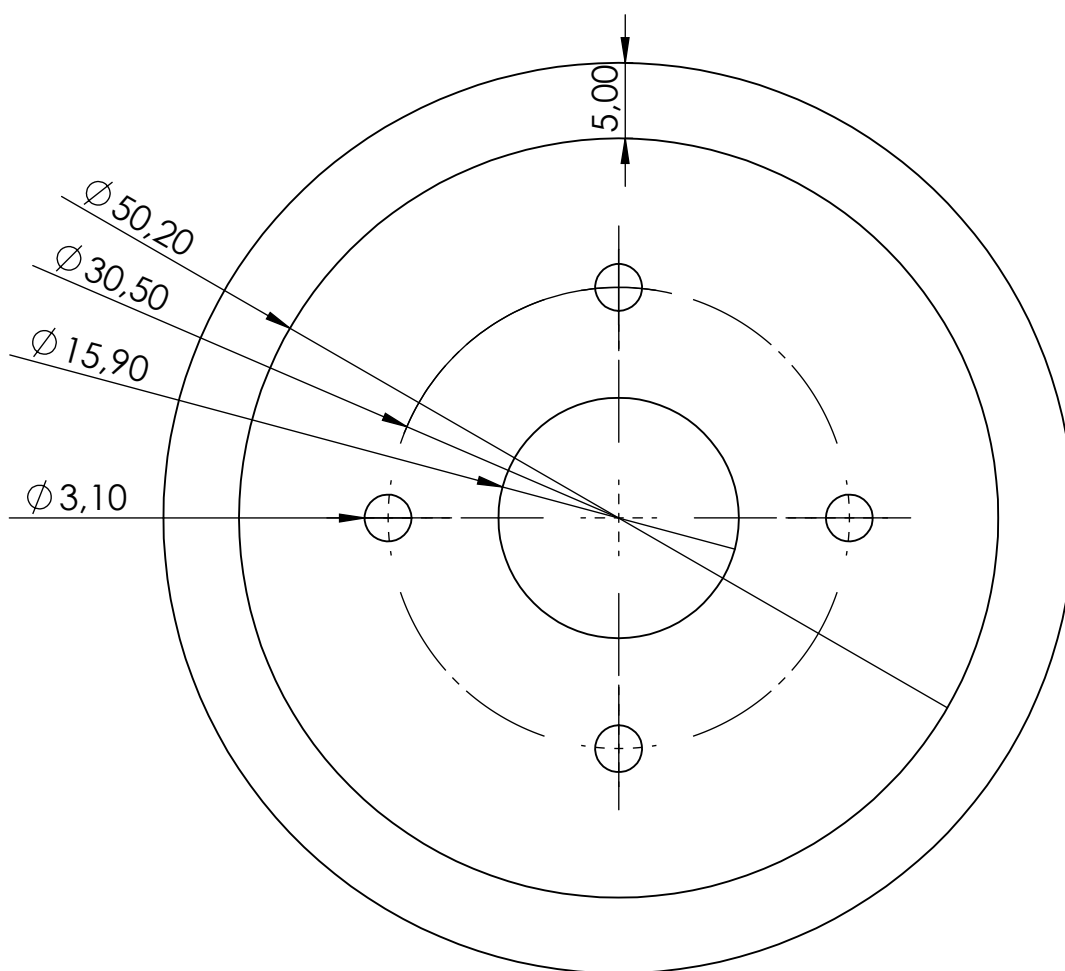
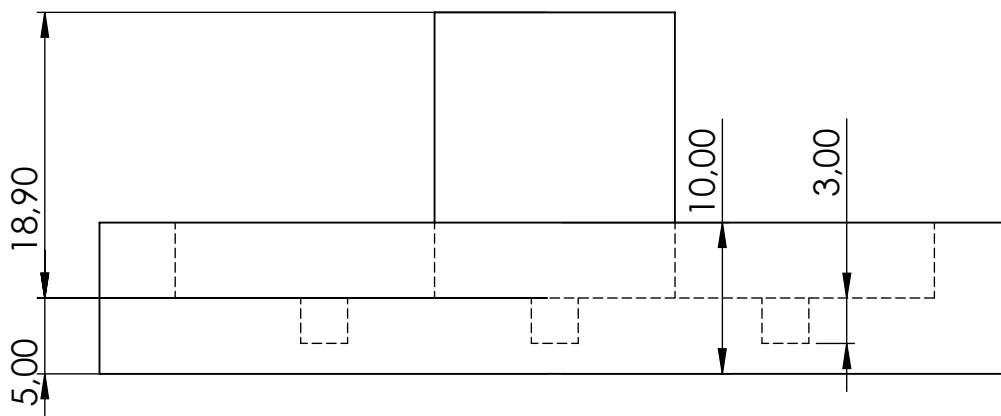
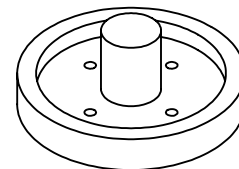
Projection



Checked by JAUME ORIOL LLADÓ 05/05/2023

Drawn by JAUME ORIOL LLADÓ 05/05/2023

Remarks



GRIPPER DESIGN FOR AN ASSISTIVE ROBOT  
IN A HOSPITAL ENVIRONMENT



UNIVERSITAT DE  
BARCELONA



Part Drawing

10

Quantity 1

Projection



ROLLER MOLD PART 2

Format:

DIN A4

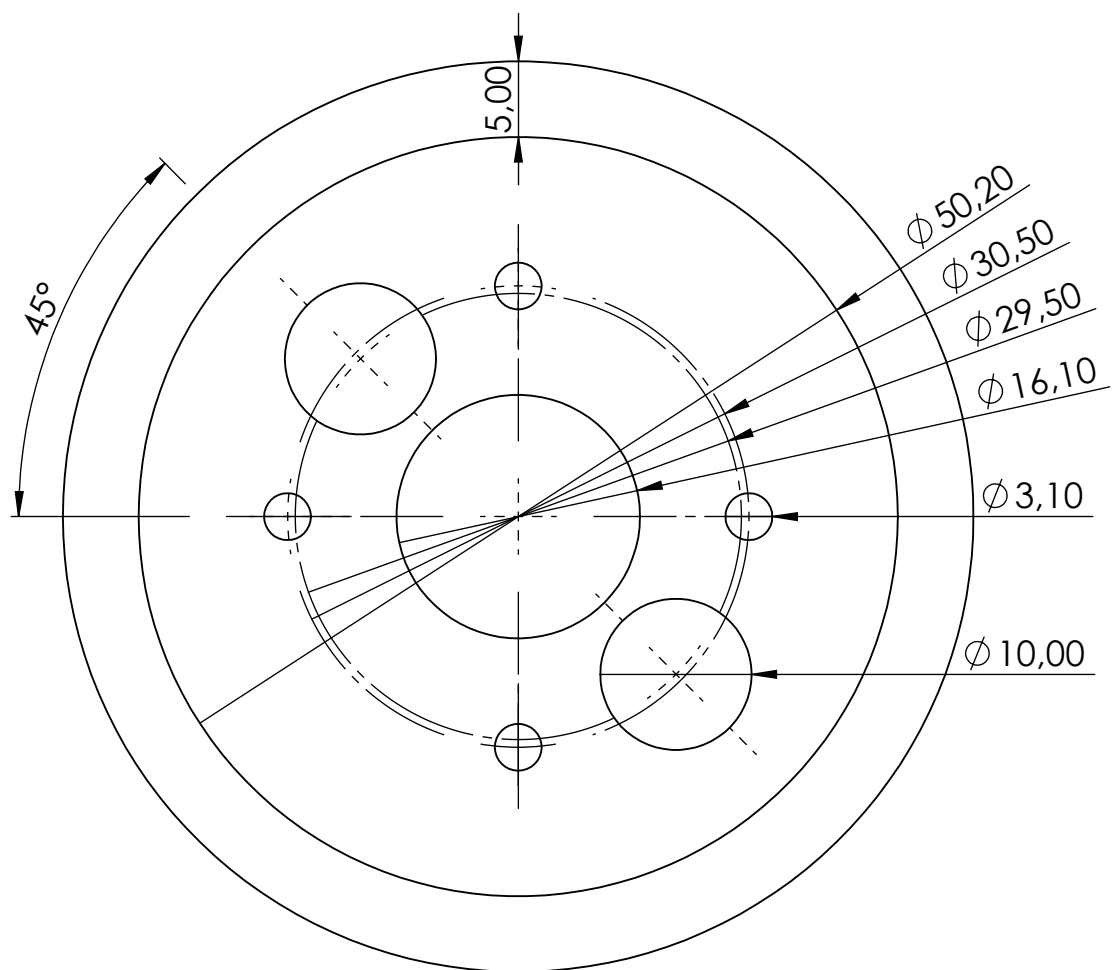
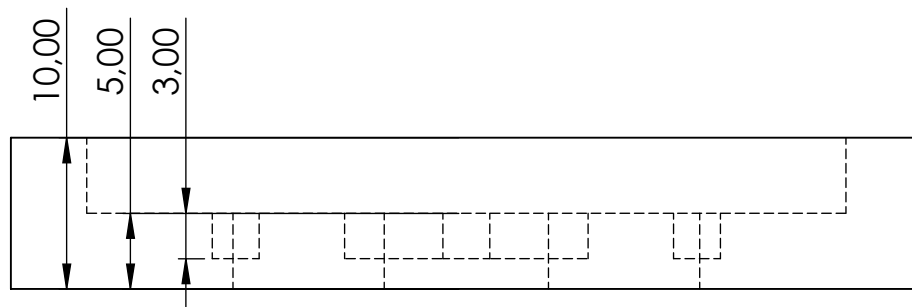
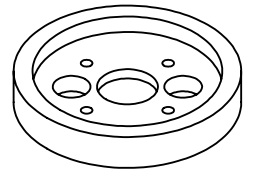
Scale

2:1

Checked by JAUME ORIOL LLADÓ 05/05/2023

Drawn by JAUME ORIOL LLADÓ 05/05/2023

Remarks



GRIPPER DESIGN FOR AN ASSISTIVE ROBOT  
IN A HOSPITAL ENVIRONMENT



UNIVERSITAT DE  
BARCELONA



Part Drawing

11

Quantity 1

ROLLER MOLD PART 3

Format:

DIN A4

Scale

2:1

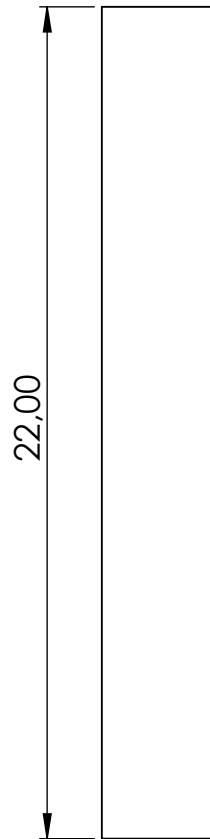
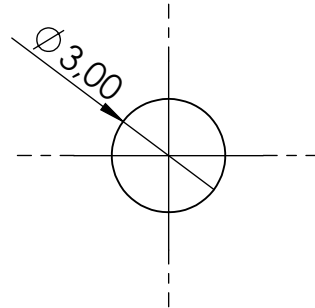
Projection






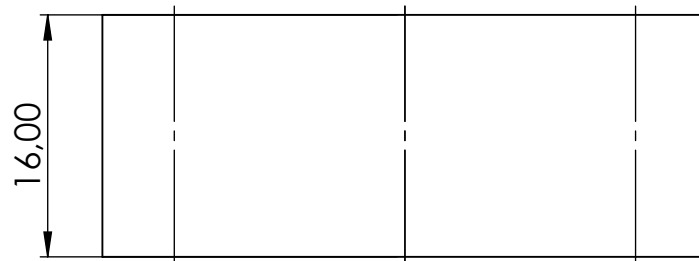
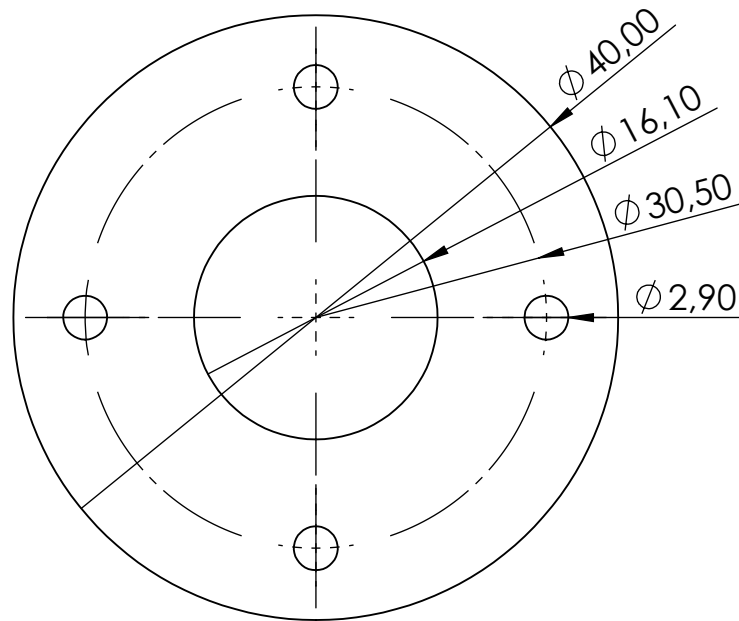
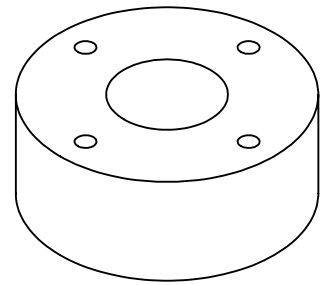
Checked by JAUME ORIOL LLADÓ 05/05/2023

Drawn by JAUME ORIOL LLADÓ 05/05/2023

Remarks



GRIPPER DESIGN FOR AN ASSISTIVE ROBOT IN A HOSPITAL ENVIRONMENT			  <div>UNIVERSITAT DE BARCELONA</div>	Part Drawing 12	
				Quantity 4	
ROD			Format: DIN A4	Scale 5:1	Projection 
Checked by	JAUME ORIOL LLADÓ	05/05/2023	Remarks		
Drawn by	JAUME ORIOL LLADÓ	05/05/2023			



GRIPPER DESIGN FOR AN ASSISTIVE ROBOT  
IN A HOSPITAL ENVIRONMENT



UNIVERSITAT DE  
BARCELONA



Part Drawing

13

Quantity 1

Projection



RESIN 80A ROLLER

Format:

DIN A4

Scale

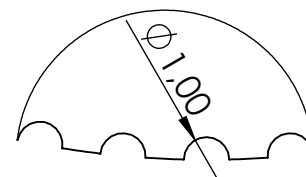
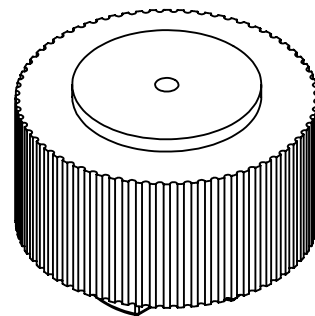
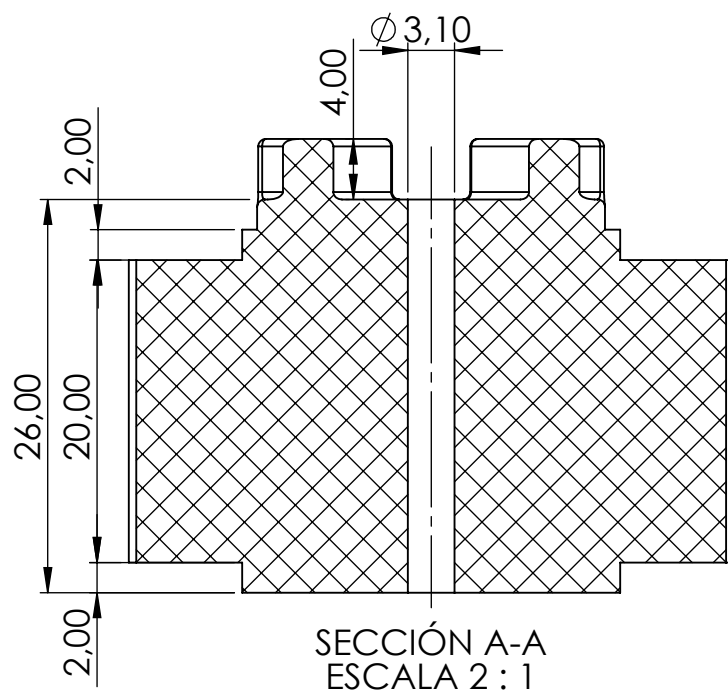
2:1

Checked by JAUME ORIOL LLADÓ 05/05/2023

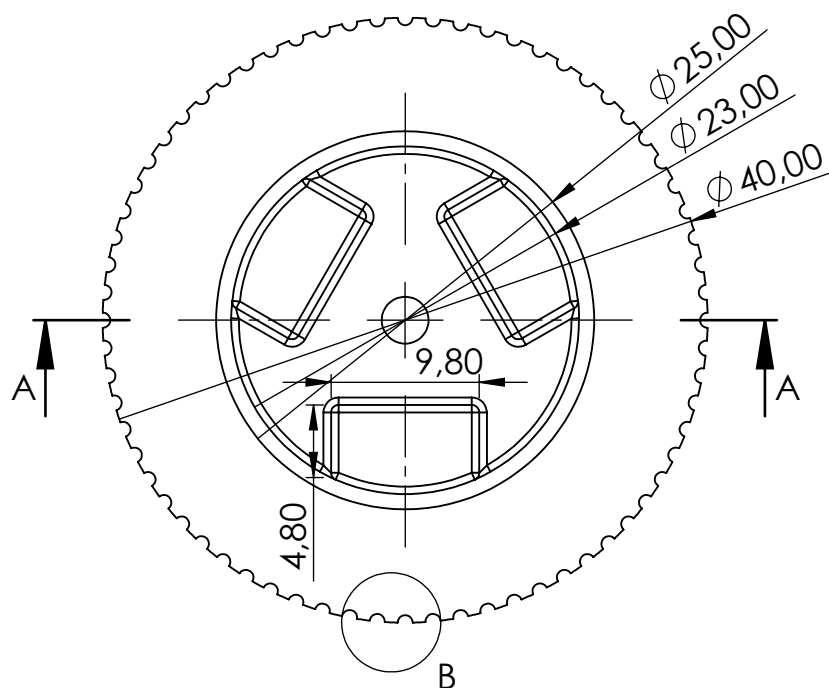
Drawn by JAUME ORIOL LLADÓ 05/05/2023

Remarks

PRINTED WITH RESIN 80A



DETALLE B  
ESCALA 6 : 1



GRIPPER DESIGN FOR AN ASSISTIVE ROBOT  
IN A HOSPITAL ENVIRONMENT



UNIVERSITAT DE  
BARCELONA



Part Drawing

14

Quantity 1

TOOTHED LATEX ROLLER

Format:

DIN A4

Scale

2:1

Projection



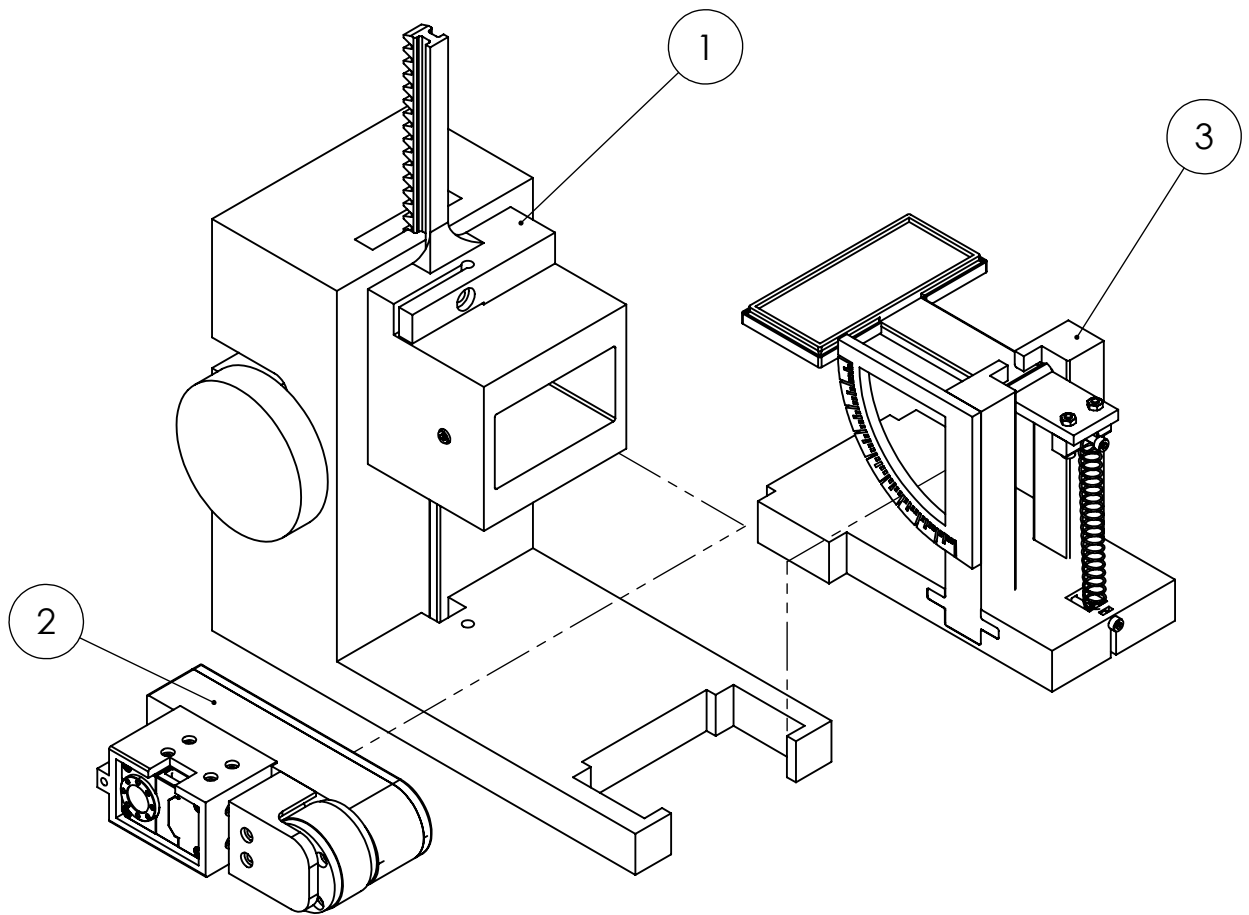
Checked by JAUME ORIOL LLADÓ 05/05/2023




Drawn by JAUME ORIOL LLADÓ 05/05/2023

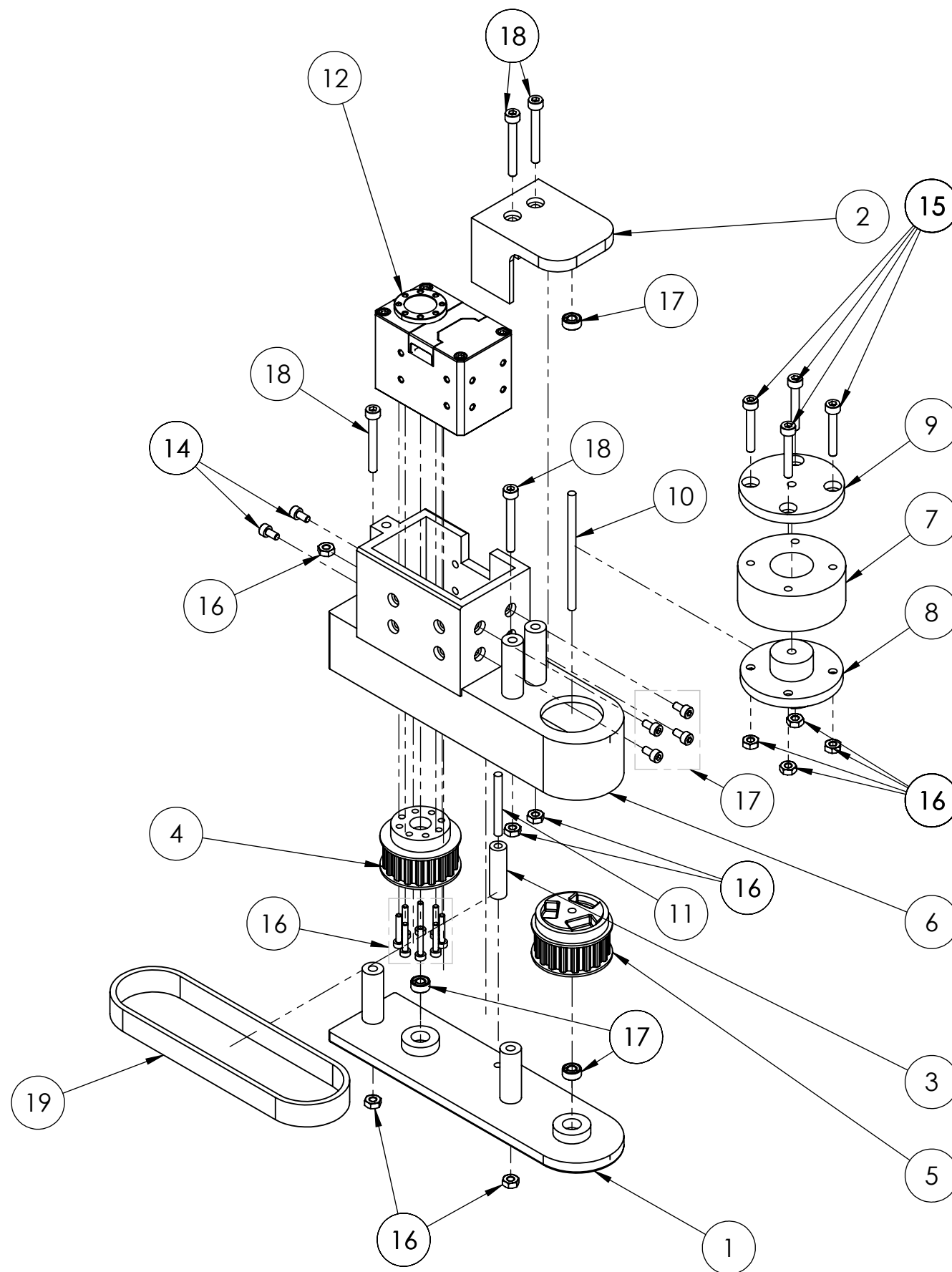
Remarks Z=68



ITEM NO.	PART NUMBER	QTY.
1	BASE	1
2	FINGER	1
3	ROCKER	1



GRIPPER DESIGN FOR AN ASSISTIVE ROBOT IN A HOSPITAL ENVIRONMENT			 UNIVERSITAT DE BARCELONA 	Part Drawing 15	
TEST-BENCH EXPLODED VIEW DIAGRAM				Quantity 1	
Checked by	JAUME ORIOL LLADÓ	10/06/2023	Format: DIN A4	Scale 1:3	Projection 
Drawn by	JAUME ORIOL LLADÓ	10/06/2023	Remarks		



ITEM NO.	PART NUMBER	QTY.
1	BASE PLATE	1
2	TOP PLATE	1
3	TENSION ROLLER	1
4	ENGINE PULLEY	1
5	ROLLER PULLEY	1
6	CASE	1
7	ROLLER	1
8	CAP PART 1	1
9	CAP PART 2	1
10	ROLLER ROD	1
11	TENSION ROLLER ROD	1
12	DUMMY_DC12.STP	1
13	ISO 4762 M2 X 12 - 12N	8
14	ISO 4762 M2.5 X 5 - 5N	6
15	ISO 4762 M3 X 20 - 20N	4
16	ISO - 4032 - M3 - D - N	9
17	ISO 15 ABB - 383 - 10,SI,NC,10_68	3
18	ISO 4762 M3 X 25 - 18N	4
19	CONTITECH SYNCHRONOUS BELT 10/T5/215 SS	1

GRIPPER DESIGN FOR AN ASSISTIVE ROBOT  
IN A HOSPITAL ENVIRONMENT



UNIVERSITAT DE  
BARCELONA



Drawing Part  
16

Quantity 1

FINGER EXPLODED VIEW DIAGRAM

Format:

DIN A3

Scale

1:2

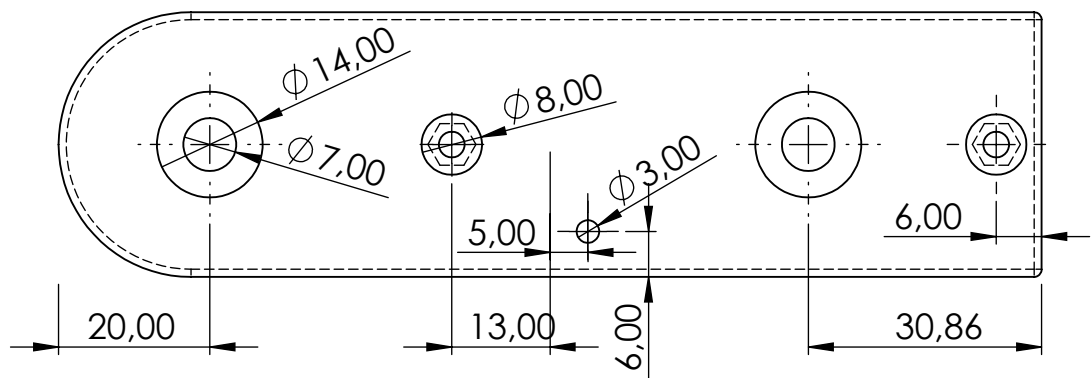
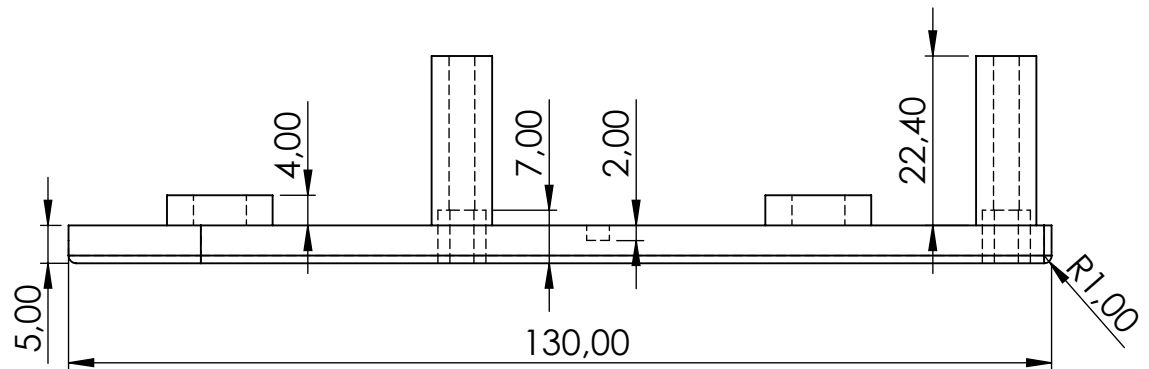
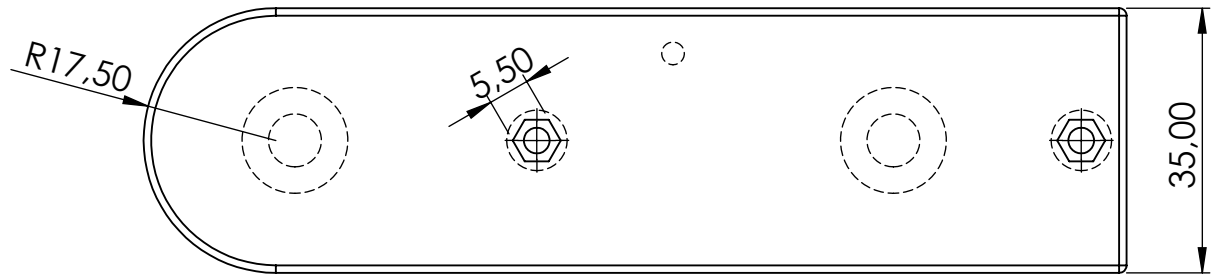
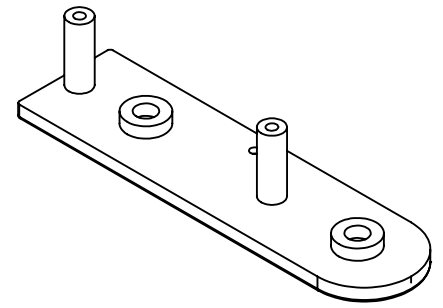
Projection



Checked by JAUME ORIOL LLADÓ 10/06/2023

Drawn by JAUME ORIOL LLADÓ 10/06/2023

Remarks



GRIPPER DESIGN FOR AN ASSISTIVE ROBOT  
IN A HOSPITAL ENVIRONMENT



UNIVERSITAT DE  
BARCELONA



Drawing Part  
17

Quantity 1

BASE PLATE

Format:

DIN A4

Scale

1:1

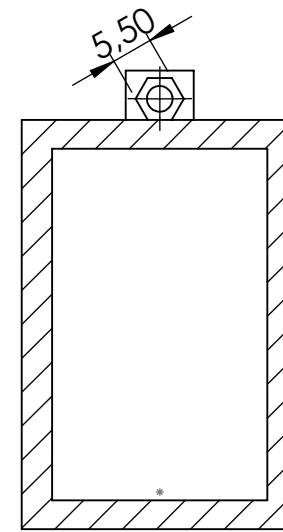
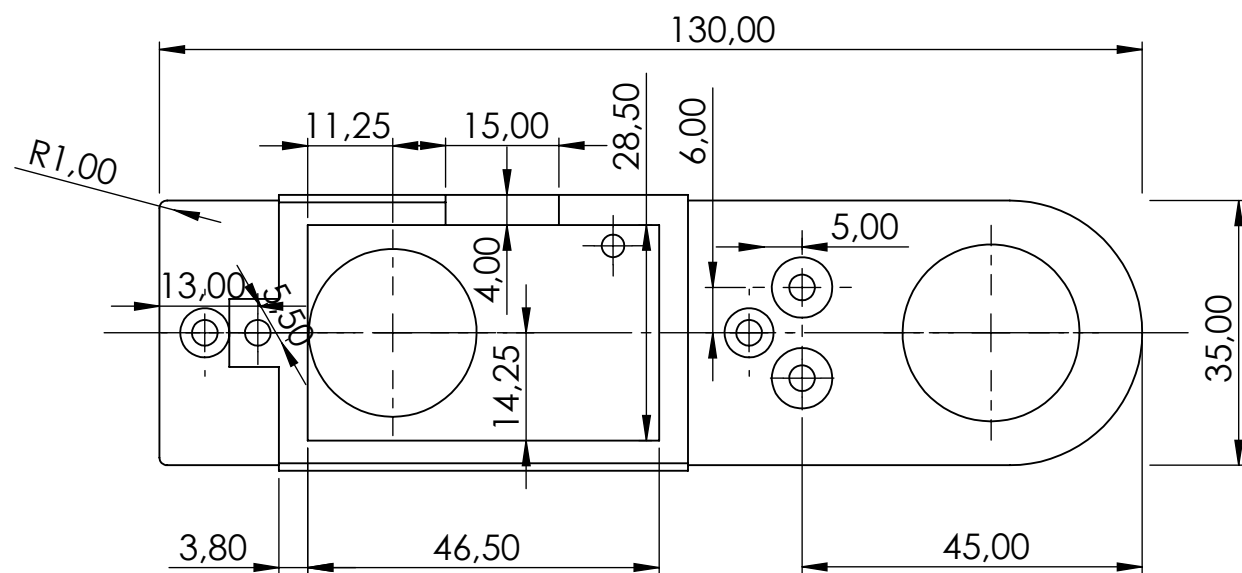
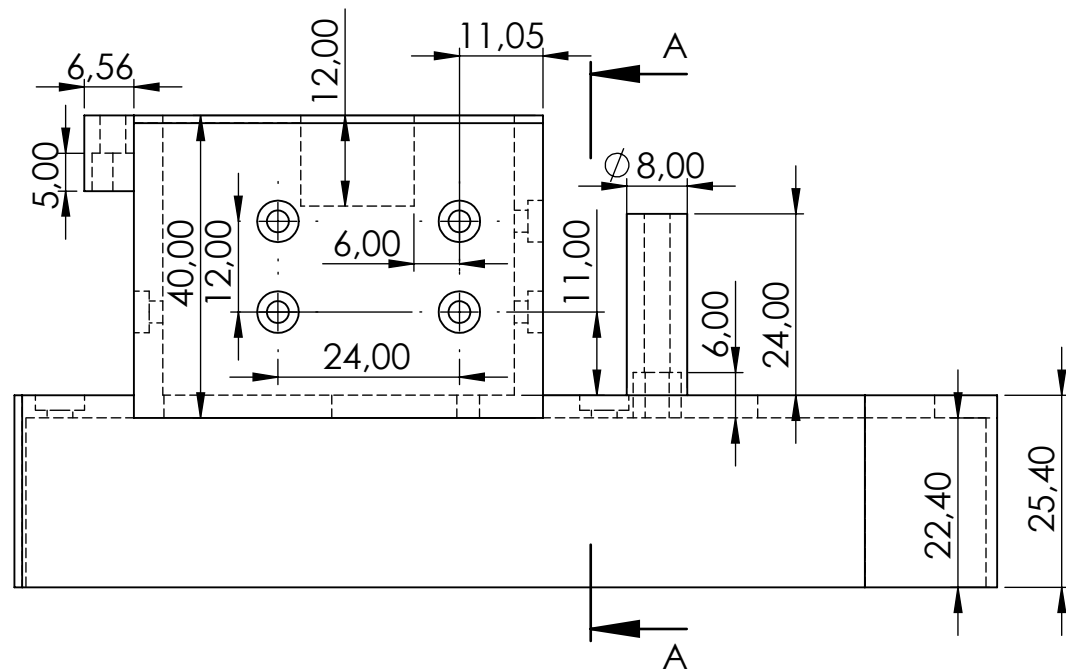
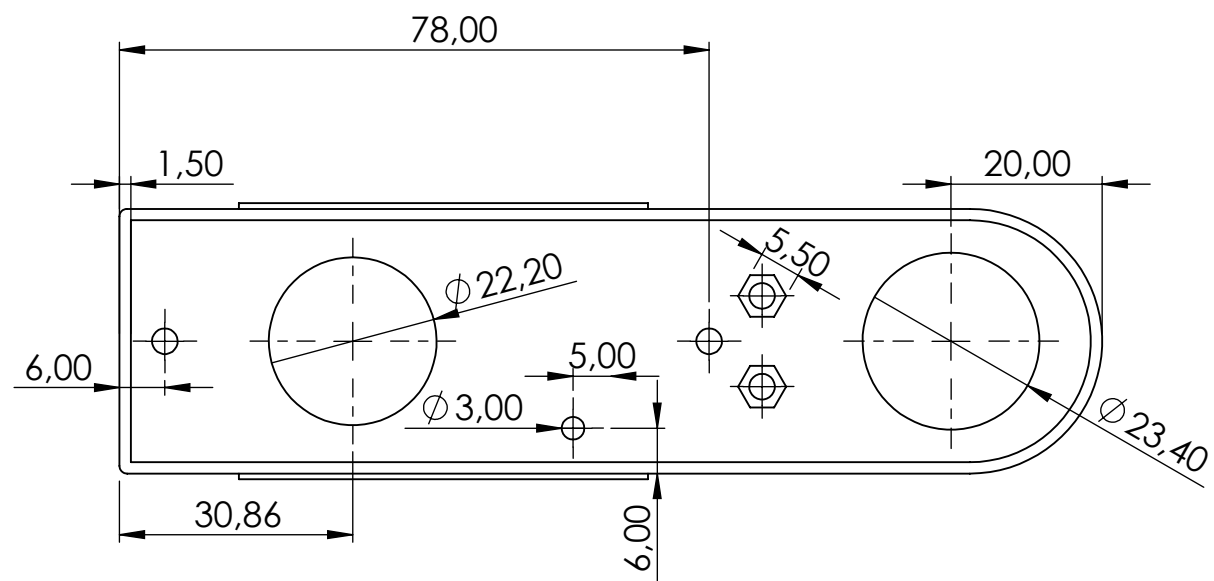
Projection



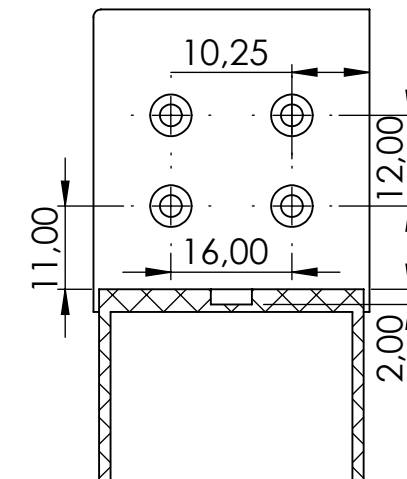
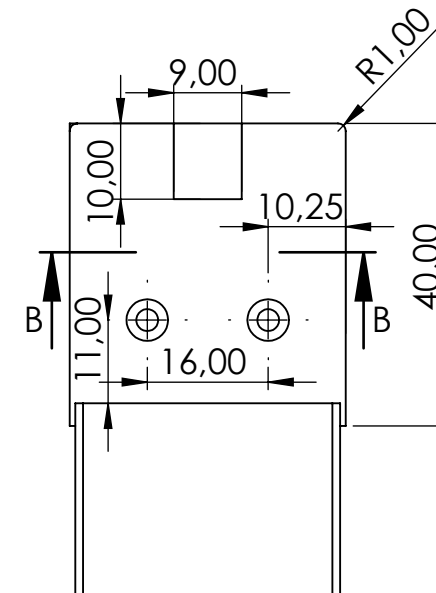
Checked by JAUME ORIOL LLADÓ 05/05/2023

Drawn by JAUME ORIOL LLADÓ 05/05/2023

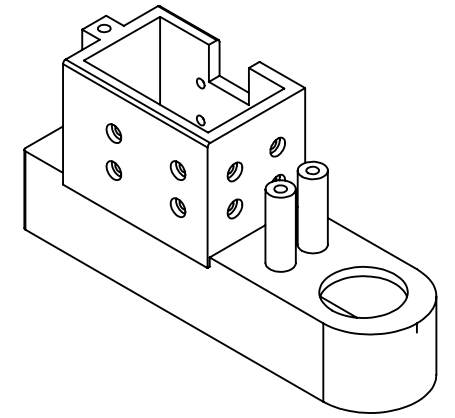
Remarks






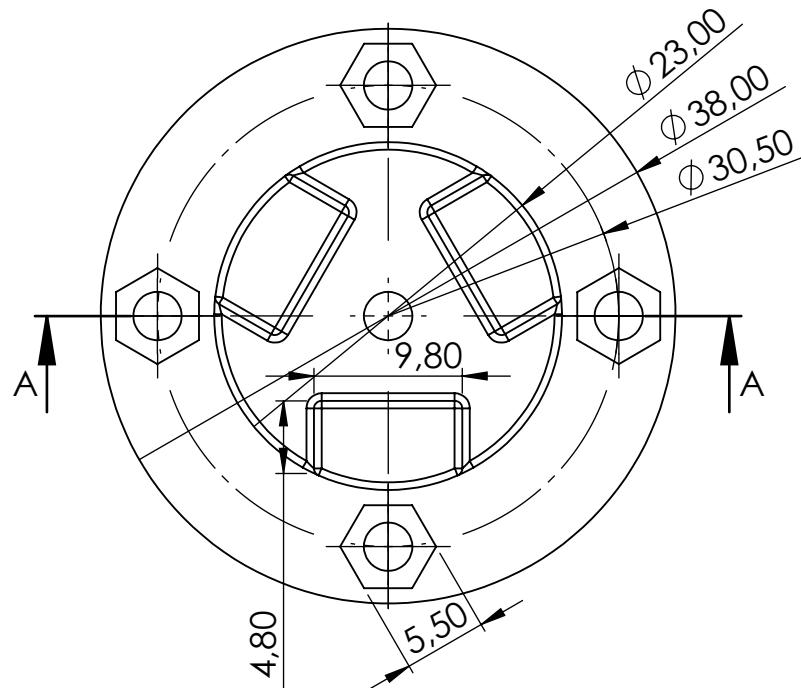
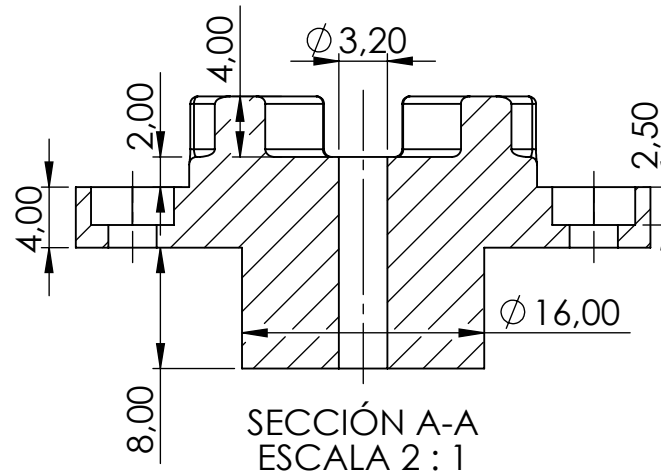
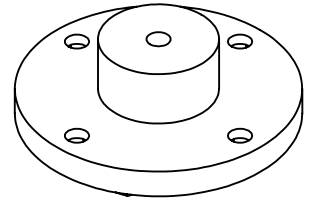
SECCIÓN B-B



SECCIÓN A-A



GRIPPER DESIGN FOR AN ASSISTIVE ROBOT IN A HOSPITAL ENVIRONMENT			  <div>UNIVERSITAT DE BARCELONA</div>	Drawing Part 18	
CASE				Quantity 1	
Checked by	JAUME ORIOL LLADÓ	05/05/2023	Format: DIN A3	Scale 1:1	Projection 
Drawn by	JAUME ORIOL LLADÓ	05/05/2023	Remarks		



GRIPPER DESIGN FOR AN ASSISTIVE ROBOT  
IN A HOSPITAL ENVIRONMENT



UNIVERSITAT DE  
BARCELONA



Drawing Part

19

Quantity 1

CAP PART 1

Format:

DIN A4

Scale

2:1

Projection

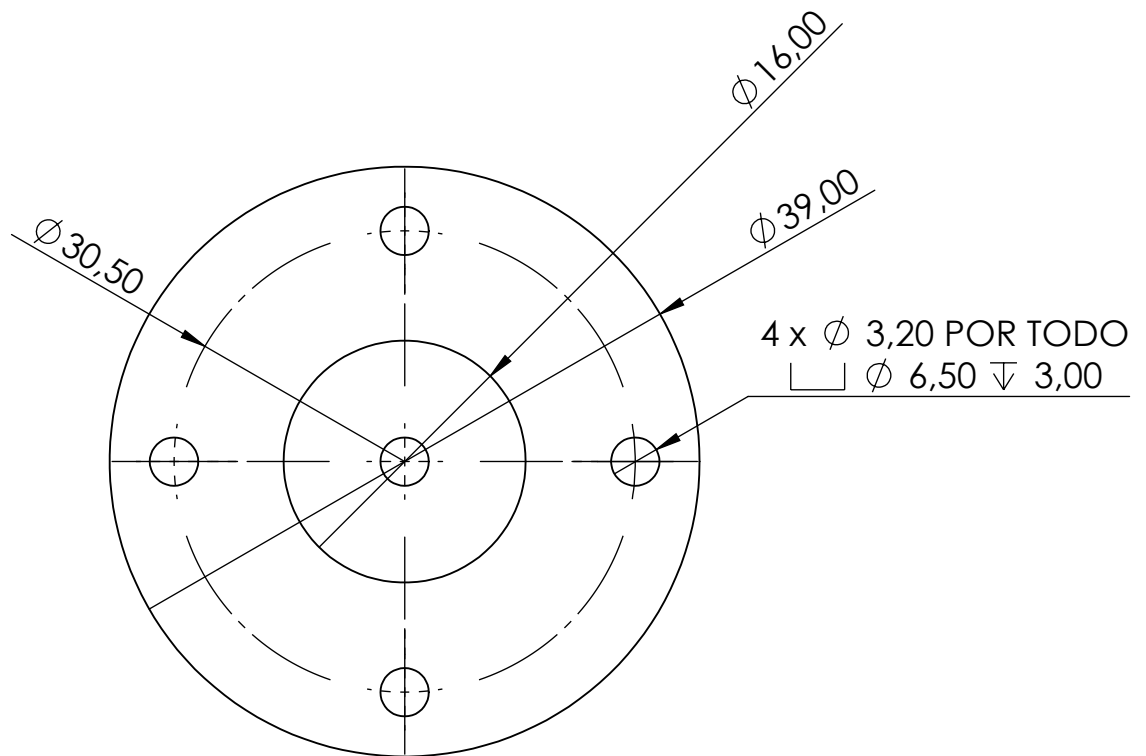
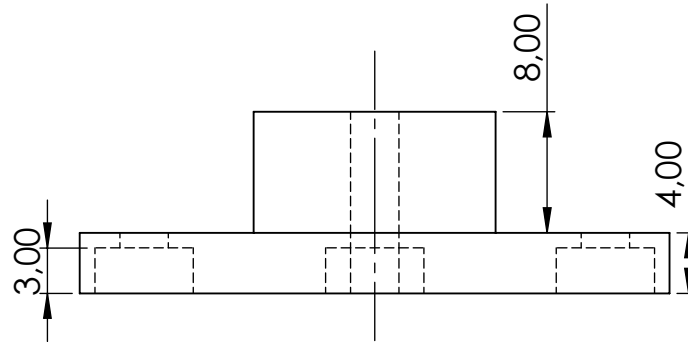
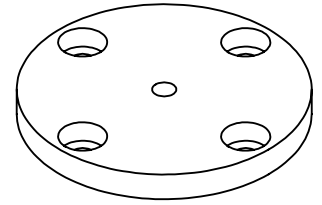


Checked by JAUME ORIOL LLADÓ 05/05/2023

Drawn by JAUME ORIOL LLADÓ 05/05/2023

Remarks

ALL ROUNDINGS ARE 0.5mm



GRIPPER DESIGN FOR AN ASSISTIVE ROBOT  
IN A HOSPITAL ENVIRONMENT



UNIVERSITAT DE  
BARCELONA



Drawing Part  
20

Quantity 1

CAP PART 2

Format:

DIN A4

Scale

2:1

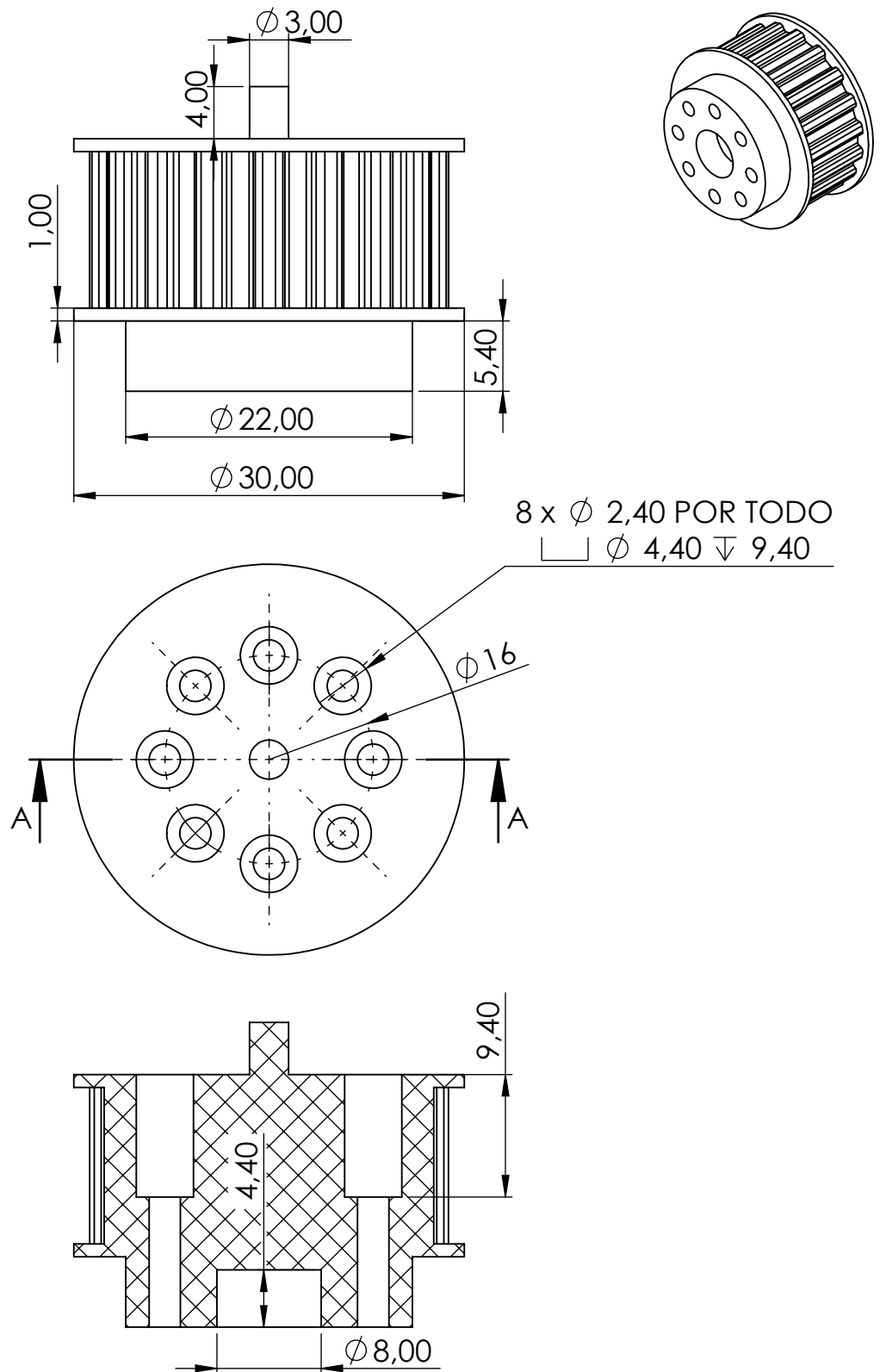
Projection



Checked by JAUME ORIOL LLADÓ 05/05/2023

Drawn by JAUME ORIOL LLADÓ 05/05/2023

Remarks



SECCIÓN A-A

GRIPPER DESIGN FOR AN ASSISTIVE ROBOT  
IN A HOSPITAL ENVIRONMENT



UNIVERSITAT DE  
BARCELONA



Drawing Part  
21

Quantity 1

ENGINE PULLEY

Format:

DIN A4

Scale

2:1

Projection



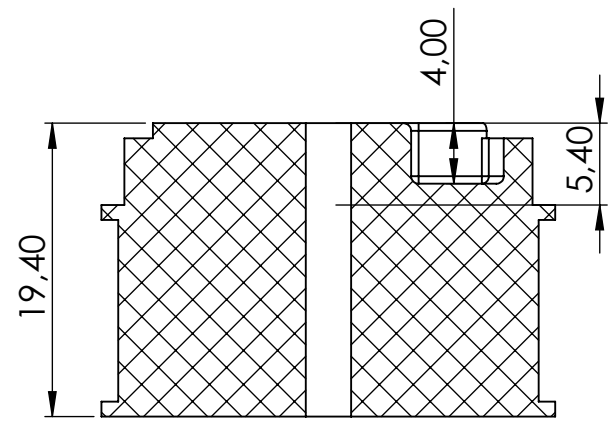
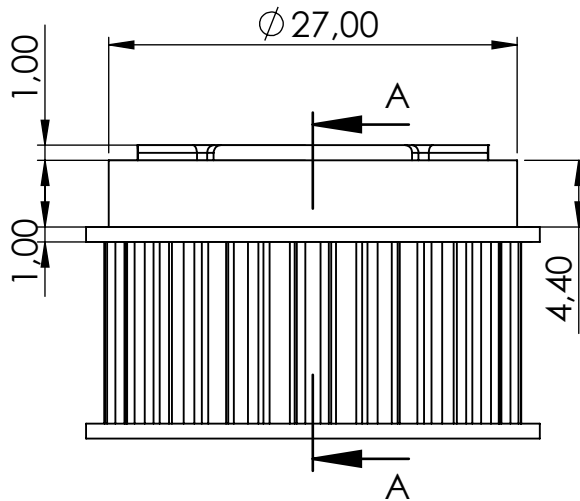
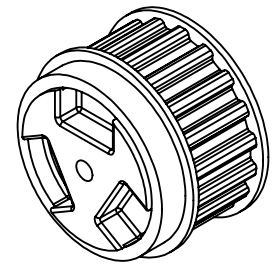
Checked by JAUME ORIOL LLADÓ 05/05/2023

Drawn by JAUME ORIOL LLADÓ 05/05/2023

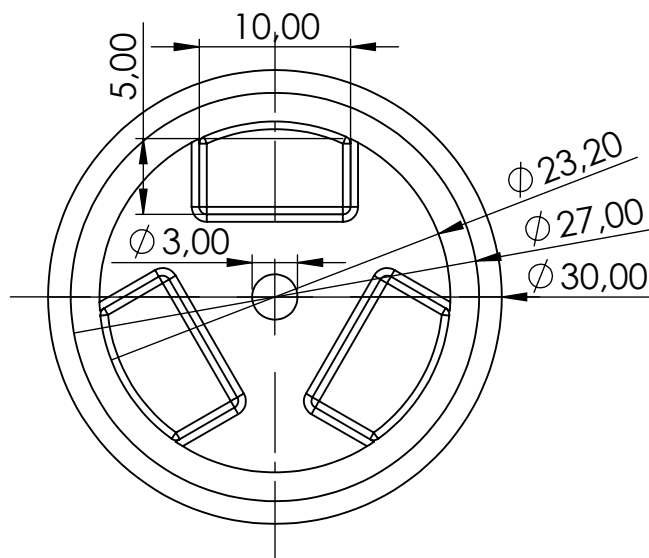
Remarks

T5 PULLEY Z=18





SECCIÓN A-A



GRIPPER DESIGN FOR AN ASSISTIVE ROBOT  
IN A HOSPITAL ENVIRONMENT



UNIVERSITAT DE  
BARCELONA



Drawing Part

22

Quantity 1

ROLLER AXIS

Format:

DIN A4

Scale

2:1

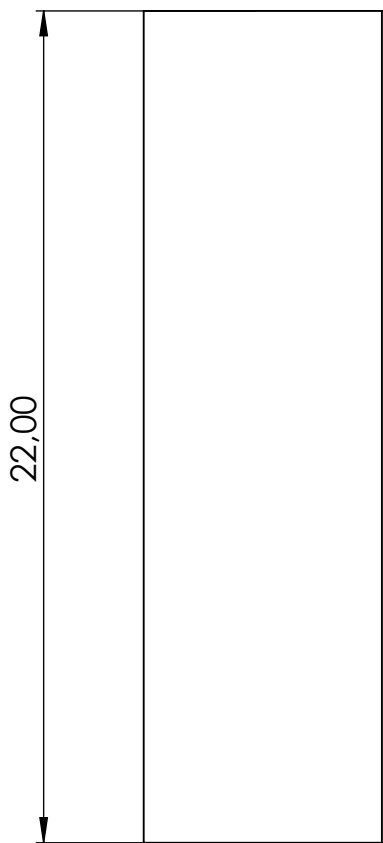
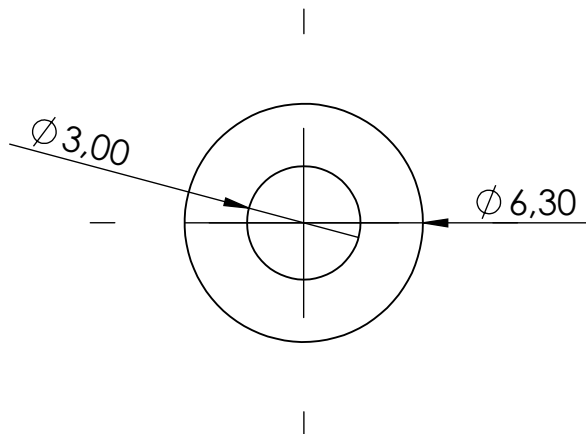
Projection



Checked by JAUME ORIOL LLADÓ 05/05/2023

Drawn by JAUME ORIOL LLADÓ 05/05/2023

Remarks T5 PULLEY Z=18, ALL ROUNDINGS ARE 0.5mm



GRIPPER DESIGN FOR AN ASSISTIVE ROBOT  
IN A HOSPITAL ENVIRONMENT



UNIVERSITAT DE  
BARCELONA



Drawing Part  
23

Quantity 1

TENSION ROLLER

Format:

DIN A4

Scale

5:1

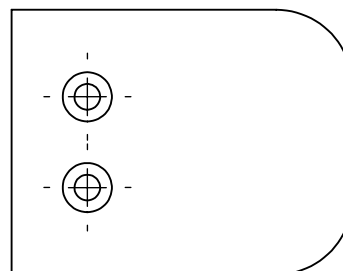
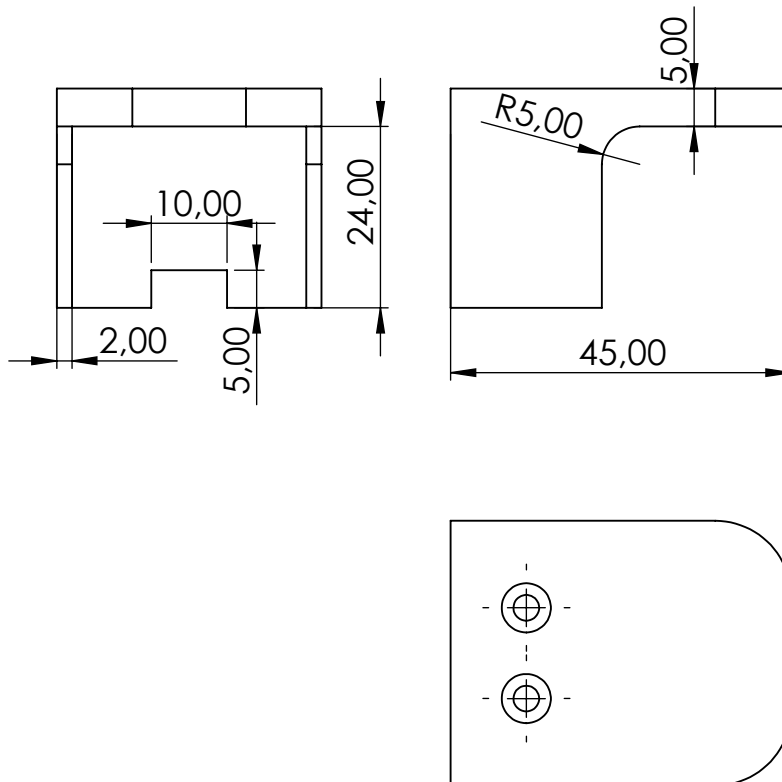
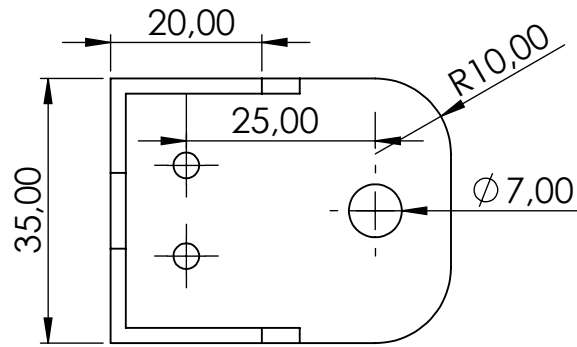
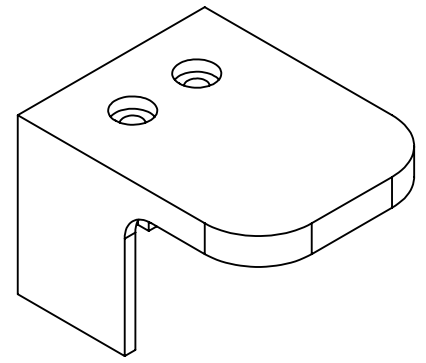
Projection



Checked by JAUME ORIOL LLADÓ 05/05/2023

Drawn by JAUME ORIOL LLADÓ 05/05/2023

Remarks



GRIPPER DESIGN FOR AN ASSISTIVE ROBOT  
IN A HOSPITAL ENVIRONMENT



UNIVERSITAT DE  
BARCELONA



Drawing Part

24

Quantity 1

TOP PLATE

Format:

DIN A4

Scale

1:1

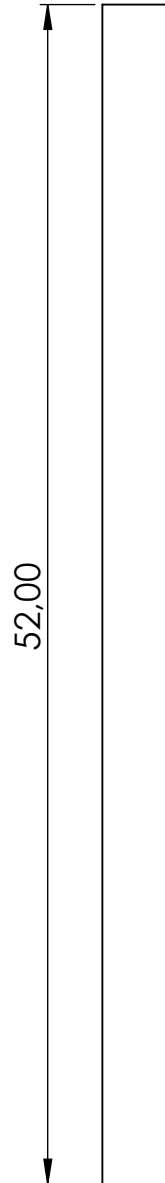
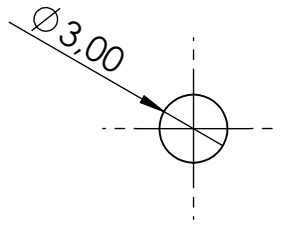
Projection



Checked by JAUME ORIOL LLADÓ 05/05/2023

Drawn by JAUME ORIOL LLADÓ 05/05/2023

Remarks



GRIPPER DESIGN FOR AN ASSISTIVE ROBOT  
IN A HOSPITAL ENVIRONMENT



UNIVERSITAT DE  
BARCELONA



Part Drawing  
25

Quantity 1

ROLLER ROD

Format:

DIN A4

Scale

3:1

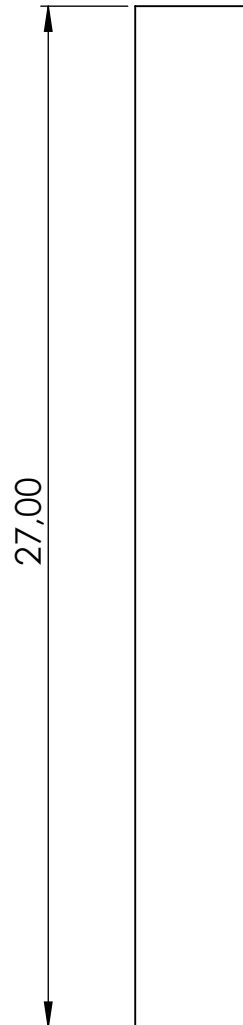
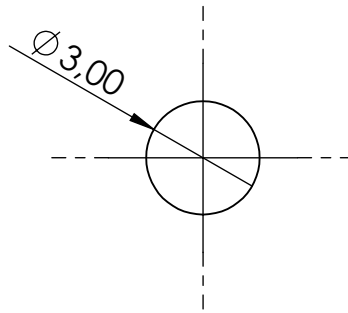
Projection



Checked by JAUME ORIOL LLADÓ 05/05/2023

Drawn by JAUME ORIOL LLADÓ 05/05/2023

Remarks



GRIPPER DESIGN FOR AN ASSISTIVE ROBOT  
IN A HOSPITAL ENVIRONMENT



UNIVERSITAT DE  
BARCELONA



Part Drawing  
26

Quantity 1

TENSION ROLLER ROD

Format:

DIN A4

Scale

5:1

Projection

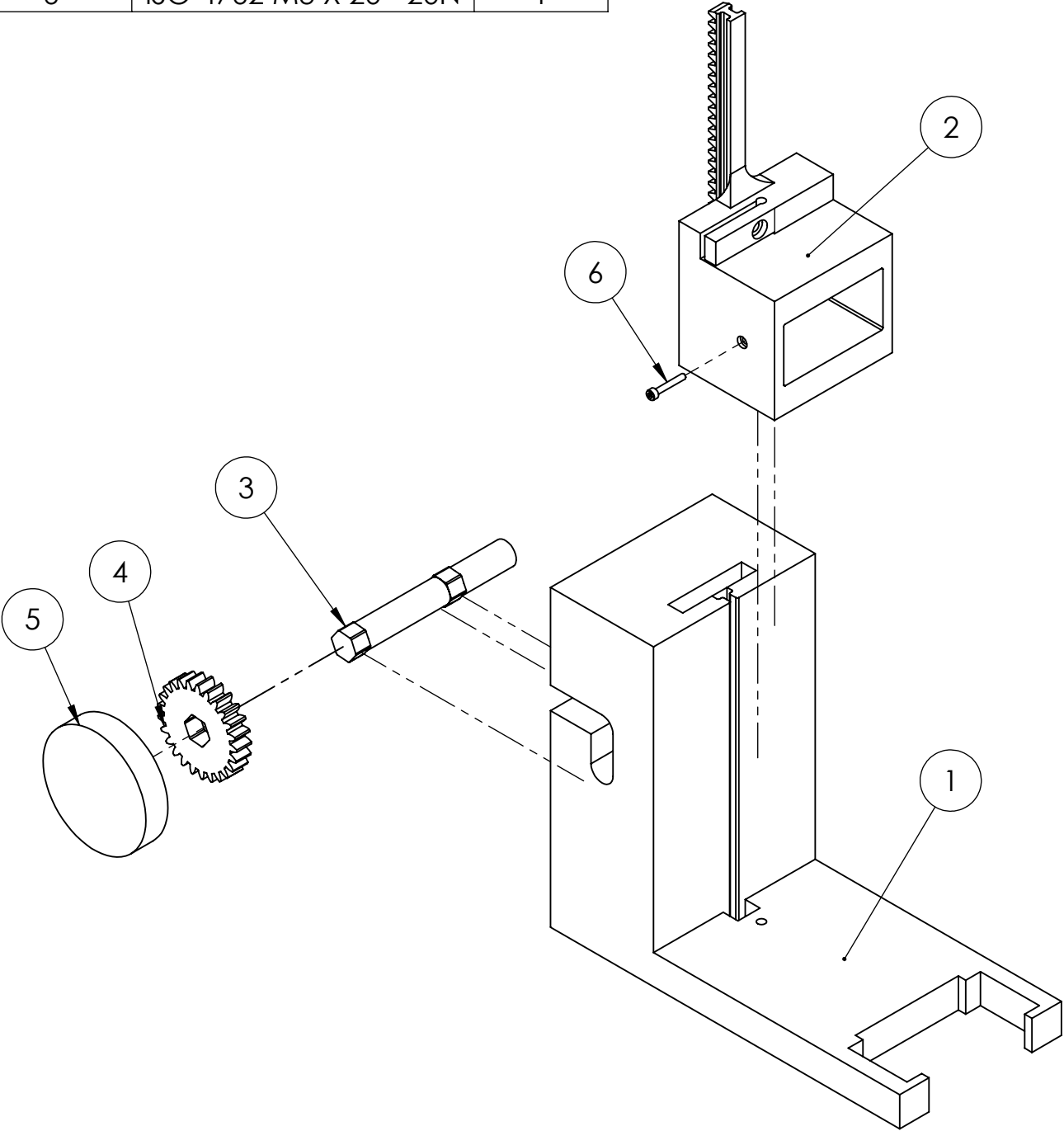





Checked by JAUME ORIOL LLADÓ 05/05/2023

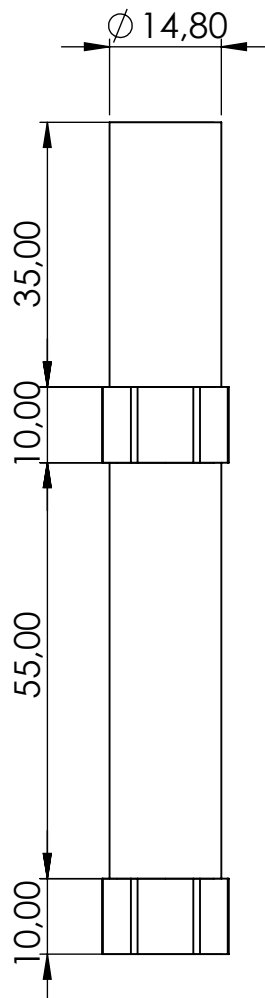
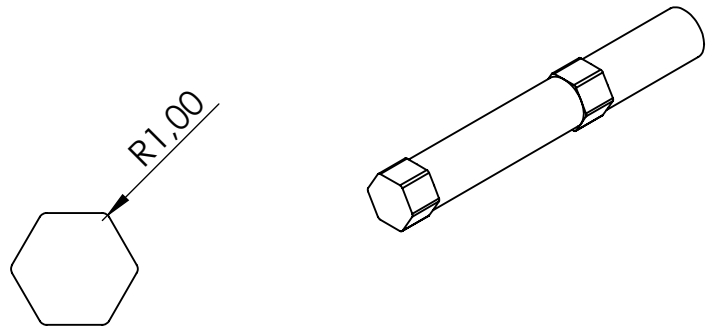
Drawn by JAUME ORIOL LLADÓ 05/05/2023



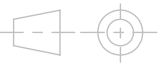
Remarks

ITEM NO.	PART NUMBER	QTY.
1	L STRUCTURE	1
2	RACK	1
3	CRANK SHAFT	1
4	GEAR	1
5	HANDLE	1
6	ISO 4762 M3 X 20 - 20N	1

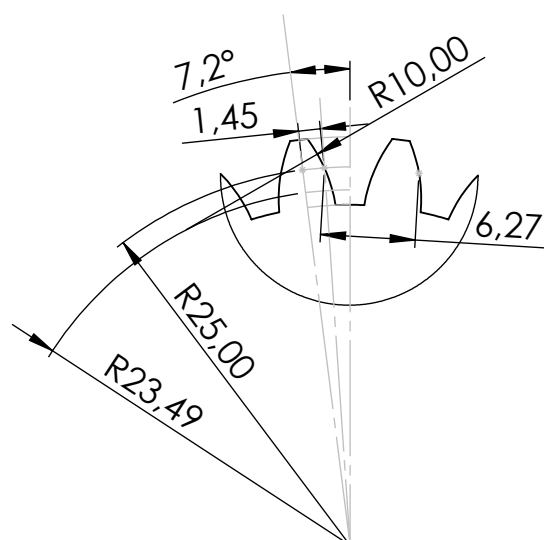
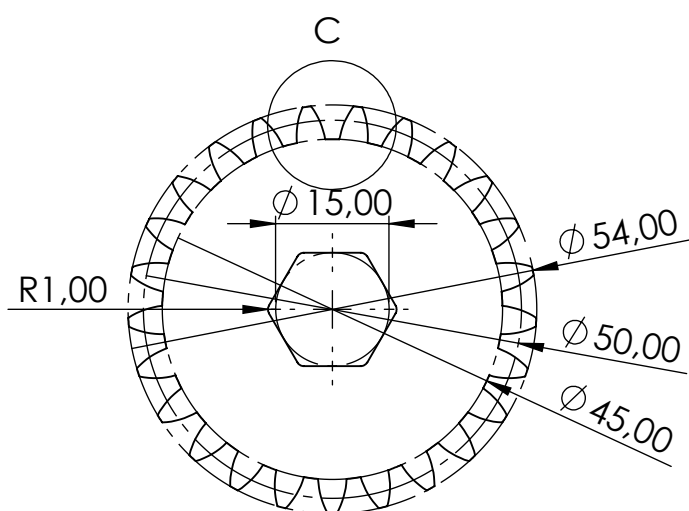
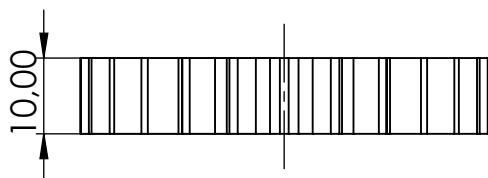
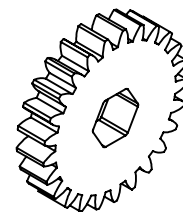


GRIPPER DESIGN FOR AN ASSISTIVE ROBOT IN A HOSPITAL ENVIRONMENT			 	Part Drawing
			27	
BASE EXPLODED VIEW DIAGRAM			Quantity	
			1	
			Format:	Scale
			DIN A4	1:3
			Projection	
				
Checked by	JAUME ORIOL LLADÓ	05/05/2023	Remarks	
Drawn by	JAUME ORIOL LLADÓ	05/05/2023		



GRIPPER DESIGN FOR AN ASSISTIVE ROBOT IN A HOSPITAL ENVIRONMENT			 UNIVERSITAT DE BARCELONA		Drawing Part 28
CRANK SHAFT					Quantity 1
Checked by	JAUME ORIOL LLADÓ	05/05/2023	Format: DIN A4	Scale 1:1	Projection 
Drawn by	JAUME ORIOL LLADÓ	05/05/2023	Remarks		





DETALLE C  
ESCALA 2 : 1

GRIPPER DESIGN FOR AN ASSISTIVE ROBOT  
IN A HOSPITAL ENVIRONMENT



UNIVERSITAT DE  
BARCELONA



Drawing Part  
29

Quantity 1

GEAR

Format:

DIN A4

Scale

1:1

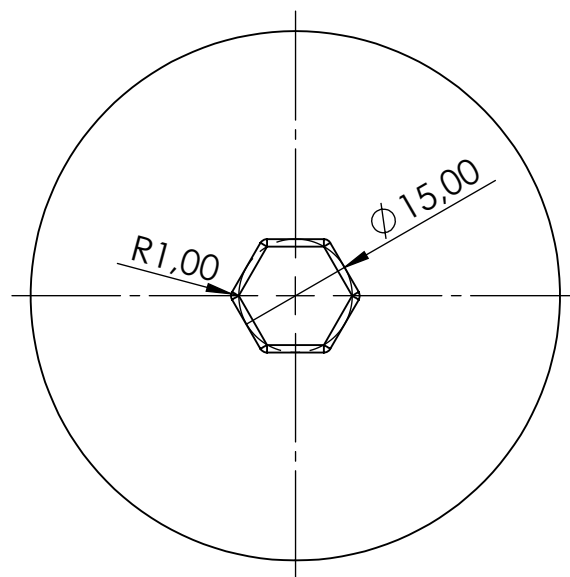
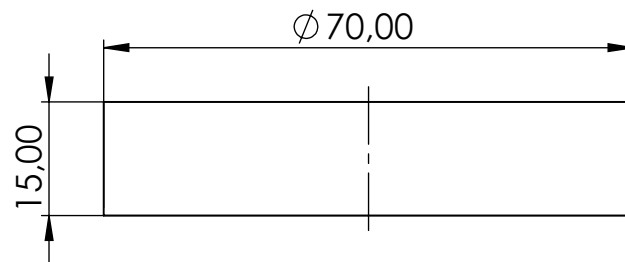
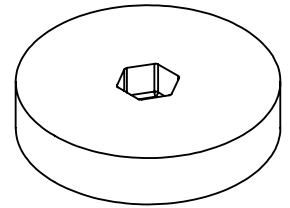
Projection



Checked by JAUME ORIOL LLADÓ 05/05/2023

Drawn by JAUME ORIOL LLADÓ 05/05/2023

Remarks



GRIPPER DESIGN FOR AN ASSISTIVE ROBOT  
IN A HOSPITAL ENVIRONMENT



UNIVERSITAT DE  
BARCELONA



Drawing Part  
30

Quantity 1

HANDLE

Format:

DIN A4

Scale

1:1

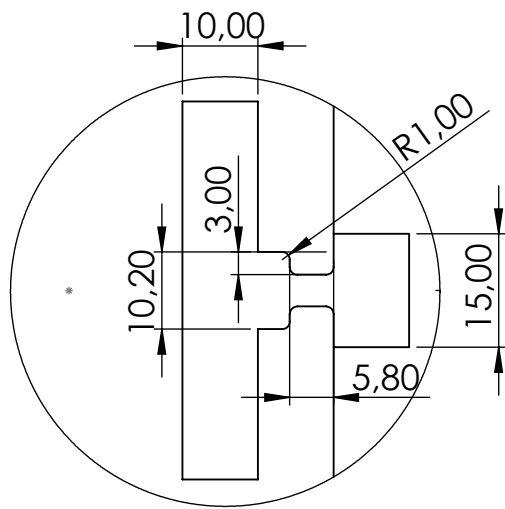
Projection



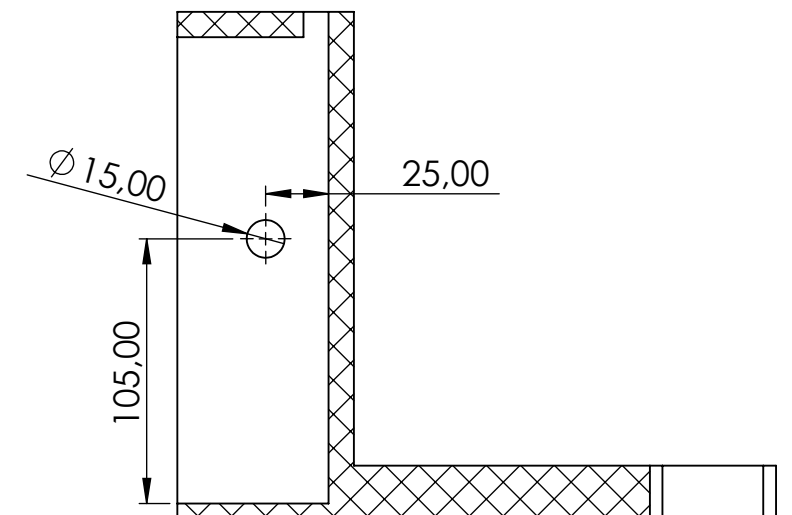
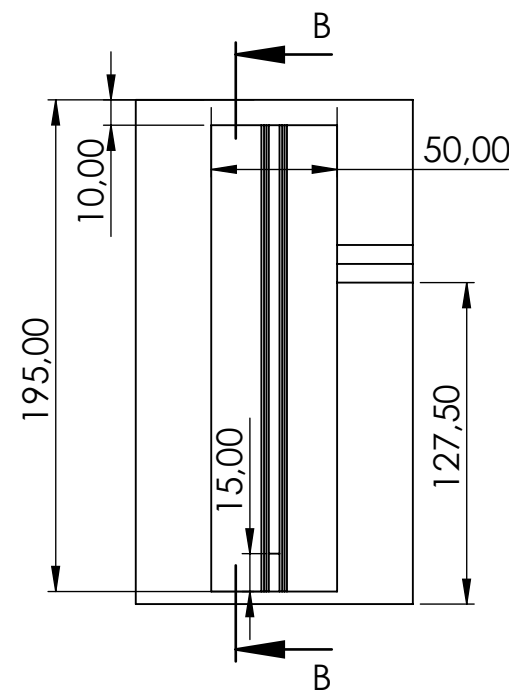
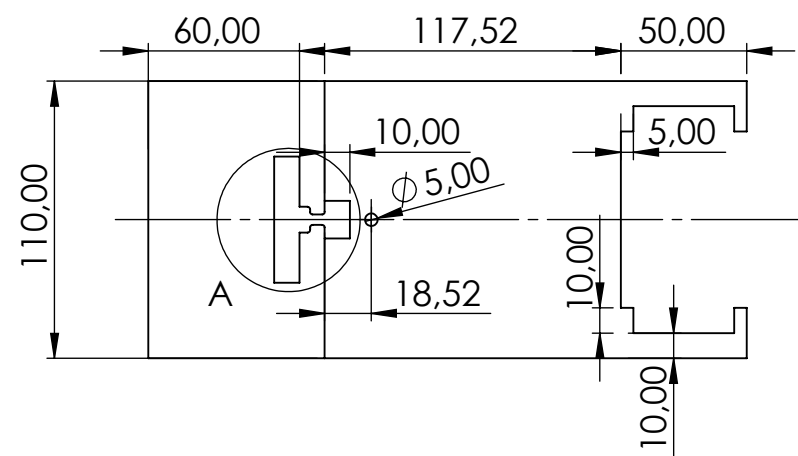
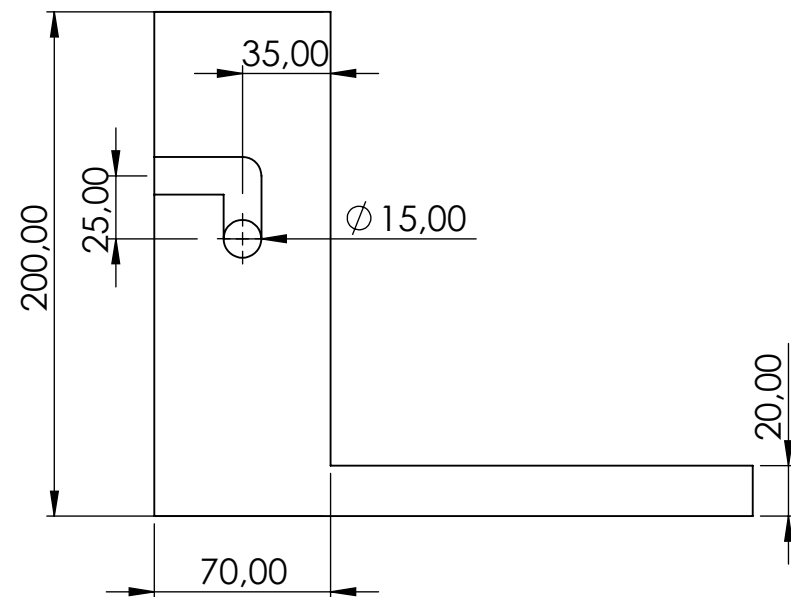
Checked by JAUME ORIOL LLADÓ 05/05/2023

Drawn by JAUME ORIOL LLADÓ 05/05/2023

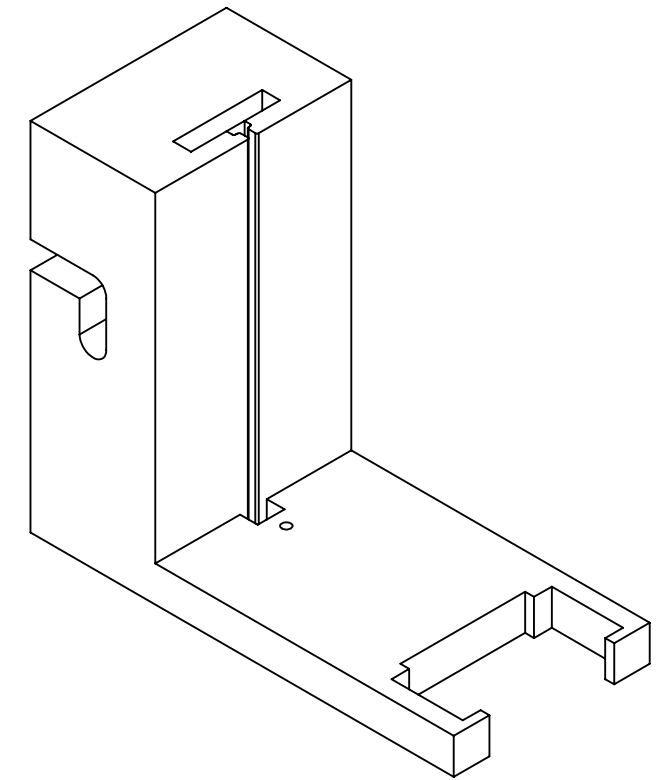
Remarks






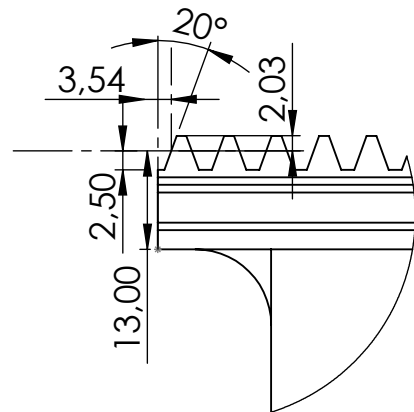
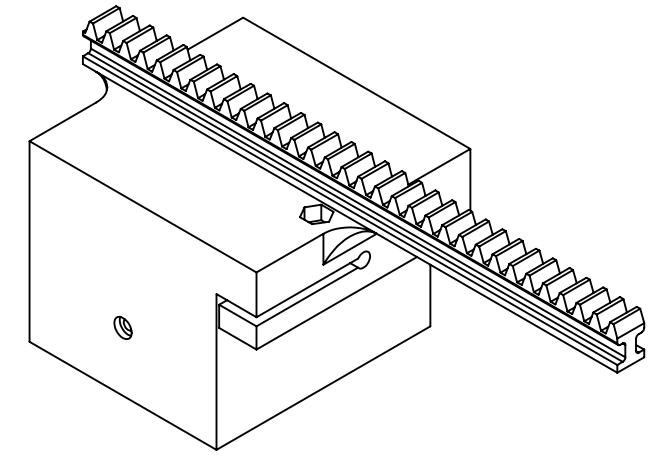
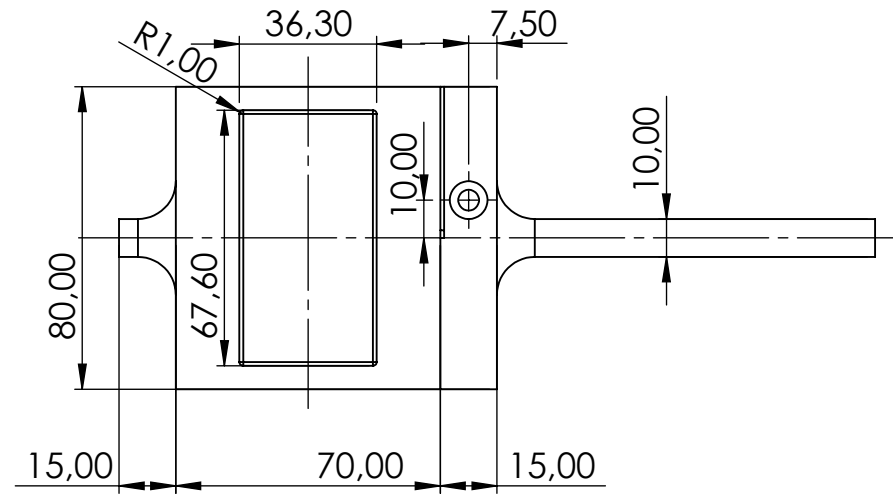
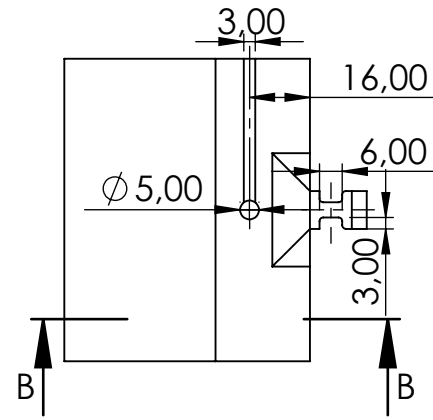
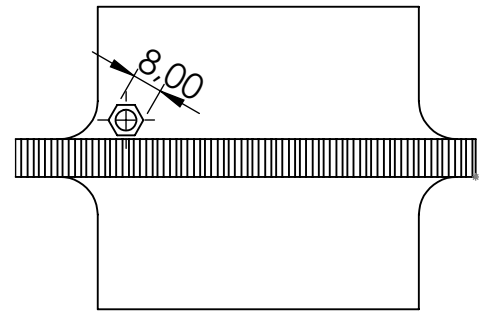
DETALLE A  
ESCALA 1 : 1



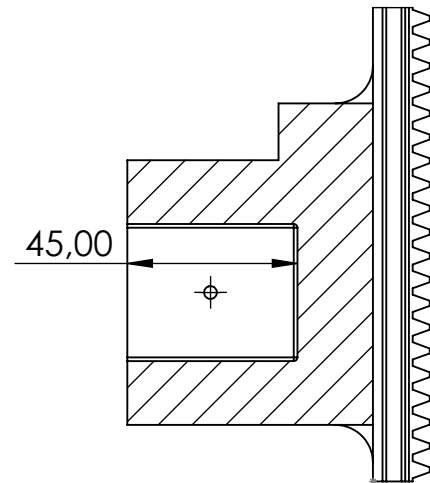
SECCIÓN B-B  
ESCALA 1 : 3



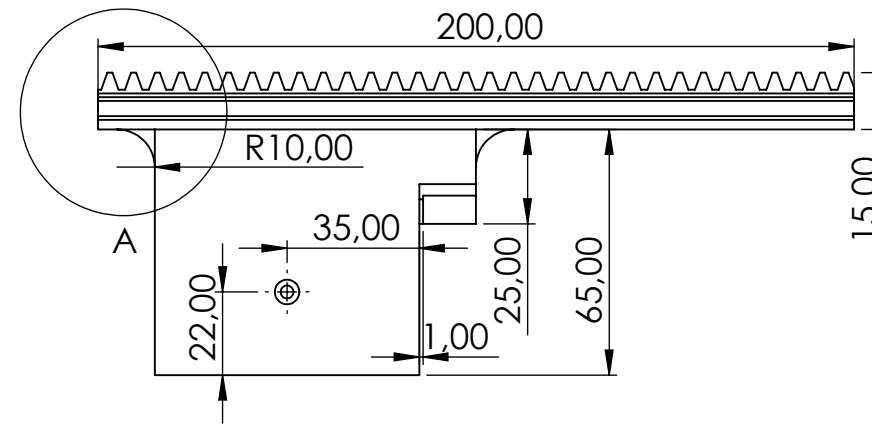
GRIPPER DESIGN FOR AN ASSISTIVE ROBOT IN A HOSPITAL ENVIRONMENT			 UNIVERSITAT DE BARCELONA		Drawing Part 31
L STRUCTURE					Quantity 1
Checked by	JAUME ORIOL LLADÓ	05/05/2023	Format: DIN A3	Scale 1:3	Projection 
Drawn by	JAUME ORIOL LLADÓ	05/05/2023	Remarks		






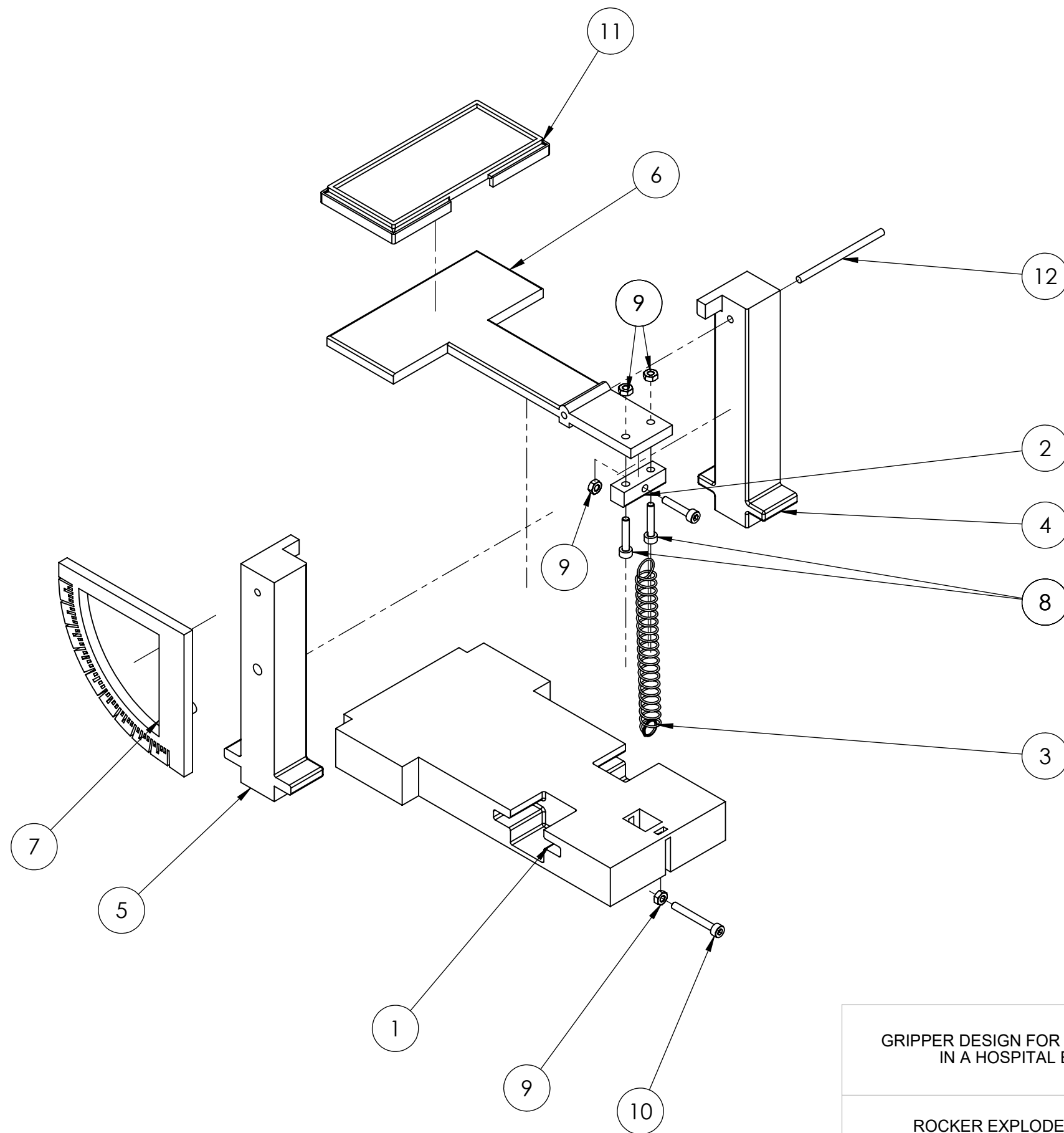
DETALLE A  
ESCALA 1 : 1



SECCIÓN B-B



GRIPPER DESIGN FOR AN ASSISTIVE ROBOT IN A HOSPITAL ENVIRONMENT			 UNIVERSITAT DE BARCELONA 	Drawing Part 32	
RACK				Quantity 1	
Checked by	JAUME ORIOL LLADÓ	05/05/2023	Format:  DIN A3	Scale  1:2	Projection 
Drawn by	JAUME ORIOL LLADÓ	05/05/2023			



ITEM NO.	PART NUMBER	QTY.
1	ROCKER BASE	1
2	SPRING CONNECTOR	1
3	SPRING	1
4	PILLAR	1
5	PILLAR WITH PROTRACTOR	1
6	ROCKER ARM	1
7	PROTRACTOR	1
8	ISO 4762 M3 X 16 - 16N	3
9	ISO - 4032 - M3 - D - N	4
10	ISO 4762 M3 X 25 - 18N	1
11	MATERIAL PLATFORM	1
12	ROCKER ROD	1

GRIPPER DESIGN FOR AN ASSISTIVE ROBOT  
IN A HOSPITAL ENVIRONMENT



UNIVERSITAT DE  
BARCELONA



Drawing Part  
33

Quantity 1

ROCKER EXPLODED VIEW DIAGRAM

Format:

DIN A3

Scale

1:2

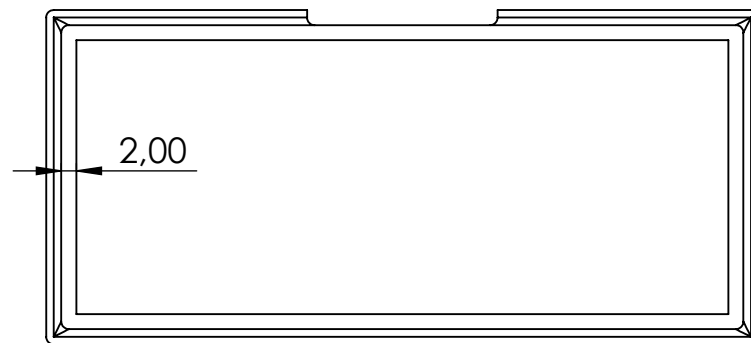
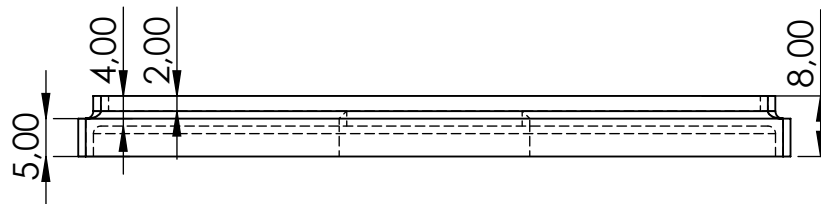
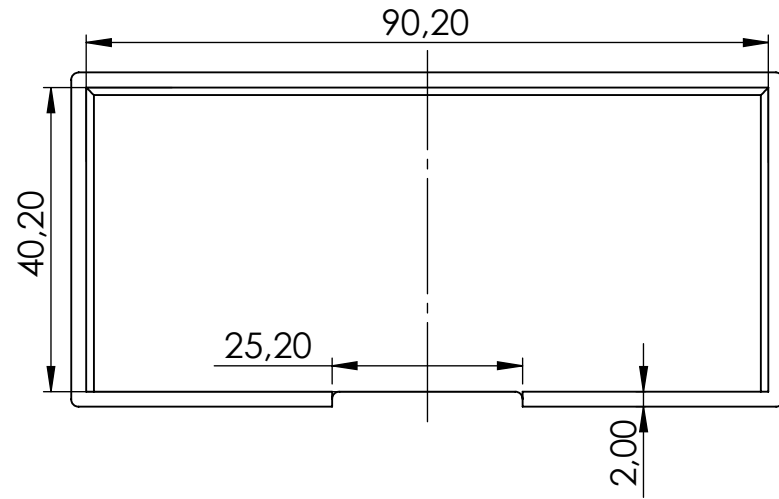
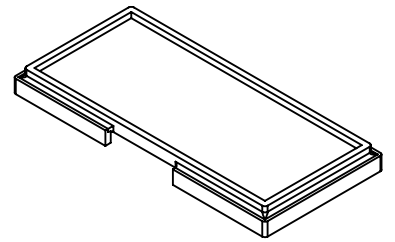
Projection



Checked by JAUME ORIOL LLADÓ 10/06/2023

Drawn by JAUME ORIOL LLADÓ 10/06/2023

Remarks



GRIPPER DESIGN FOR AN ASSISTIVE ROBOT  
IN A HOSPITAL ENVIRONMENT



UNIVERSITAT DE  
BARCELONA



Drawing Part

34

Quantity 1

MATERIAL PLATFORM

Format:

DIN A4

Scale

1:1

Projection

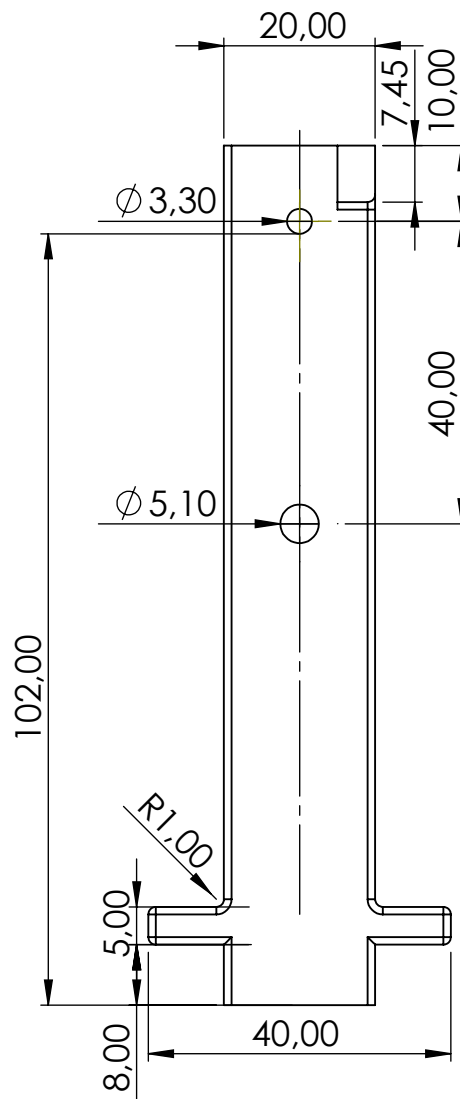
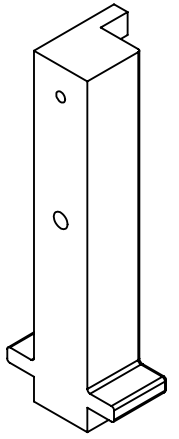
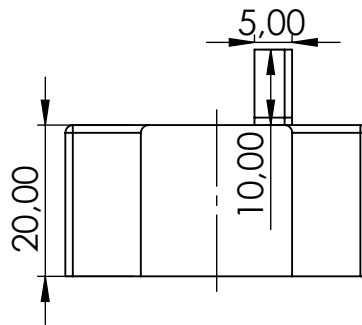


Checked by JAUME ORIOL LLADÓ 17/05/2023

Drawn by JAUME ORIOL LLADÓ 17/05/2023

Remarks

ALL ROUNDINGS ARE OF 1mm



GRIPPER DESIGN FOR AN ASSISTIVE ROBOT  
IN A HOSPITAL ENVIRONMENT



UNIVERSITAT DE  
BARCELONA



Drawing Part  
35

Quantity 1

PILLAR WITH PROTRACTOR

Format:

DIN A4

Scale

1:1

Projection

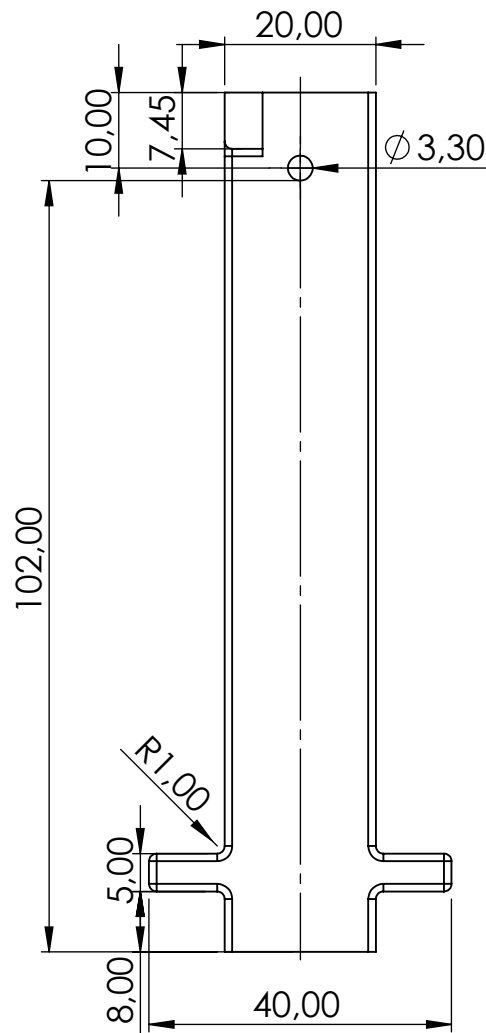
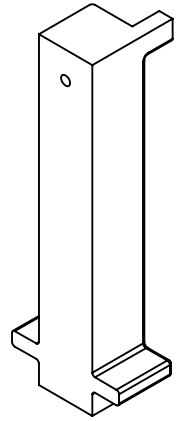
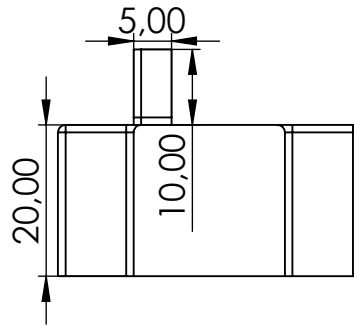


Checked by JAUME ORIOL LLADÓ 17/05/2023

Drawn by JAUME ORIOL LLADÓ 17/05/2023

Remarks





GRIPPER DESIGN FOR AN ASSISTIVE ROBOT  
IN A HOSPITAL ENVIRONMENT



UNIVERSITAT DE  
BARCELONA



Drawing Part

36

Quantity 1

PILLAR

Format:

DIN A4

Scale

1:1

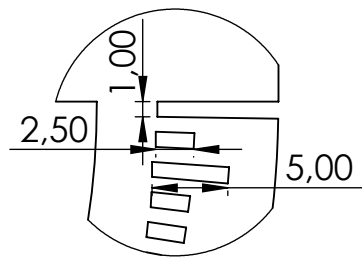
Projection



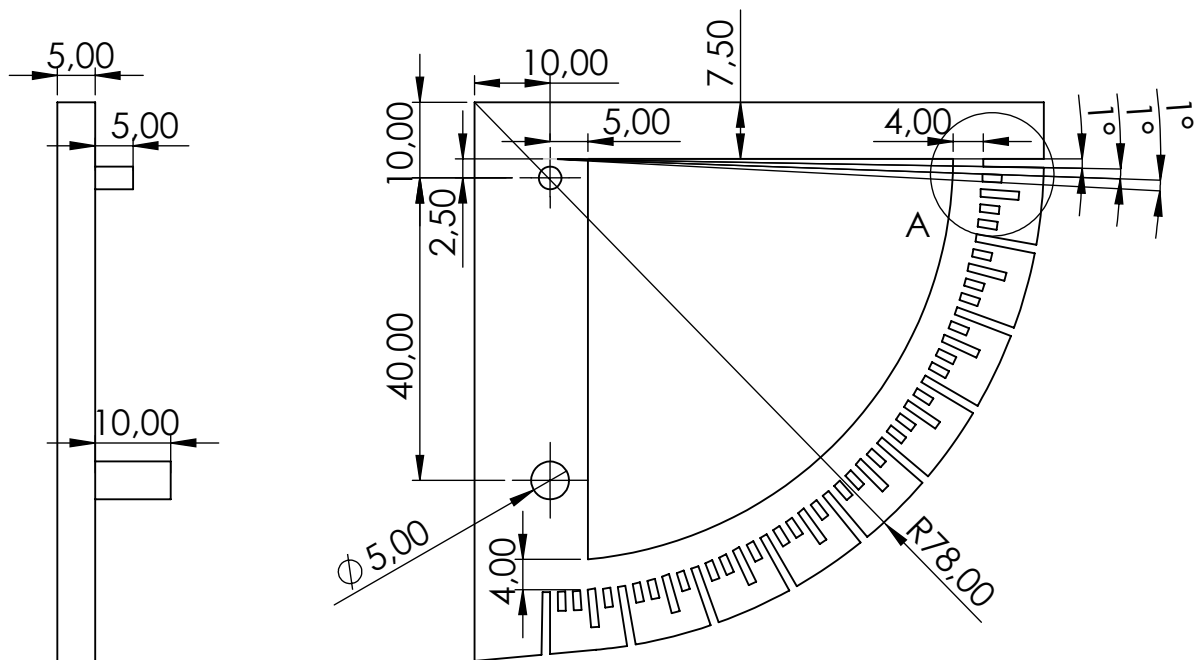
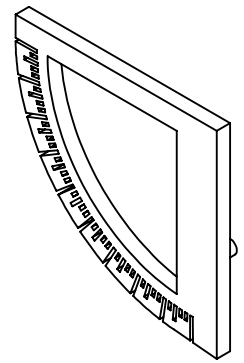
Checked by JAUME ORIOL LLADÓ 17/05/2023

Drawn by JAUME ORIOL LLADÓ 17/05/2023

Remarks



DETALLE A  
ESCALA 2 : 1



GRIPPER DESIGN FOR AN ASSISTIVE ROBOT  
IN A HOSPITAL ENVIRONMENT



UNIVERSITAT DE  
BARCELONA



Drawing Part  
37

Quantity 1

PROTRACTOR

Format:

DIN A4

Scale

1:1

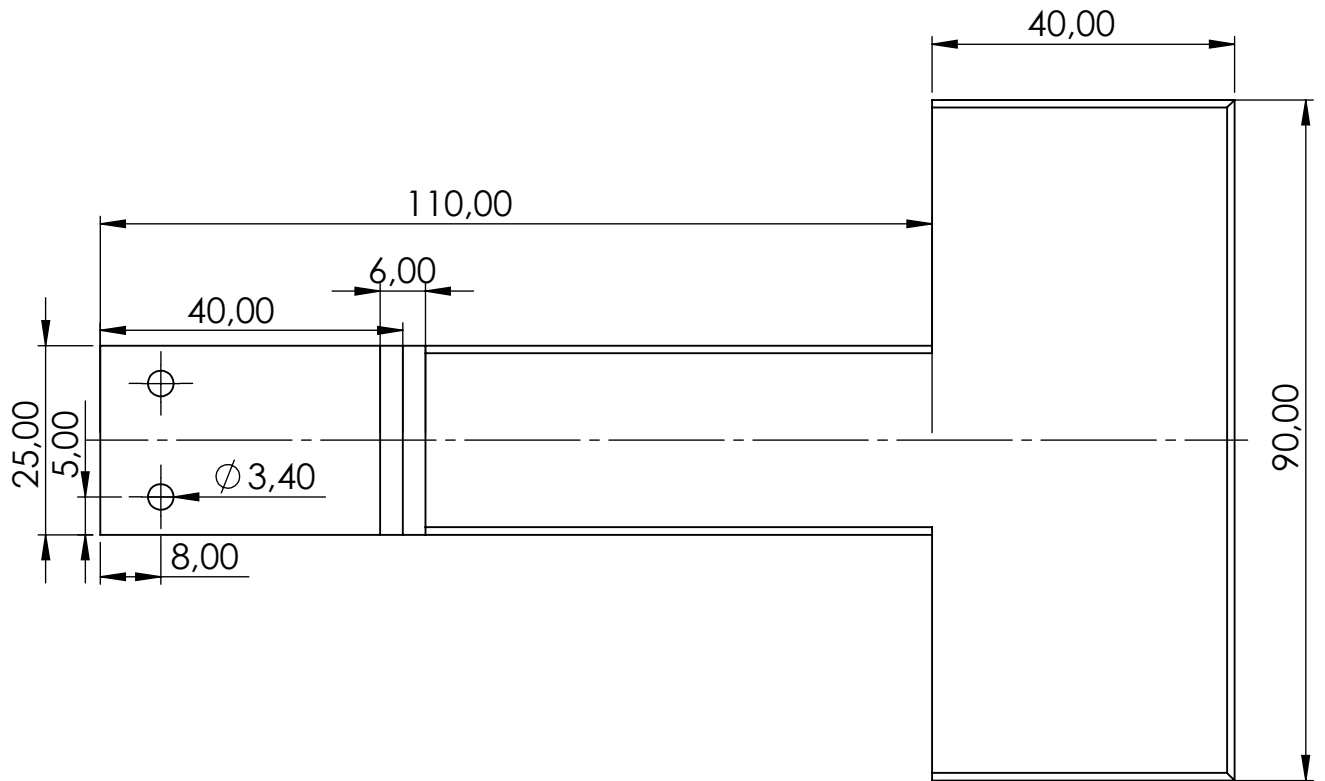
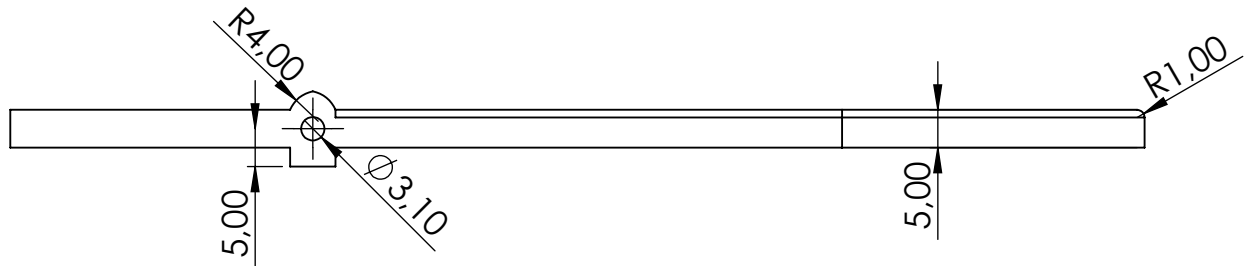
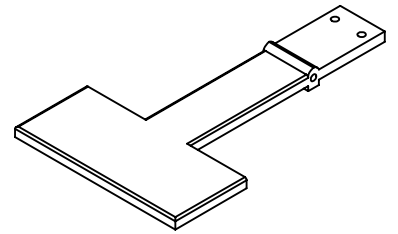
Projection



Checked by JAUME ORIOL LLADÓ 17/05/2023

Drawn by JAUME ORIOL LLADÓ 17/05/2023

Remarks



GRIPPER DESIGN FOR AN ASSISTIVE ROBOT  
IN A HOSPITAL ENVIRONMENT



UNIVERSITAT DE  
BARCELONA



Drawing Part  
38

Quantity 1

ROCKER ARM

Format:

DIN A4

Scale

1:1

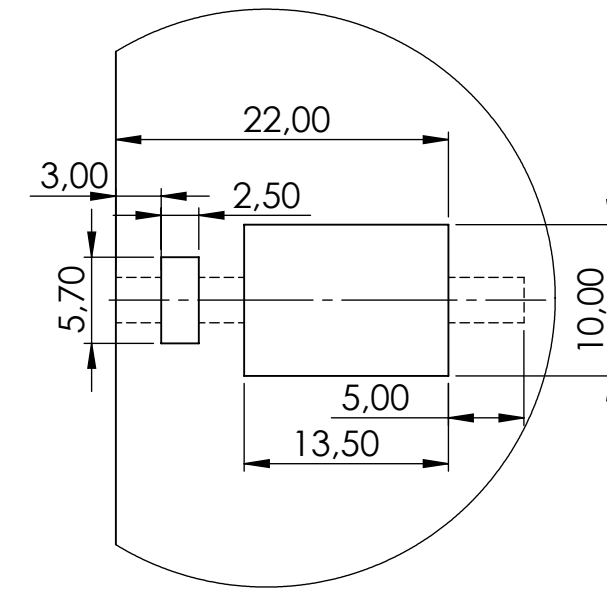
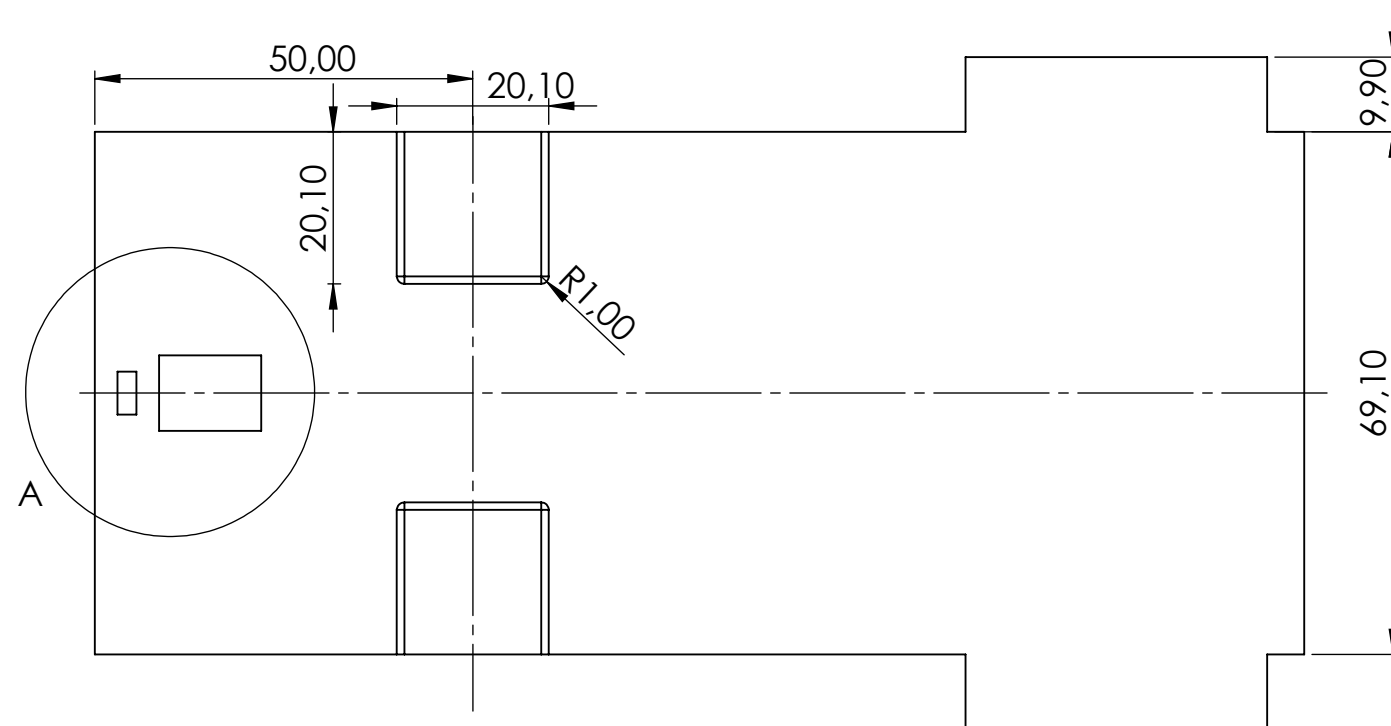
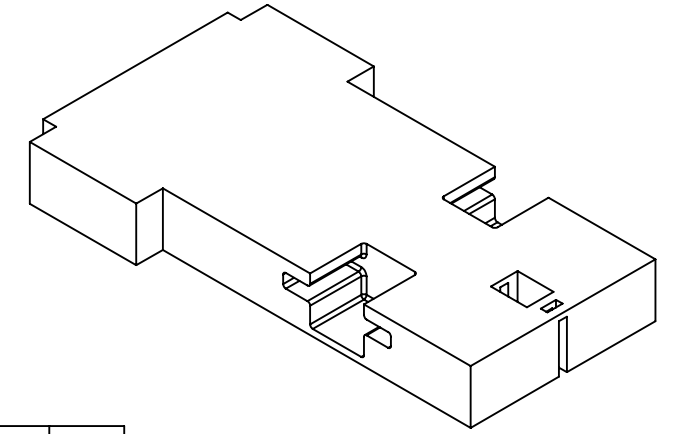
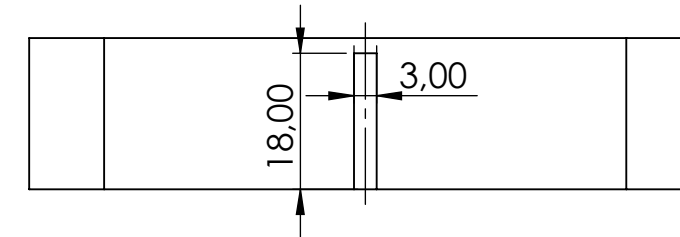
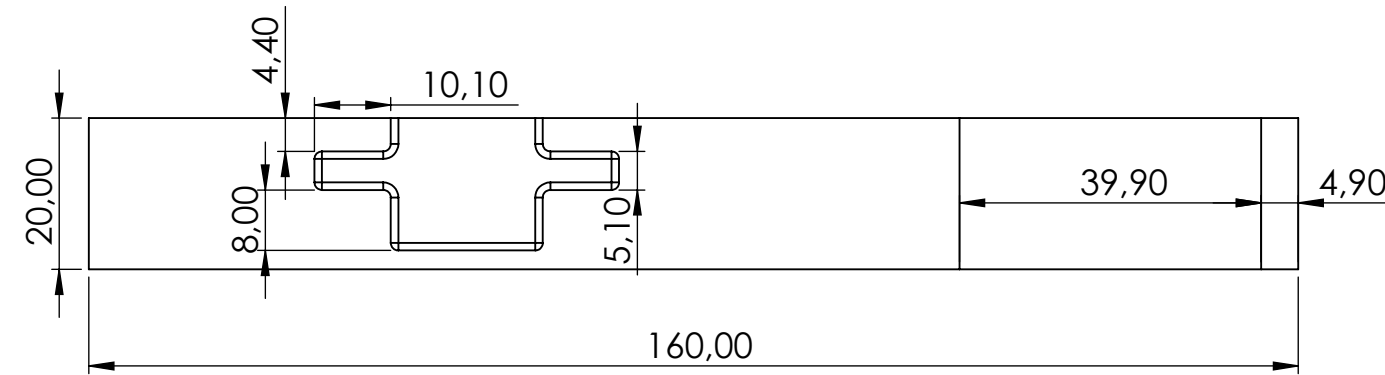
Projection






Checked by JAUME ORIOL LLADÓ 17/05/2023

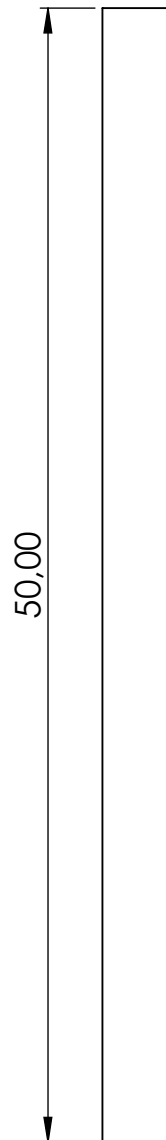
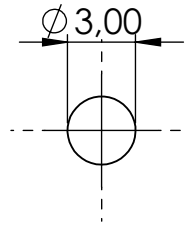
Drawn by JAUME ORIOL LLADÓ 17/05/2023




Remarks

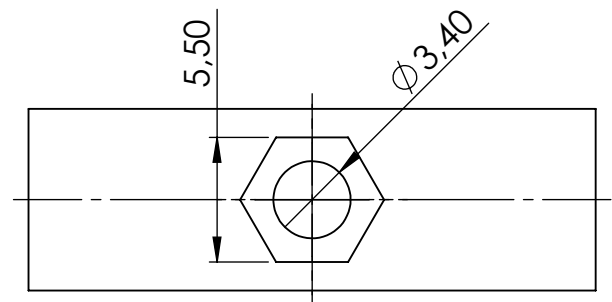
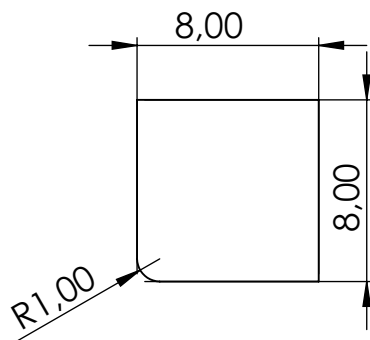
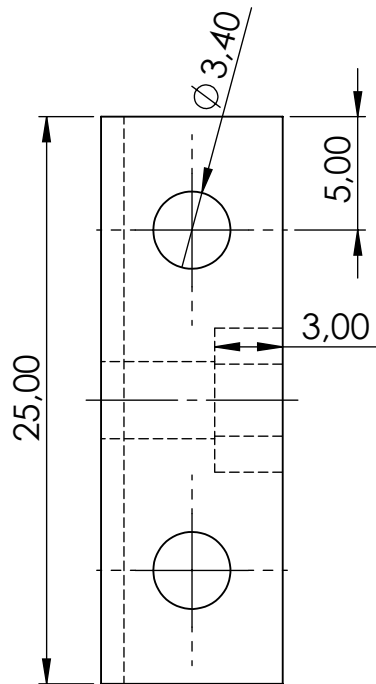
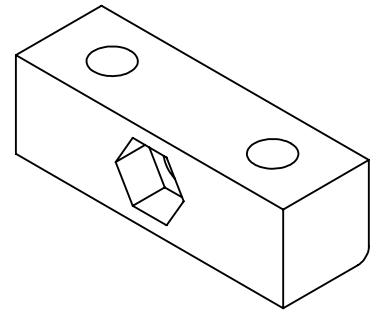


DETALLE A  
ESCALA 2 : 1

GRIPPER DESIGN FOR AN ASSISTIVE ROBOT IN A HOSPITAL ENVIRONMENT			 UNIVERSITAT DE BARCELONA 	Drawing Part 39	
ROCKER BASE				Quantity 1	
Checked by	JAUME ORIOL LLADÓ	17/05/2023	Format: DIN A3	Scale 1:1	Projection 
Drawn by	JAUME ORIOL LLADÓ	17/05/2023	Remarks		



GRIPPER DESIGN FOR AN ASSISTIVE ROBOT IN A HOSPITAL ENVIRONMENT			 UNIVERSITAT DE BARCELONA 		Part Drawing 40
					Quantity 1
ROCKER ROD			Format: DIN A4	Scale 3:1	Projection 
Checked by	JAUME ORIOL LLADÓ	17/05/2023	Remarks		
Drawn by	JAUME ORIOL LLADÓ	17/05/2023			



GRIPPER DESIGN FOR AN ASSISTIVE ROBOT  
IN A HOSPITAL ENVIRONMENT



UNIVERSITAT DE  
BARCELONA



Drawing Part

41

Quantity 1

SPRING CONNECTOR

Format:

DIN A4

Scale

3:1

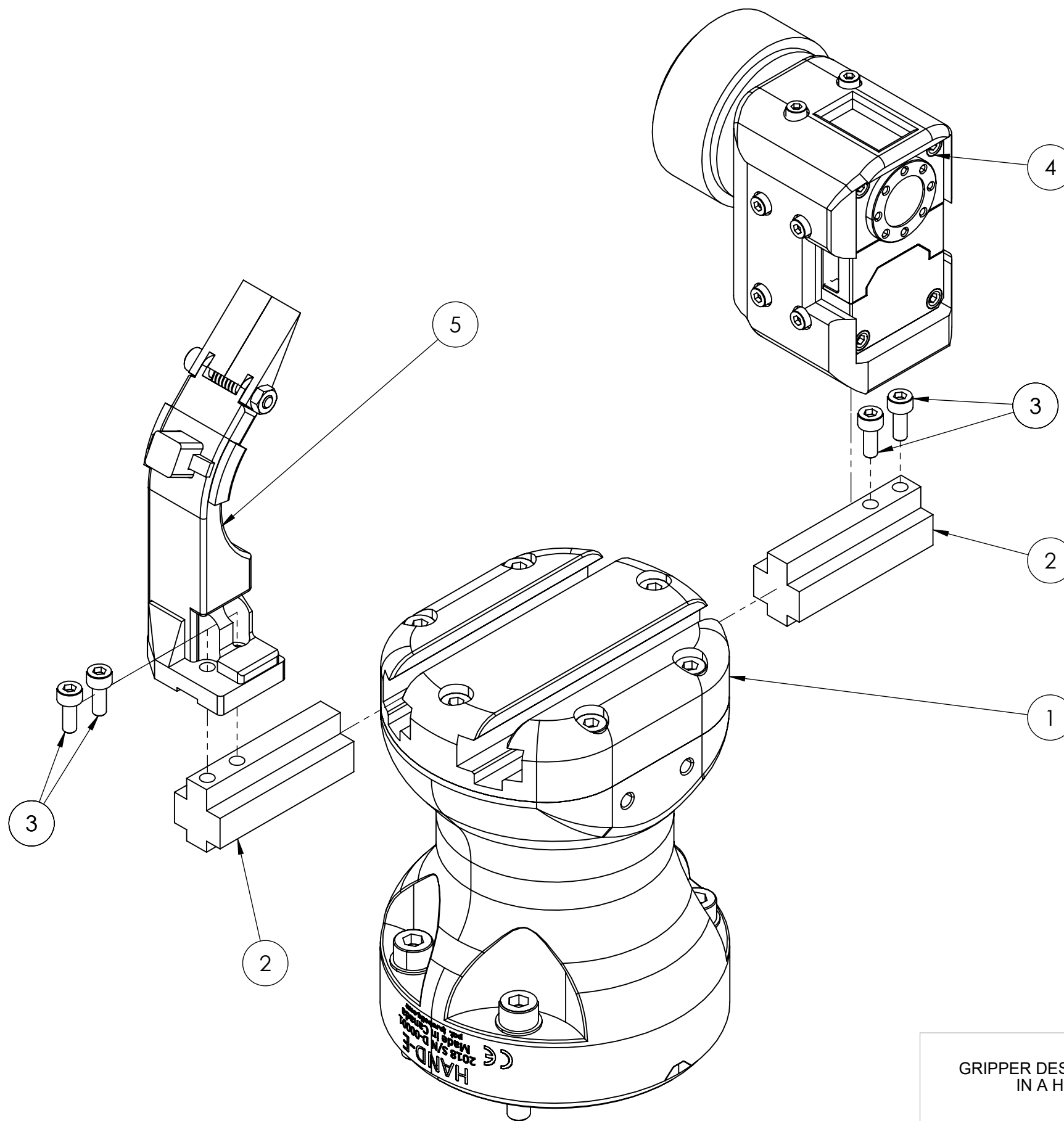
Projection



Checked by JAUME ORIOL LLADÓ 17/05/2023

Drawn by JAUME ORIOL LLADÓ 17/05/2023

Remarks



ITEM NO.	PART NUMBER	QTY.
1	ROBOTIQ_HAND-E_DEFEATURE_20181026.STEP	1
2	RACK	2
3	ISO 4762 M3 X 8 - 8N	4
4	FINGER A	1
5	FINGER B	1

GRIPPER DESIGN FOR AN ASSISTIVE ROBOT  
IN A HOSPITAL ENVIRONMENT



Drawing Part  
42

GRIPPER EXPLODED VIEW DIAGRAM

Format:  
DIN A3

Scale  
1:1

Quantity 1

Projection

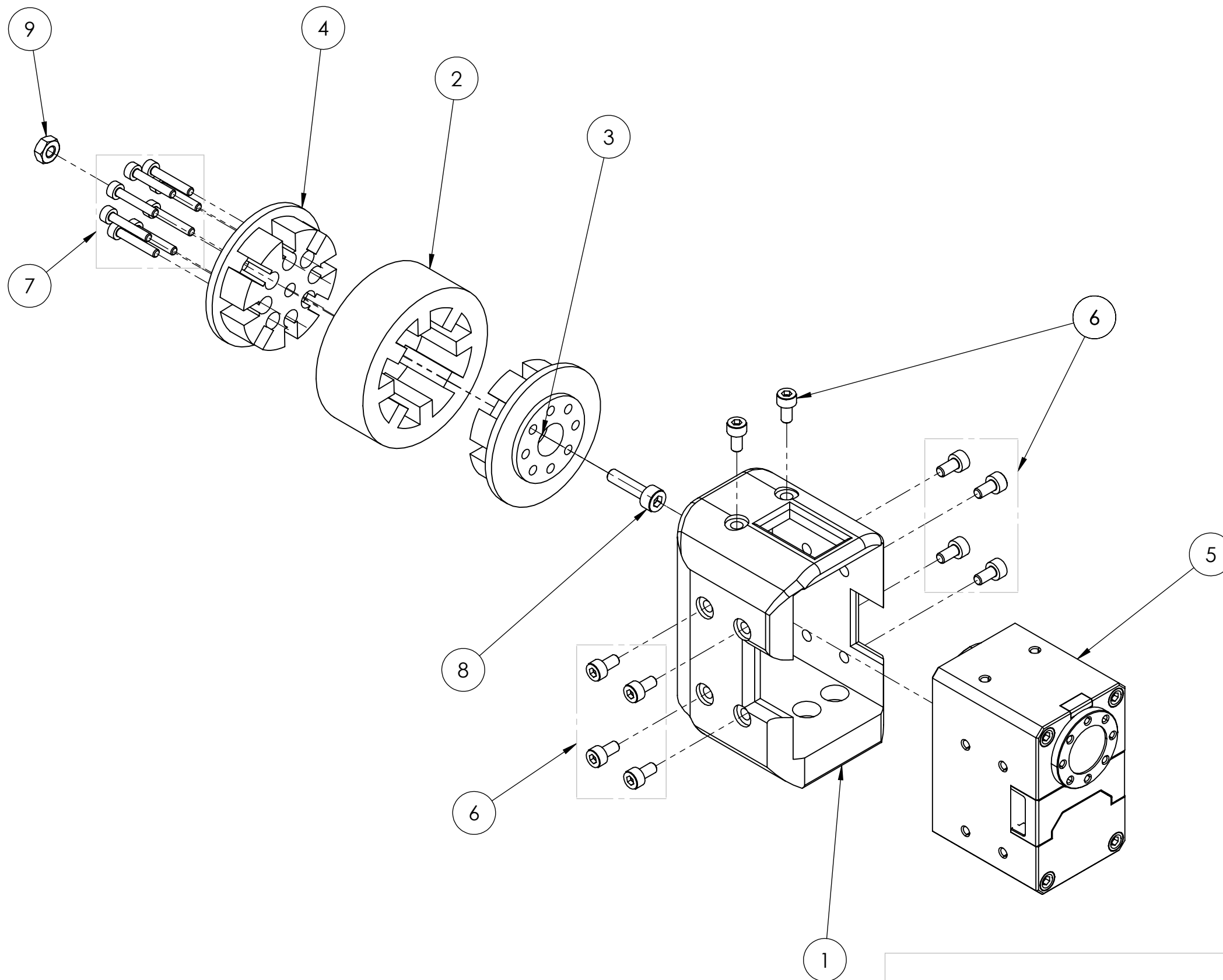


Checked by JAUME ORIOL LLADÓ 12/06/2023

Drawn by JAUME ORIOL LLADÓ 12/06/2023

Remarks





ITEM NO.	PART NUMBER	QTY.
1	BASE	1
2	ROLLER	1
3	ROLLER CAP PART 1	1
4	ROLLER CAP PART 2	1
5	ENGINE	1
6	ISO 4762 M2.5 X 5 - 5N	10
7	ISO 4762 M2 X 12 - 12N	8
8	ISO 4762 M3 X 12 - 12N	1
9	ISO - 4032 - M3 - D - N	1

GRIPPER DESIGN FOR AN ASSISTIVE ROBOT  
IN A HOSPITAL ENVIRONMENT



Drawing Part  
43

FINGER A EXPLODED VIEW DIAGRAM

Format:  
DIN A3

Scale  
1:1

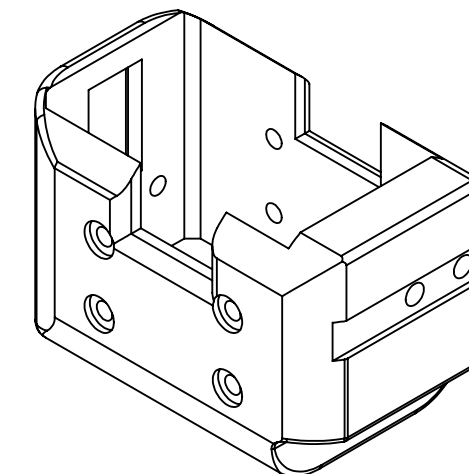
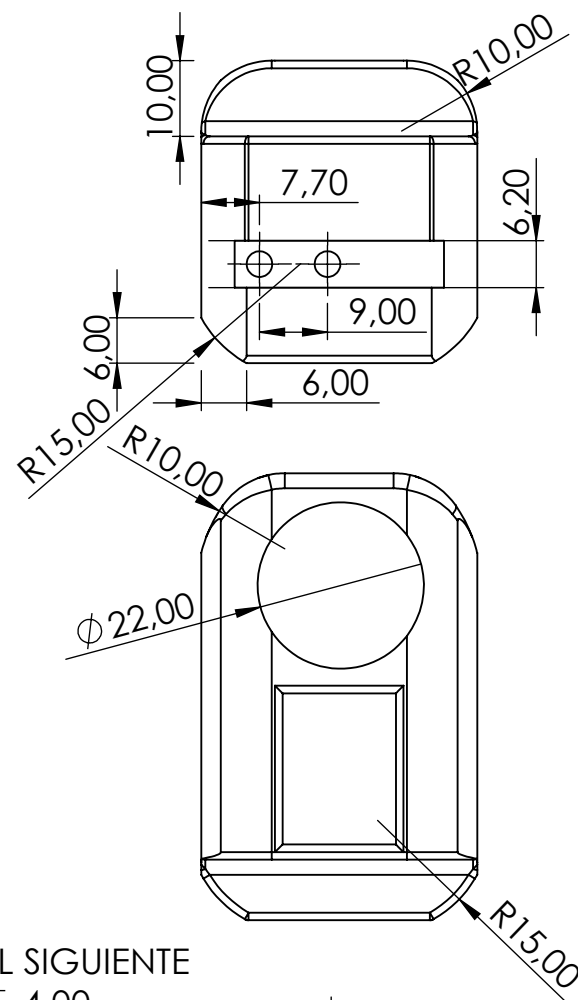
Projection



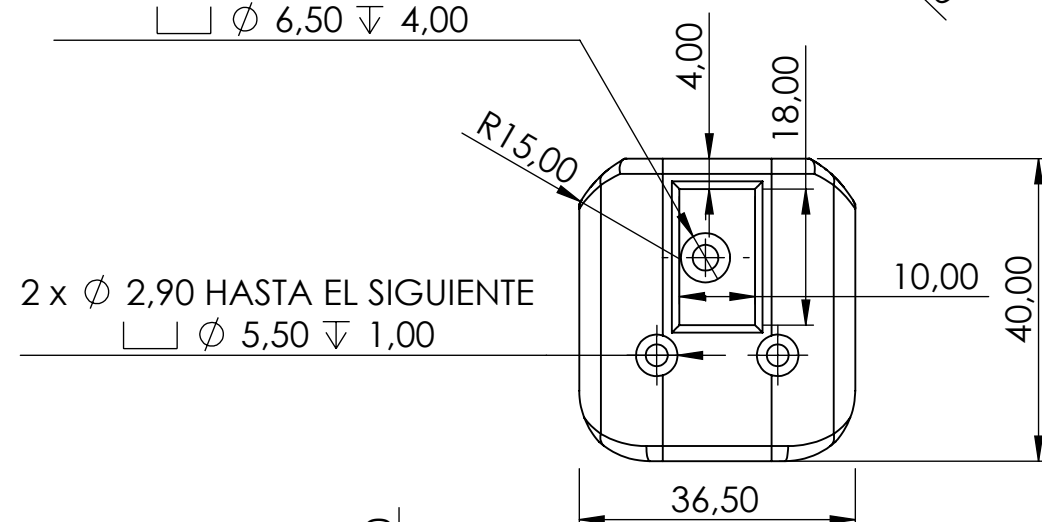
Checked by JAUME ORIOL LLADÓ 12/05/2023

Drawn by JAUME ORIOL LLADÓ 12/05/2023

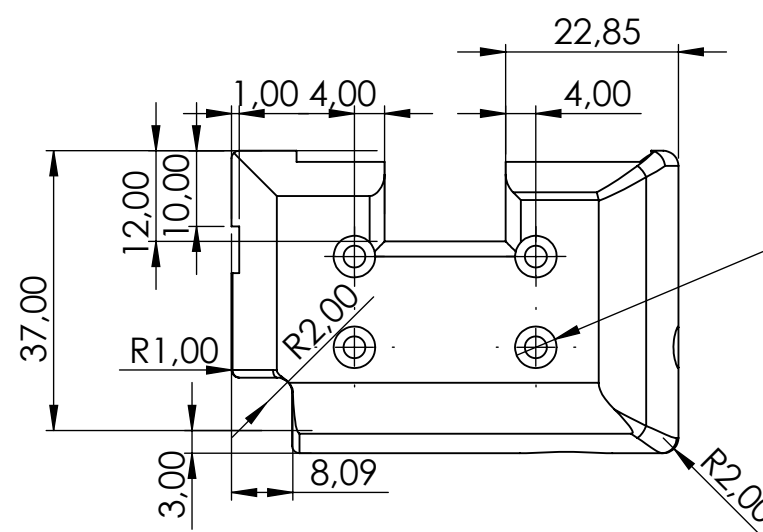
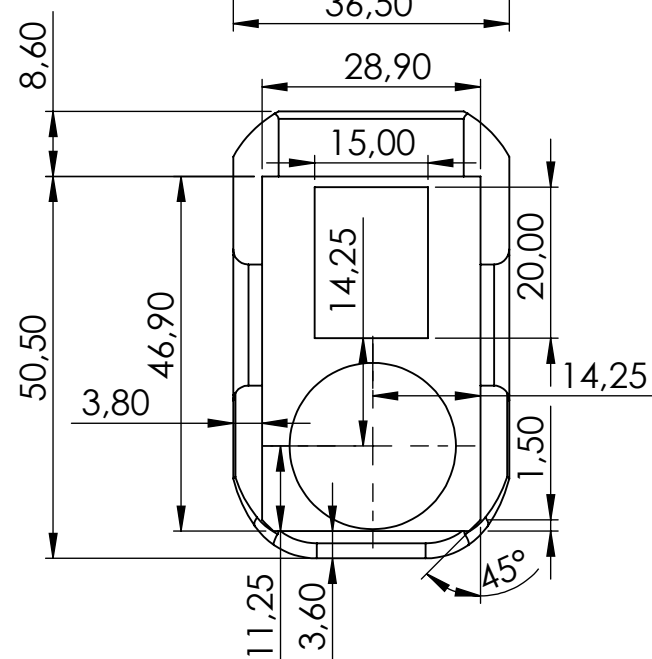
Remarks



2 x  $\varnothing$  3,40 HASTA EL SIGUIENTE  
□  $\varnothing$  6,50  $\nabla$  4,00



2 x  $\varnothing$  2,90 HASTA EL SIGUIENTE  
□  $\varnothing$  5,50  $\nabla$  1,00



8 x  $\varnothing$  2,90 HASTA EL SIGUIENTE  
□  $\varnothing$  5,50  $\nabla$  1,00

GRIPPER DESIGN FOR AN ASSISTIVE ROBOT  
IN A HOSPITAL ENVIRONMENT



Drawing Part  
44

Quantity 1

FINGER A BASE

Format:  
DIN A3

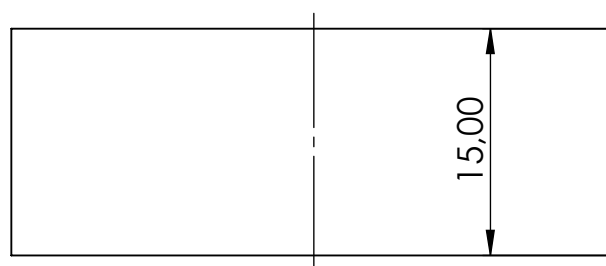
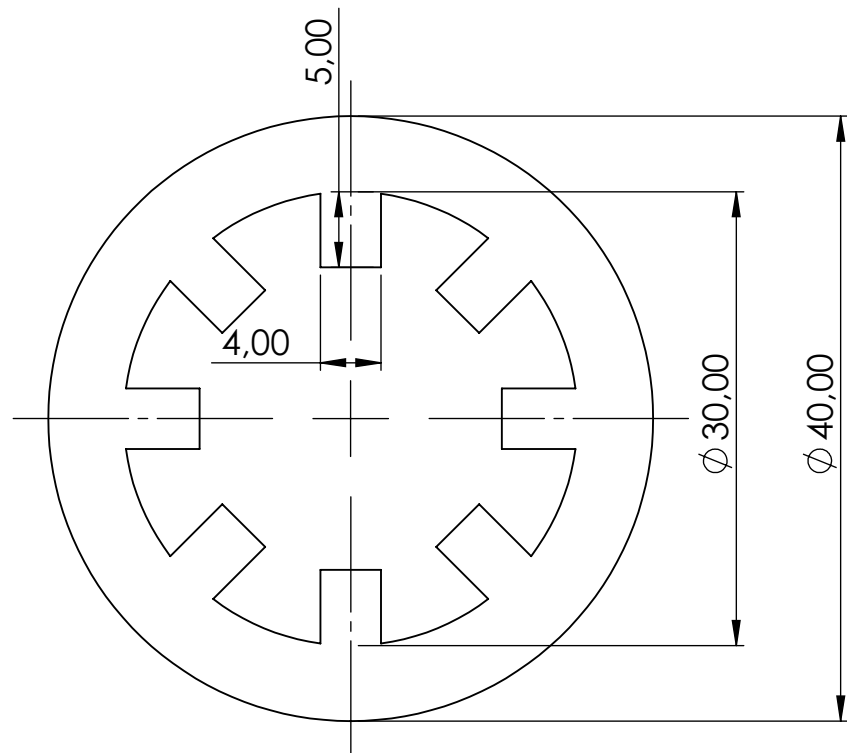
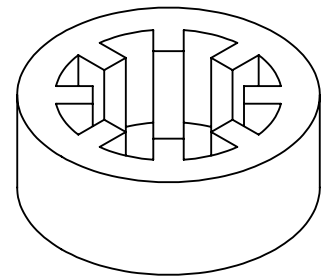
Scale  
1:1

Projection

Checked by JAUME ORIOL LLADÓ 13/06/2023

Drawn by JAUME ORIOL LLADÓ 13/06/2023

Remarks



GRIPPER DESIGN FOR AN ASSISTIVE ROBOT  
IN A HOSPITAL ENVIRONMENT



UNIVERSITAT DE  
BARCELONA



Part Drawing

45

Quantity 1

GRIPPER'S ROLLER

Format:

DIN A4

Scale

2:1

Projection

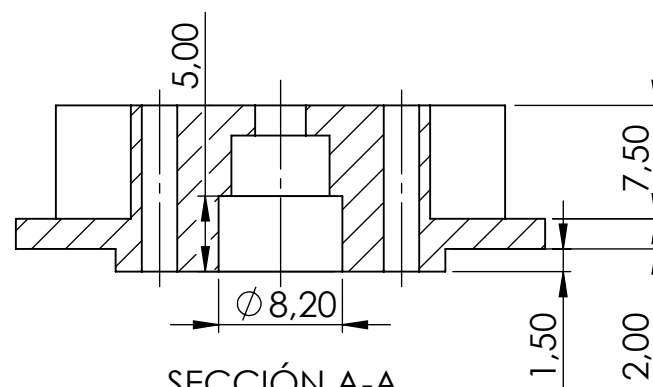
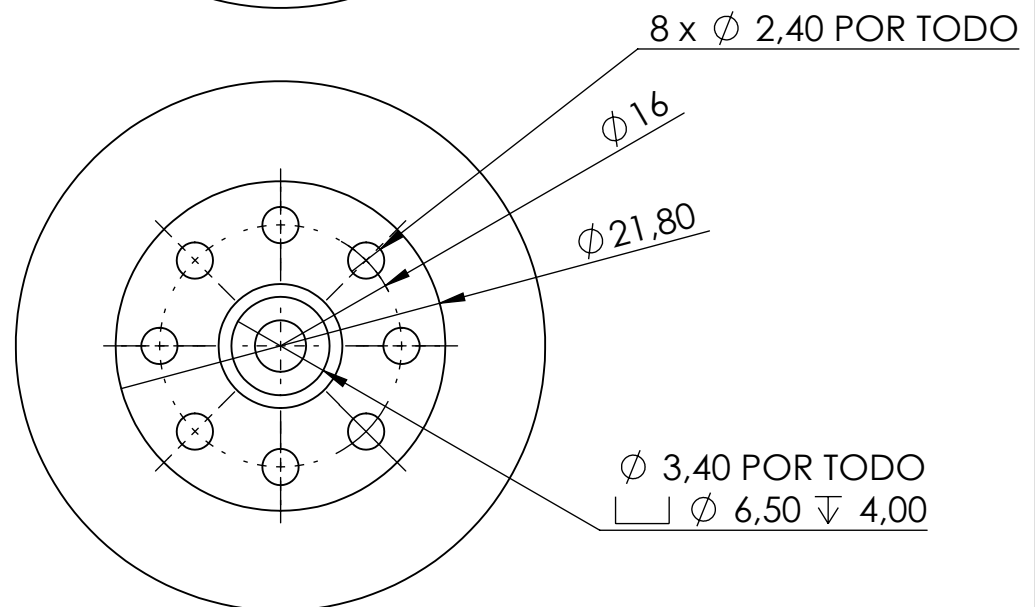
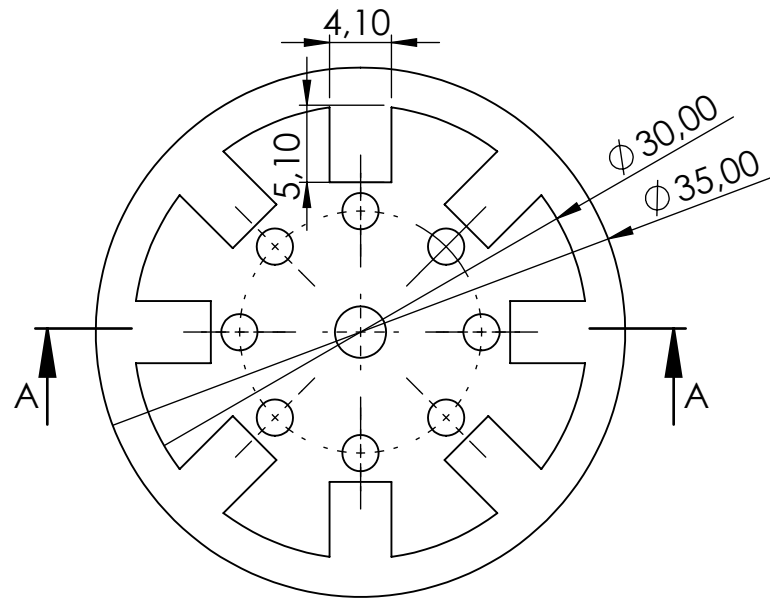
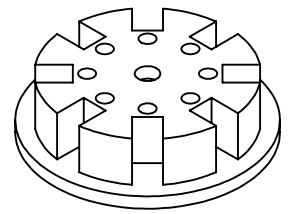


Checked by JAUME ORIOL LLADÓ 13/06/2023

Drawn by JAUME ORIOL LLADÓ 13/06/2023

Remarks

Printed with Resin 80A



SECCIÓN A-A  
ESCALA 2 : 1

GRIPPER DESIGN FOR AN ASSISTIVE ROBOT  
IN A HOSPITAL ENVIRONMENT



UNIVERSITAT DE  
BARCELONA



Part Drawing

46

Quantity 1

ROLLER CAP PART 1

Format:

DIN A4

Scale

2:1

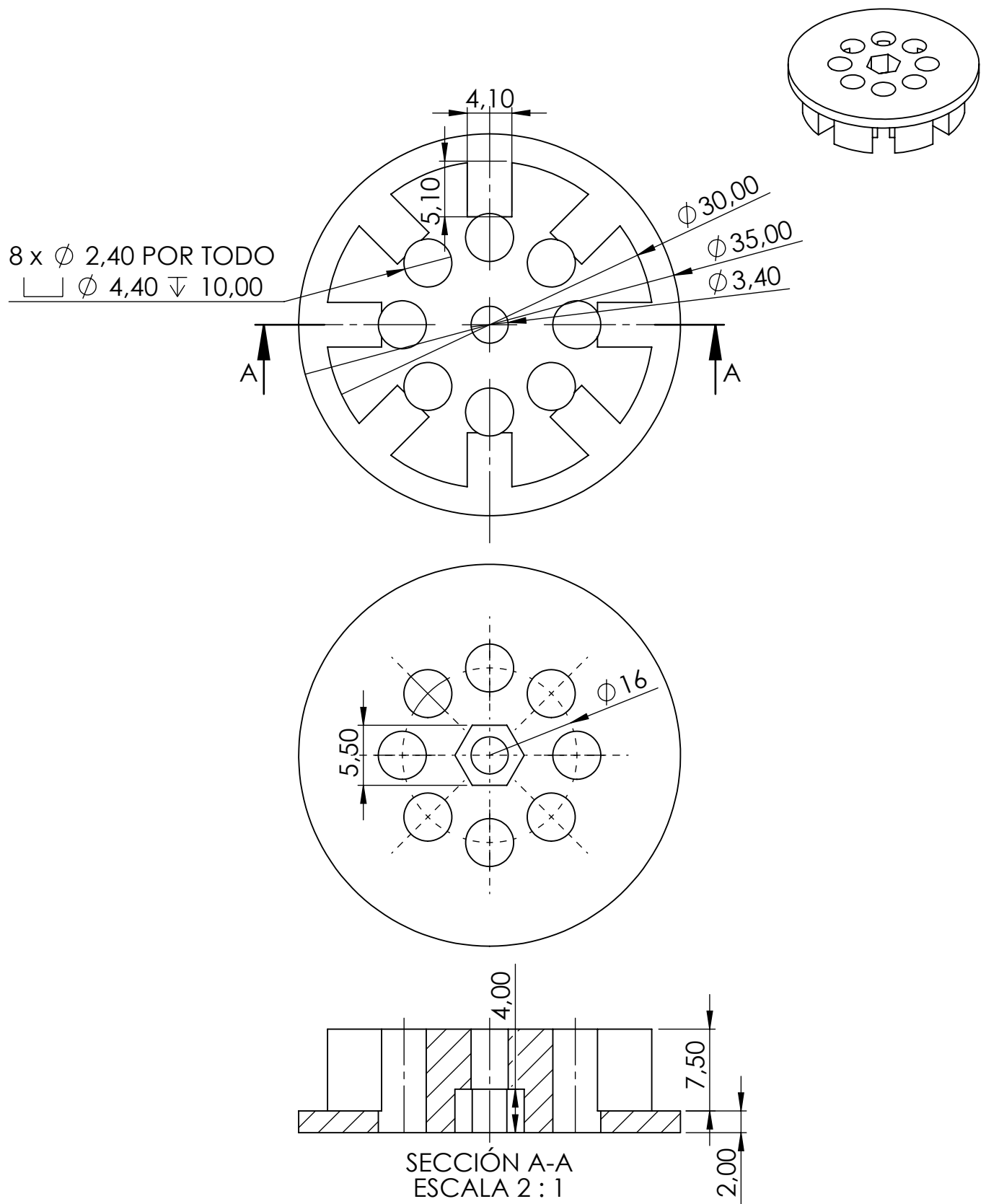
Projection



Checked by JAUME ORIOL LLADÓ 13/05/2023

Drawn by JAUME ORIOL LLADÓ 13/05/2023

Remarks



GRIPPER DESIGN FOR AN ASSISTIVE ROBOT  
 IN A HOSPITAL ENVIRONMENT



UNIVERSITAT DE  
 BARCELONA



Part Drawing

47

Quantity 1

ROLLER CAP PART 2

Format:

DIN A4

Scale

2:1

Projection

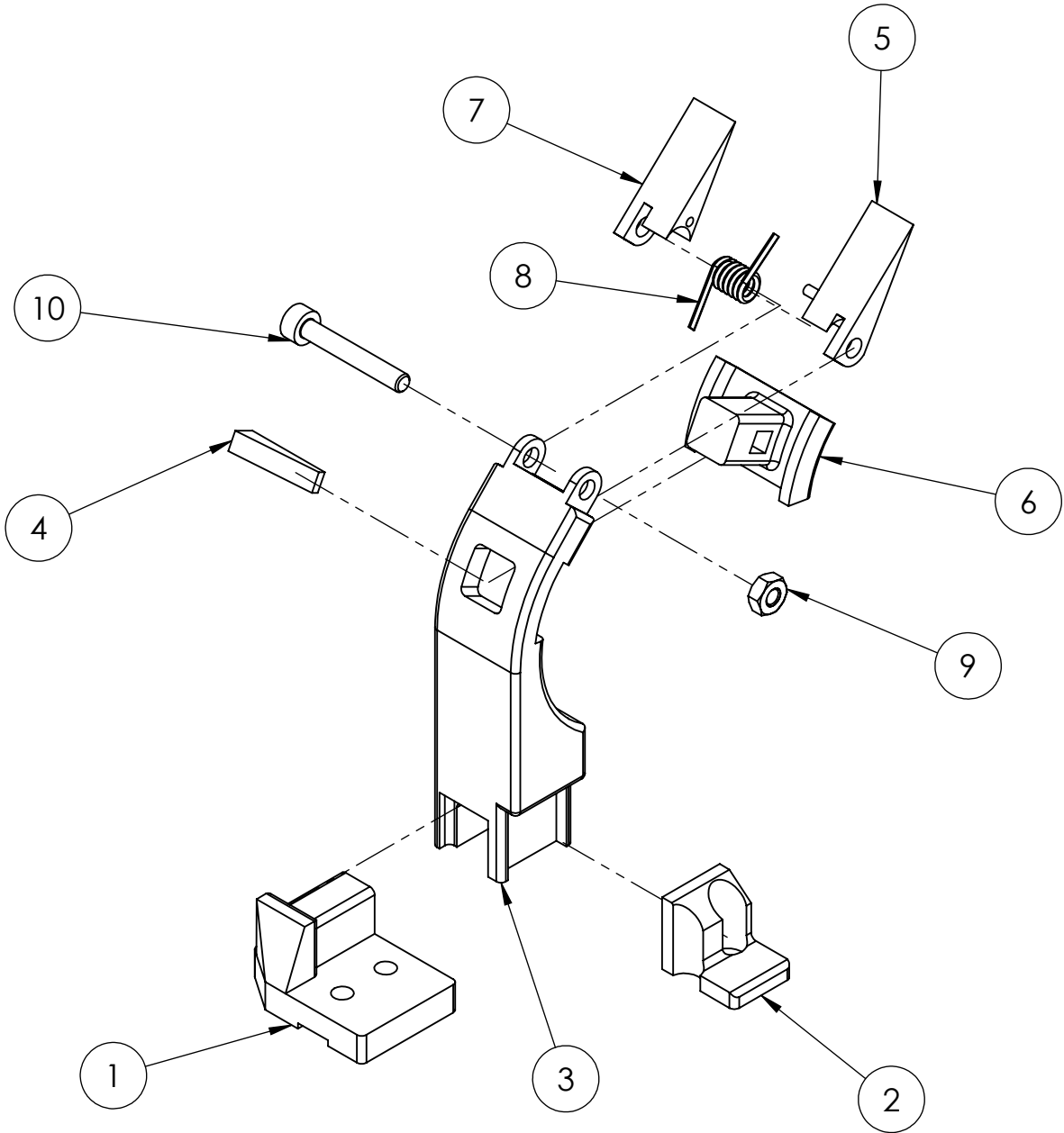





Checked by JAUME ORIOL LLADÓ 13/06/2023

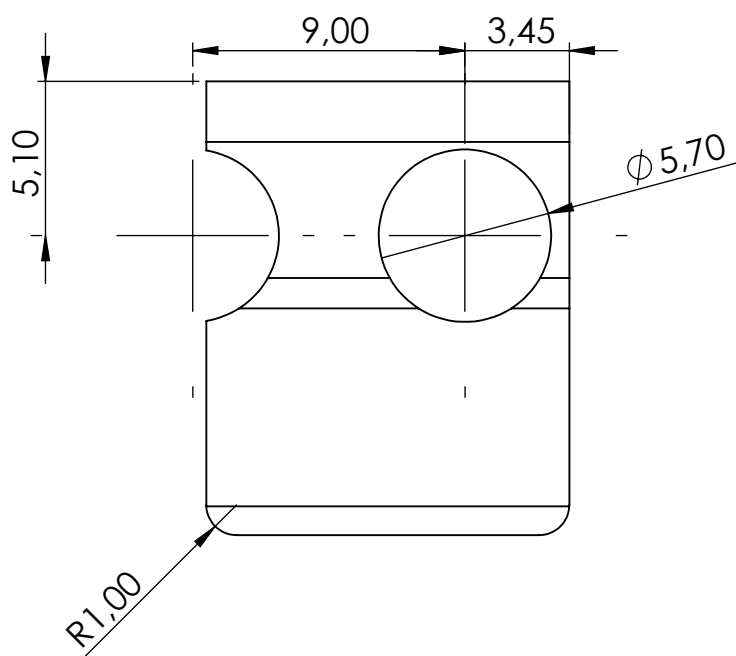
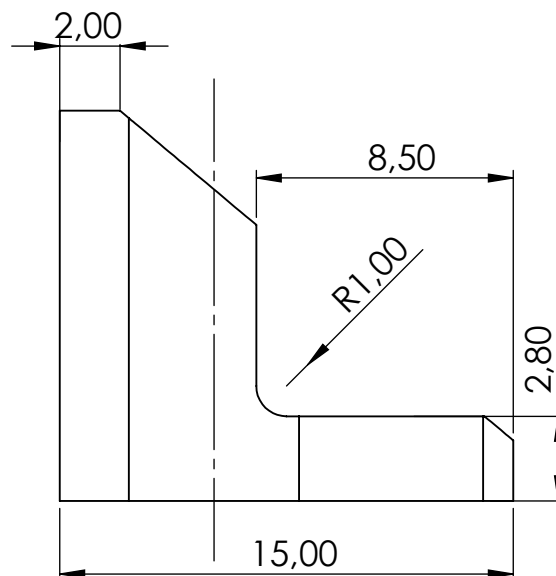
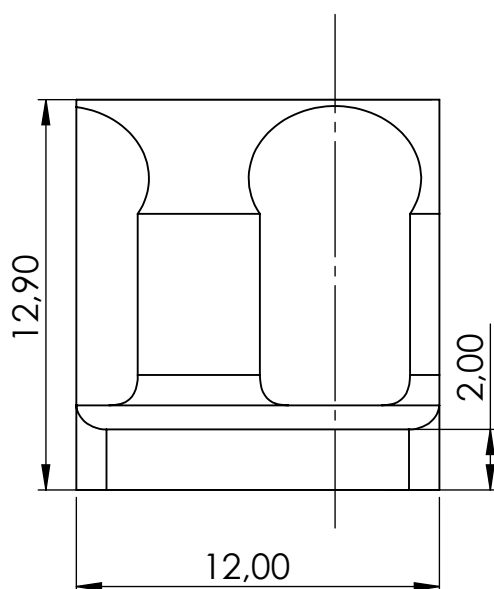
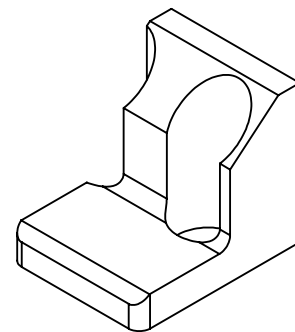
Drawn by JAUME ORIOL LLADÓ 13/06/2023

Remarks

ITEM NO.	PART NUMBER	QTY.
1	BASE	1
2	CARTEL	1
3	BODY	1
4	WEDGE	1
5	LEFT TIP	1
6	MATERIAL SURFACE	1
7	RIGHT TIP	1
8	SPRING	1
9	ISO - 4032 - M3 - D - N	1
10	ISO 4762 M3 X 20 - 20N	1



GRIPPER DESIGN FOR AN ASSISTIVE ROBOT IN A HOSPITAL ENVIRONMENT			<div> UNIVERSITAT DE BARCELONA</div> <div> UPC</div>		Part Drawing 48
FINGER B EXPLODED VIEW DIAGRAM					Quantity 1
Checked by	JAUME ORIOL LLADÓ	12/06/2023	Format: DIN A4	Scale 1:1	Projection 
Drawn by	JAUME ORIOL LLADÓ	12/06/2023	Remarks		



GRIPPER DESIGN FOR AN ASSISTIVE ROBOT  
IN A HOSPITAL ENVIRONMENT



UNIVERSITAT DE  
BARCELONA



Part Drawing

49

Quantity 1

CARTEL

Format:

DIN A4

Scale

4:1

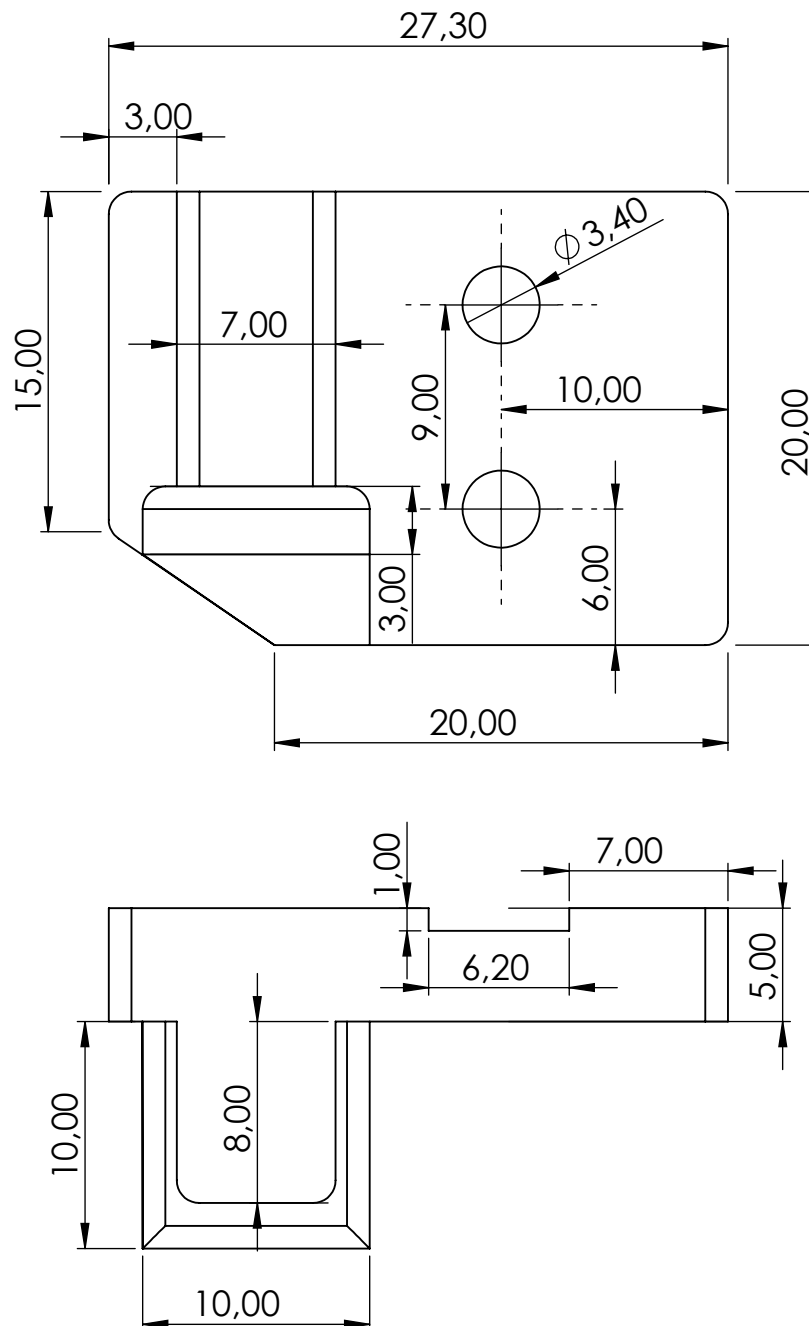
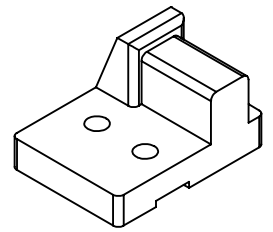
Projection



Checked by JAUME ORIOL LLADÓ 13/06/2023

Drawn by JAUME ORIOL LLADÓ 13/06/2023

Remarks



GRIPPER DESIGN FOR AN ASSISTIVE ROBOT  
IN A HOSPITAL ENVIRONMENT



UNIVERSITAT DE  
BARCELONA



Part Drawing

50

Quantity 1

Projection



FINGER B BASE

Format:

DIN A4

Scale

3:1

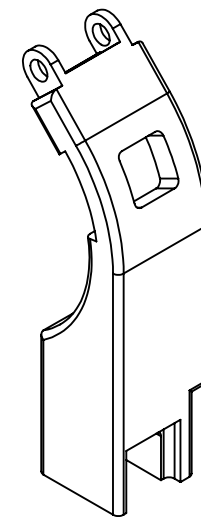
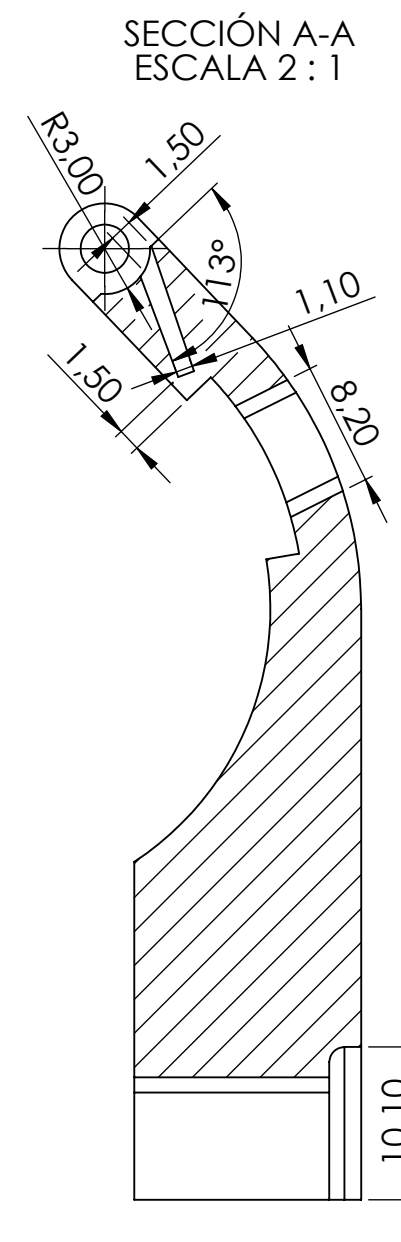
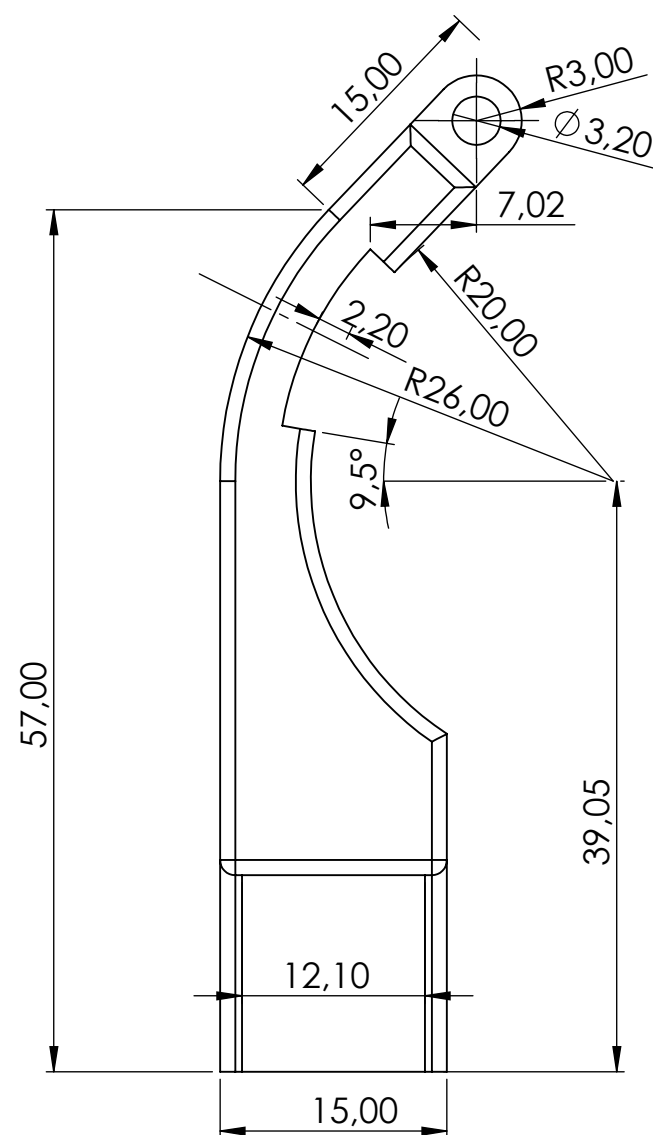
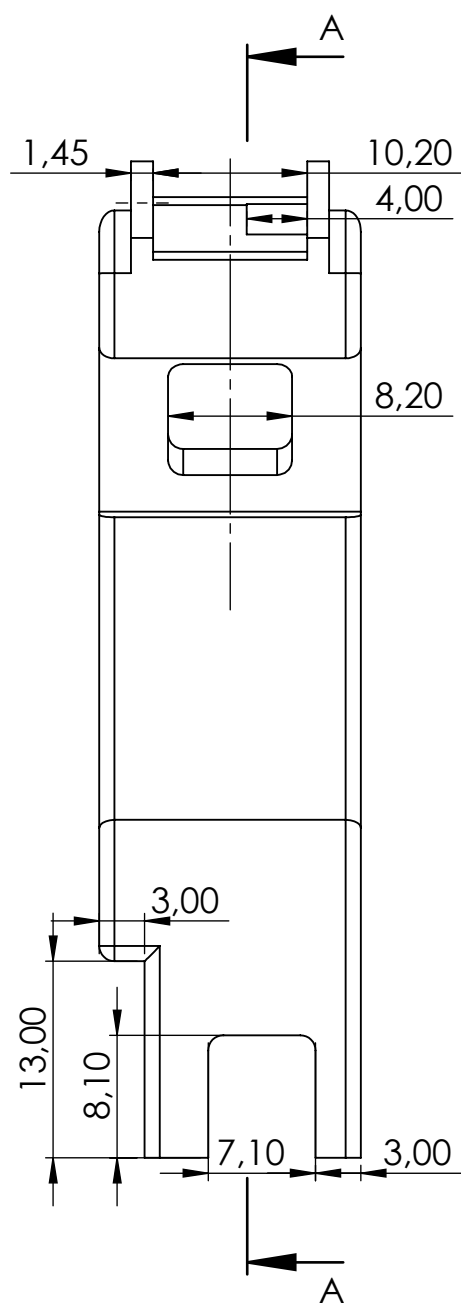
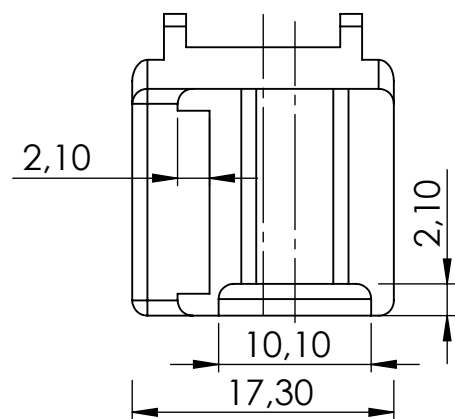
Checked by JAUME ORIOL LLADÓ 13/06/2023

Drawn by JAUME ORIOL LLADÓ 13/06/2023

Remarks

All roundings are 1mm





GRIPPER DESIGN FOR AN ASSISTIVE ROBOT  
IN A HOSPITAL ENVIRONMENT



UNIVERSITAT DE  
BARCELONA



Drawing Part

51

Quantity 1

FNGER B BODY

Format:

DIN A3

Scale

2:1

Projection

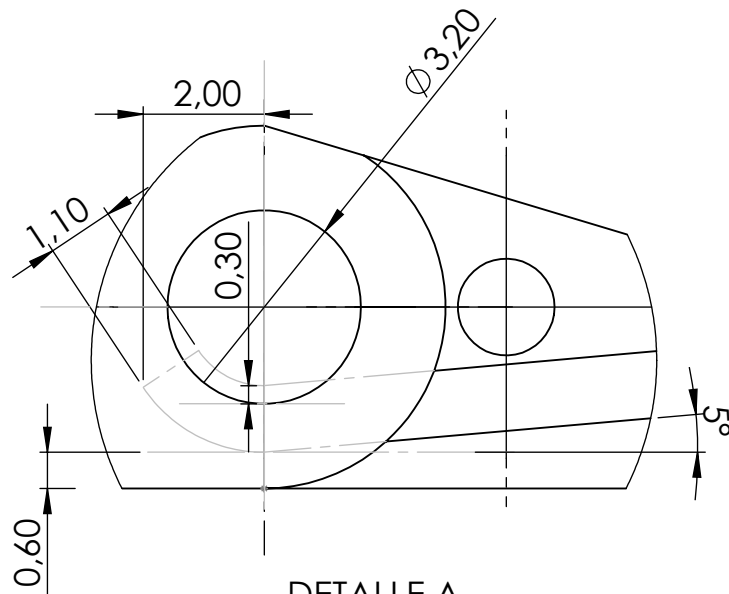


Checked by JAUME ORIOL LLADÓ 13/06/2023

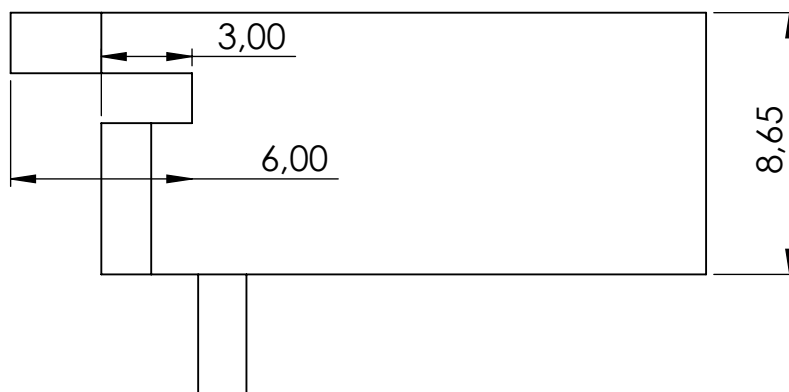
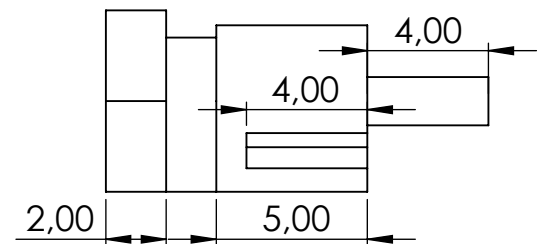
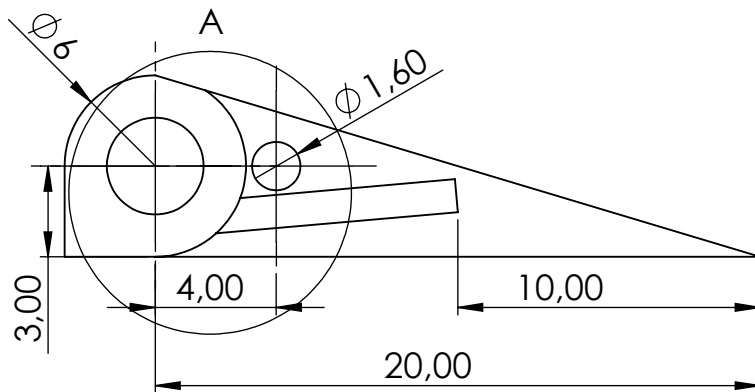
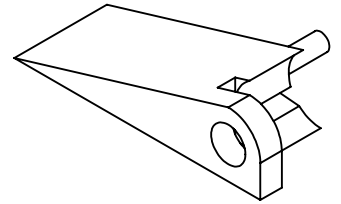
Drawn by JAUME ORIOL LLADÓ 13/06/2023

Remarks

All roundings are 1mm



DETALLE A  
ESCALA 8 : 1



GRIPPER DESIGN FOR AN ASSISTIVE ROBOT  
IN A HOSPITAL ENVIRONMENT



UNIVERSITAT DE  
BARCELONA



Part Drawing

52

Quantity 1

LEFT TIP

Format:

DIN A4

Scale

4:1

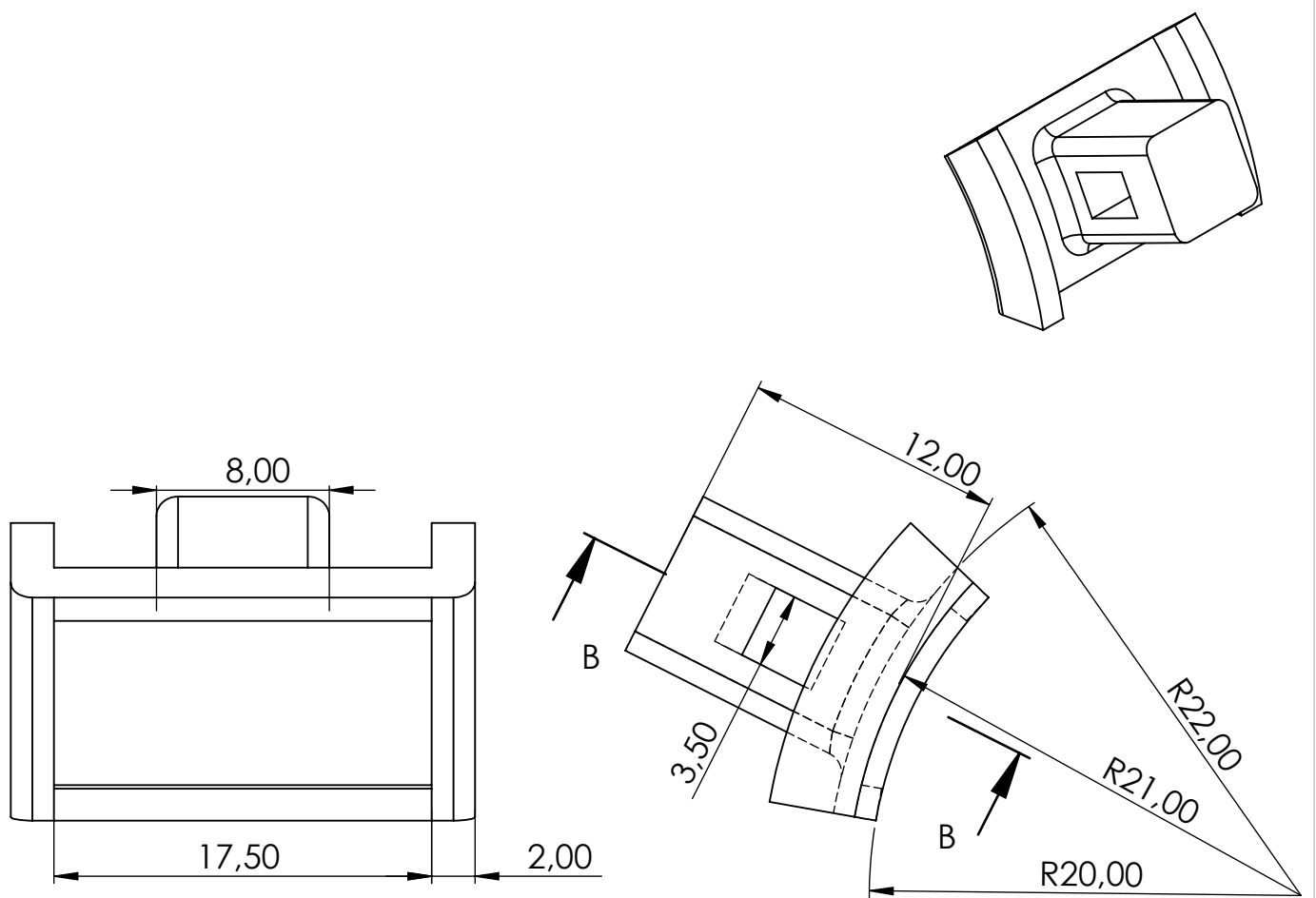
Projection



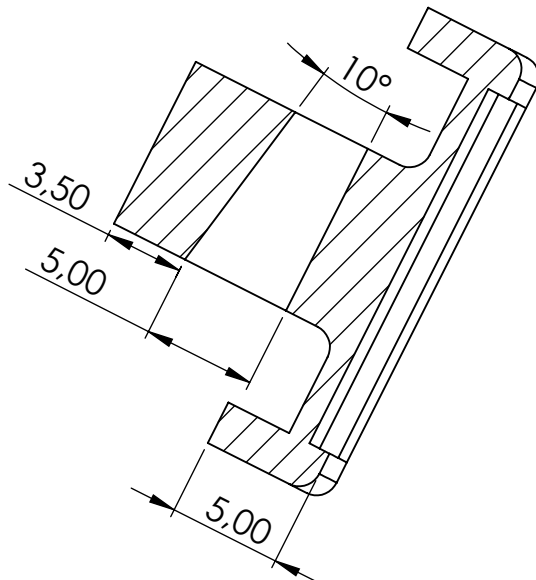
Checked by JAUME ORIOL LLADÓ 13/06/2023

Drawn by JAUME ORIOL LLADÓ 13/06/2023

Remarks



SECCIÓN B-B  
ESCALA 3 : 1



GRIPPER DESIGN FOR AN ASSISTIVE ROBOT  
IN A HOSPITAL ENVIRONMENT



UNIVERSITAT DE  
BARCELONA



Part Drawing

53

Quantity 1

MATERIAL SURFACE

Format:

DIN A4

Scale

3:1

Projection

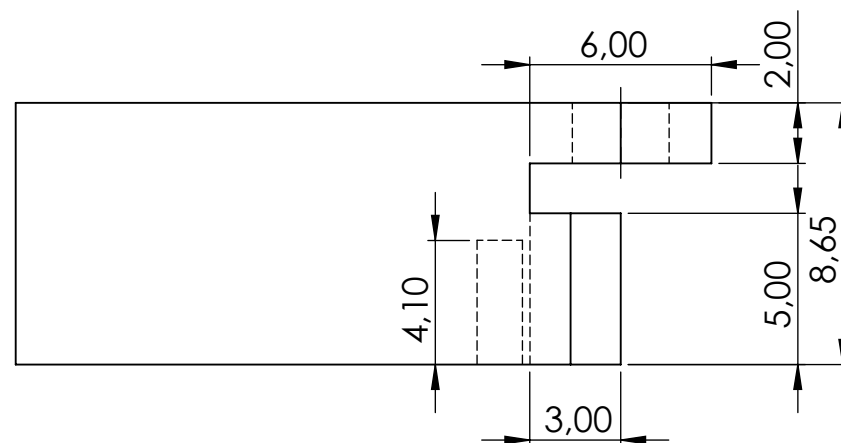
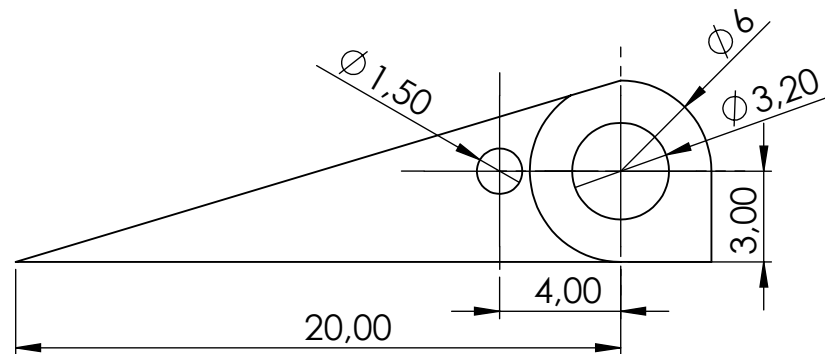
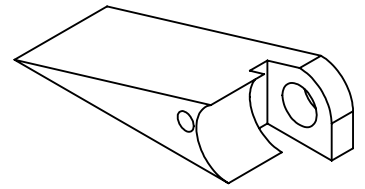


Checked by JAUME ORIOL LLADÓ 13/06/2023

Drawn by JAUME ORIOL LLADÓ 13/06/2023

Remarks

All roundings are 1mm



GRIPPER DESIGN FOR AN ASSISTIVE ROBOT  
IN A HOSPITAL ENVIRONMENT



UNIVERSITAT DE  
BARCELONA



Part Drawing

54

Quantity 1

RIGHT TIP

Format:

DIN A4

Scale

4:1

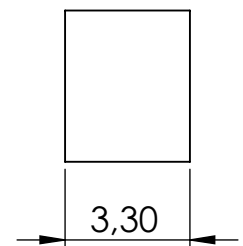
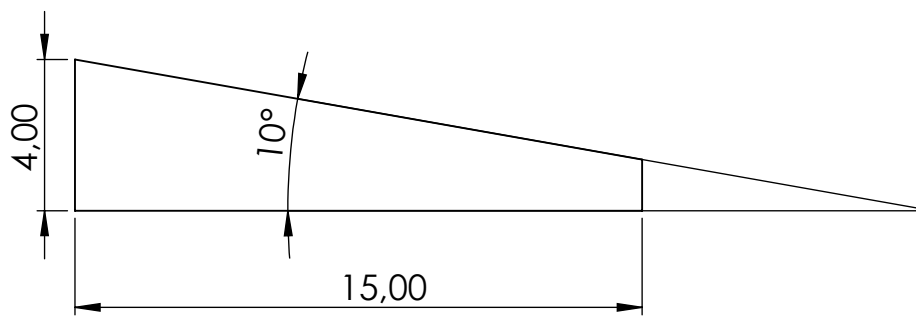
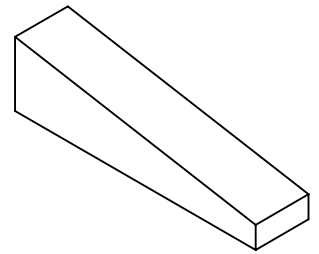
Projection



Checked by JAUME ORIOL LLADÓ 13/06/2023

Drawn by JAUME ORIOL LLADÓ 13/06/2023

Remarks



GRIPPER DESIGN FOR AN ASSISTIVE ROBOT  
IN A HOSPITAL ENVIRONMENT



UNIVERSITAT DE  
BARCELONA



Part Drawing

55

Quantity 1

WEDGE

Format:

DIN A4

Scale

5:1

Projection



Checked by JAUME ORIOL LLADÓ 13/06/2023

Drawn by JAUME ORIOL LLADÓ 13/06/2023

Remarks